博士論文

Effect of catalysis or oxidation actions of typical corrosion products on the generation of disinfection byproducts in water supply pipeline

水道パイプラインにおける消毒副産物の生成に対する代表的な腐食生成物の触媒作用または酸化作用の影響

北九州市立大学国際環境工学研究科

2023 年 3 月

傅凌霄（フ　リョウショウ）

FU LINGXIAO

Doctoral Thesis

Effect of catalysis or oxidation actions of typical corrosion products on the generation of disinfection byproducts in water supply pipeline

Mar 2023

FU LINGXIAO

The University of Kitakyushu

Faculty of Environmental Engineering

Department of Architecture

Gao Laboratory

ACKNOWLEDGEMENTS

EFFECT OF CATALYSIS OR OXIDATION ACTIONS OF TYPICAL CORROSION PRODUCTS ON THE GENERATION OF DISINFECTION BY-PRODUCTS IN WATER SUPPLY PIPELINE

ABSTRACT

Drinking water safety is one of the issues that people are most concerned about in daily life, and it is the basic guarantee for life health and quality of life. In the drinking water distribution process, a series of complex biochemical reactions will occur within the drinking water distribution systems (DWDS), resulting in "secondary pollution" of drinking water. Copper and lead elements are widely present in daily-use pipe materials. In complex pipe network environments, they will be corroded to form pipe corrosion products (PCPs), which affect the initiation or attribution of biochemical reactions in DWDS. In this study, we selected extracellular polymeric substances (EPS) secreted by pipe network microbial biofilms as precursors to explore the catalytic formation of disinfection byproducts (DBPs) by copper corrosion products (CCPs) during the chlorination process; study the oxidation of lead corrosion products (PbO_2) to EPS in I-containing water is studied, and the generation mechanism, kinetics, toxicity effect and control strategy of I-DBPs in EPS as precursors are also studied.

The presence of CCPs can promote the DBPs formation, especially for nitrogenous disinfection byproducts (N-DBPs). The catalysis of the two CCPs is different. Cu^{2+} catalysis is homogeneous catalysis initiated by the complexation of Cu^{2+} and EPS, while CuO catalysis is heterogeneous catalysis caused by the Cl atoms in the polarized $HOCl/OCl^-$ by CuO. With the pH increases, the catalytic effect of CCPs increases, because alkaline conditions can promote electrostatic interactions among CCPs, EPS,

and HOCl/OCl$^-$. The presence of Br$^-$ will weaken the catalytic effect of CCPs. CCPs have a better catalytic effect on the protein component of EPS due to its more phenolic and unsaturated/conjugated structure. Among the amino acids that make up EPS protein, CCPs have the best catalytic effect on the reaction of tyrosine (Tyr) to form trihalomethane (THMs), while has the best catalytic effect to histidine (His) on the haloacetic acids (HAAs), haloacetonitrile (HANs) and haloacetamide (HAcAms) formation.

In the PbO$_2$/I$^-$/EPS system, the I$^-$ oxidation rate decreases with the increase of pH, the H$^+$ reaction order was 0.79, and the constant rate (k) is 1.6×10^{11} M$^{-2.79}$ s^{-1}. In the presence of EPS, most of the formed I$_2$/HOI (> 92%) was converted to total organic iodine (TOI). Compared with humic acid, EPS had lower C-IDBPs formation potential (FPs) and higher N-IDBPs FPs, so it had higher chronic cytotoxicity. pH, I$^-$ concentration and PbO$_2$ dosage had significant effects on the FPs of I-DBPs. The EPS proteins component had a higher C- and N-IDBPs FPs than the polysaccharide component because it contains more electrophilic sites and higher nitrogen content. Then, the chemical composition of the EPS proteins components was analyzed, and twenty amino acids monomers were detected. Among them, aspartic acid (Asp) was the main precursor of iodinated trihalomethanes (I-THMs), iodinated haloaceticacids (I-HAAs), iodinated haloacetonitriles (I-HANs) and iodinated haloacetamides (I-HAcAms) In addition, asparagine (Asn) and tyrosine (Tyr) were also important precursors of I-HANs and I-HAcAms.

In the MnO$_2$/I$^-$/EPS system, the ratio of I$^-$ to IO$_3^-$ and TOI was only 3.8% and 69.2%, which was due to the low oxidation ability of MnO$_2$. The increase of pH weakens the polarization and oxidation-reduction potential of MnO$_2$, resulting in a decreased in the generation FPs of I-THMs, I-HANs and I-HAAs. However, the FPs of I-HAcAms mainly depended on the difference between the hydrolysis rate of I-HANs and the decomposition rated of I-HAcAms, which reached the maximum at pH 6.0. In addition,

the FPs of I-DBPs was positively correlated with I⁻ concentration, and negatively correlated with MnO_2 dose. Similarly, the protein component had a higher C- and N-IDBPs production potential than the polysaccharide component, and Asp was the main precursor of the four I-DBPs.

In this study, the effect of two different PCPs on the formation of DBPs was studied when extracellular polymers were used as precursors. This will help to control the formation and conversion of DBPs, prevent the drinking water "secondary pollution", and ensure the safety and health of the water quality during the transmission and distribution of drinking water.

Keywords: oxidation corrosion products, disinfection by-products, extracellular polymer, catalysis, oxidation

TABLE OF CONTENTS

ACKNOWLEDGEMENT

PROLOGUE

1.1 Experimental conditions

Drinking water quality is closely related to people's life and health. With the development of China's economic level and the improvement of living standards, people's demand for drinking water quality also increases. Providing safe, clean and healthy drinking water for people is of great scientific and strategic significance for protecting people's life and health and promoting sustainable development of society. In order to ensure the safety of drinking water, scientists have done a lot of research from drinking water source protection, new water treatment technology and drinking water treatment process, but the water supply network is often neglected. The water supply pipe network is an important part of the water supply system connecting the water plant and the user terminal. The drinking water will stay in the water supply pipe network for a long time after long-distance transportation. In this process, the drinking water will be in contact with the pipe internal surface and other equipment, leading to a variety of complex biochemical reactions. As a result, some water quality indices such as turbidity, chroma, total number of bacteria and heavy metal content have changed obviously, and even "yellow water" phenomenon may occur when it is serious, it is a serious threat to people's daily life and safety.

Generally speaking, all the water quality indices of finished water can meet the standards for drinking water quality formulated by the National Ministry of Health. However, water quality generally has a downward trend after long distance transportation and stay in the pipe network. The ministry of Construction of China's water supply survey of 45 cities found that compared with the finished water, the network of drinking water chroma increased by 0.45 CU, the turbidity increased by 0.38 NTU, the concentration of iron and manganese increased by 0.04 mg L^{-1} and 0.02 mg L^{-1} respectively, the total number of bacteria increased by 18 CFU L^{-1}, the number of *Escherichia coli* increased by 0.4 L^{-1}, and the qualified rate of water quality decreased by about 16.6%[1].Therefore, preventing the deterioration of drinking water in the pipe network and transporting healthy drinking water safely to the user terminal is still a difficult problem.

The control of disinfection by-products (DBPs) is the key to reduce the potential risk of drinking water in the process of transportation. The formation of DBPs is closely related to pipe network corrosion [1]. On the other hand, Pipe scale produced by pipe network corrosion will provide a site

for the growth and proliferation of microorganisms in the pipe network, and reduce the effect of disinfectants. In addition, it can dissolve heavy metals into the water, leading to the deterioration of water quality [2]. In addition to natural organic matter (NOM) in water, extracellular polymeric substances (EPS) secreted by microbial cells and soluble organic matter (DOM) produced by rupture are both precursors of DBPs [2]. At present, most studies on DBPs generation take exogenous NOM as the precursor, but ignore endogenous EPS. EPS contains a large number of biomolecules, such as nucleic acids, proteins, polysaccharides and lipids and other compounds, which will produce a large number of nitrogen-containing disinfection by-products (N-DBPs) which are more toxic than carbon containing disinfection by-products (C-DBPs). On the other hand, corrosion products directly affect DBPs generation through catalysis, oxidation and reduction [3, 4]. In cast iron tubes, PbO_2 and MnO_2 are widely detected as corrosion products. In thermodynamics, MnO_2 and PbO_2 can oxidize I^- to free iodine (I_2/HOI), and then react with the active part of organic matter to produce more toxic iodine disinfection by-products (I-DBPs). The interaction among PCPs, microorganisms and drinking water quality: PCPs changes the biochemical reaction process in pipe network through catalysis or oxidation, thus affecting water quality conditions; The stability of PCPs and physiological activities of microorganisms were affected by the change of water quality conditions. The physiological activities of microorganisms can directly affect water quality conditions and also change the composition structure of PCPs[3].

This project is from the National Natural Science Foundation of China Youth Project "study on the mechanism of microbial extracellular polymer transformation into disinfection by-products in water distribution system"(51808496), which is of great significance for ensuring the stability and safety of drinking water quality in the process of transmission and distribution.

1.2 Pipe network corrosion

After drinking water leaves the water plant and enters the pipe network, it will bring substances to the pipe network, such as particulate matter, microorganism, nutrient elements and so on. Due to the existence of these substances, the pipe network may be corroded to form pipe scale[5].Pipe network corrosion refers to the release of metal ions into water or the formation of pipe scale in the corrosion process of metal elements in pipe network materials. Pipe network corrosion can be

divided into overall corrosion and local corrosion. Overall corrosion generates more consistent corrosion scale, while local corrosion generates massive corrosion structure[6].Pipeline corrosion is a very complicated process, in the drinking water in the process of long distance transmission and can produce a series of reactions, such as nitration reaction, such as the formation of biofilms, these all can promote the corrosion of pipeline, and physical and chemical properties of pipe material, the biofilms on the pipe wall and pipe materials and the interaction between the water material will significantly affect the corrosion of pipeline[7-10].

Corrosion products are the end products of the interaction between rust (metal oxides) and sediment (particulate matter in water, etc.). After the reaction of different pipes, different corrosion substances will be generated. For example, lead oxides such as lead dioxide (PbO_2) are the main corrosion products in lead pipes [11, 12].In copper tubes, copper oxides such as copper oxide (CuO) and basic copper carbonate ($Cu_2(OH)_2CO_3$) are the main corrosion products[13, 14].In China's urban water supply pipe network system, the main materials of water supply pipe network are cast iron pipe, galvanized pipe, copper pipe, PVC pipe, etc[15].Secondly, corrosion products in pipe network directly affect the formation of DBPs through catalysis, oxidation and reduction, so the corrosion hazard of metal should be paid attention to.

1.2.1 Catalytic corrosion products

Due to its excellent corrosion resistance and resistance to microbial growth, copper is widely used in pipes of drinking water distribution systems around the world[14].Although copper is a relatively stable metal, it is prone to react in water containing oxygen electrolytes[16].In the past few decades, the corrosion products of copper tube are mainly CuO and ($Cu_2(OH)_2CO_3$).During copper corrosion, copper ions are released and form copper oxide on the tube wall[18].Too much copper released from copper pipes can cause water to turn blue-green and pose a health risk.Hu et al.[4] studied that the existence of two copper corrosion products (CuO and Cu^{2+}) can significantly catalyze the generation of DBPs under the condition of chlorine disinfection, and the catalytic effect is mainly achieved by promoting electrophilic substitution, oxidative decarboxylation and ring-opening reactions. Li et al. [18] studied the generation of Cu^{2+}, CuO and Cu_2O disinfection by-products in the disinfection process, and found that these three corrosion products all played a catalytic role in the generation of THMs in the two phases.

1.2.2 Oxidation corrosion products

Studies have reported that lead scale exists in the release of lead in drinking water, in which PbO_2 is not only an important constituent form but also a strong oxidant, oxidizing I^- in water to generate free iodine (I_2/HOI) and reacting with natural organic matter to generate I-DBPs [19].Lin et al. [20] reported that the oxidation of I^- is I_3^-, and the reaction equation is (1)−(3).In addition, TIM is generated under NOM. In addition, high levels of MnO_2 solids were first detected in the distribution system in the city of Tegucigalpa in 1998 and continue to cause occasional serious "blackwater" cooler problems in household taps, which have caused complaints [21]. Allard et al. [22] found that MnO_2 has oxidation capacity, which can oxidize I^- in water to form HOI/I_2. The oxidation rate of iodide decreases with the increase of pH value, and the H^+ reaction order is 2.3.

$$PbO_2 + 2I^- + 4H^+ \rightarrow Pb^{2+} + I_2 + 2H_2O \tag{1}$$

$$I_2 + H_2O \rightleftharpoons I^- + HOI + H^+ \tag{2}$$

$$I_2 + I^- \rightleftharpoons I_3^- \tag{3}$$

1.2.3 Reduced corrosion products

Cast iron pipe is widely used because of low cost, corrosion resistance, suitable for buried laying and so on, and it is also the most widely used pipe in our country. However, long-term use of iron pipe will produce metal corrosion products, and reduced corrosion products are mainly concentrated in cast iron pipe network. Studies have found that the corrosion substances of iron pipe are mainly composed of α-FeOOH, γ-FeOOH, Fe_3O_4, γ-Fe_2O_3, $5Fe_2O_3·9H_2O$, $FeCO_3$, $Fe(OH)_2$, $Fe(OH)_3$, $CaCO_3$ and rust tumors (manganese, silicon, phosphorus, lead, etc.)[23, 24].Although zero-valent metals (i.e., iron, zinc and copper) can be used as potential reductants to reduce a variety of halogenated disinfection by-products and, according to previous studies, they can enhance the generation of DBPs or produce more toxic DBPs during water treatment[25].Chu et al.[26] found that zero-valent iron (ZVI) could reduce three chloramphenicol antibiotics to produce chloroacetamide and dichloroacetamide in the absence of disinfectants. Previous studies have reported that in the presence of ZVI, iodized X-ray contrast agents and iodate can also serve as

sources of iodine for I-DBPs and produce more toxic I-DBPs [27]. Galvanized pipe because of its low price, good performance, long life, etc., in the drinking water distribution system of pipes occupy a certain proportion. The corrosion products of galvanized pipe are mainly composed of ZnO, $Zn_4CO_3(OH)_6 \cdot H_2O$, $Zn_5(CO_3)_2(OH)_6$, etc. Wang et al. [28] found that Zn, $Zn(OH)_2$ and ZnO on the surface of galvanized pipe would all affect HAAs generation under reduction, and Zn had the greatest influence.

1.2.4 Generation path and method of PCPs

In China's water supply pipe system, cast iron pipe is the main, and there is also a certain amount of metal iron in other pipes. Therefore, taking cast iron pipes as an example, the generation path and method of PCPs are briefly introduced. Corrosion products of cast iron pipes mainly include iron hydroxide ($Fe(OH)_3$), goethite (α-FeOOH), fibroite (γ-FeOOH), hydroite ($5Fe_2O_3 \cdot 9H_2O$), magnetite (Fe_3O_4), siderite ($FeCO_3$), etc. [29-31]. Among them, α-FeOOH and Fe_3O_4 are relatively stable and are also the main products of corrosion of cast iron pipes. α-FeOOH contains only ferric iron and is not conductive, so it is very stable [32]. Fe_3O_4 is the final product of the further oxidation reaction of α-FeOOH and β-FeOOH with γ-FeOOH and $Fe(OH)_2$ under aerobic conditions [33].

The mechanism of iron corrosion reaction was observed according to Siderite model and Lytle iron-sulfur transformation model:

Siderite model [34]: After iron in cast iron pipe is corroded, Fe^{2+} will be generated and substances containing iron divalent components will dissolve in drinking water, which leads to the increase of iron content in water phase. Fe^{2+} can react with CO_3^{2-} to form $FeCO_3$, which can then be further reacted to form α-FeOOH and Fe_3O_4. As follows:

Stage 1:

$$Fe \rightarrow Fe^{2+} + 2e^- \tag{1-1}$$

$$0.5O_2 + H_2O + 2e^- \rightarrow 2OH^- \tag{1-2}$$

$$HCO_3^- + OH^- \rightarrow CO_3^{2-} + H_2O \tag{1-3}$$

Stage 2:

$$Ca^{2+} + CO_3^- \rightarrow CaCO_3 \tag{1-4}$$

$$Fe^{2+} + CO_3^- \rightarrow FeCO_3 \tag{1-5}$$

$$2Fe^{2+} + 0.5O_2 + 4OH^- \rightarrow 2\alpha\text{-FeOOH(s)} + H_2O \tag{1-6}$$

Stage 3:

$$2FeCO_3(s) + 0.5O_2 + H_2O \rightarrow 2\alpha\text{-FeOOH(s)} + 2CO_2 \tag{1-7}$$

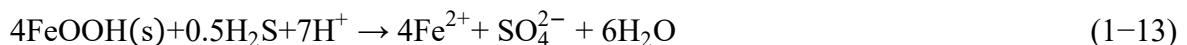$$3FeCO_3(s) + 0.5O_2 \rightarrow Fe_3O_4(s) + 3CO_2 \tag{1-8}$$

Lytle iron-sulfur transformation model [35]: Sulfate-reducing bacteria in the corroded material of pipe network can reduce sulfates to sulfide by using organic matter and hydrogen in anaerobic environment. Sulfide can reduce FeOOH and release Fe^{2+} into the water. As follows:

Stage 1：

$$Fe \rightarrow Fe^{2+} + 2e^- \tag{1-9}$$

$$SO_4^{2-} + 4H_2 \rightarrow S^{2-} + 4H_2O \tag{1-10}$$

$$Fe^{2+} + S \rightarrow FeS \tag{1-11}$$

Stage 2：

$$FeOOH(s) + H_2S + 4H^+ \rightarrow 2Fe^{2+} + S^0 + 4H_2O \tag{1-12}$$

$$4FeOOH(s) + 0.5H_2S + 7H^+ \rightarrow 4Fe^{2+} + SO_4^{2-} + 6H_2O \tag{1-13}$$

More research is needed on the corrosion process in water supply networks because no single type of pipe is made of a single material or metal. Take cast iron pipe as an example, it contains a small amount of manganese metal and copper metal and other metal elements, and these metal elements may promote or inhibit the corrosion of iron pipe through electron transfer or competition. In addition, the water quality parameters of the pipe network, such as pH, dissolved oxygen, alkalinity, inorganic ions, will also affect the corrosion of cast iron pipe.

pH：Iron corrosion products are usually released into the water as Fe^{2+} or attached to the surface of the pipe network as sediments. According to the galvanic corrosion principle, the iron corrosion reaction decreases with the increase of pH. Some studies show that the increase of pH will promote

iron corrosion reaction, lead to uneven corrosion phenomenon, and promote the release of iron corrosion products into the water phase [36, 37].

Dissolved oxygen: Although iron corrosion reaction can occur in the absence of oxygen [38], the existence of dissolved oxygen (DO) can significantly accelerate iron corrosion reaction.DO is the main electron acceptor of iron corrosion reaction, so the higher the concentration of DO, the faster the iron corrosion reaction. In addition, DO can further oxidize the generated Fe^{2+} into ferric, which can cover the surface of the iron tube, thus inhibiting the further corrosion of the iron tube. Therefore, according to the different water quality conditions, the role of DO in iron corrosion reaction will be different.

Alkalinity: The increase of alkalinity can limit iron corrosion from two aspects [39] : On the one hand, CO_3^{2-} in water reacts with Ca^{2+} and Mg^{2+} to form $CaCO_3$ and $MgCO_3$, which will deposit on the surface of iron pipe and block the contact path between DO in water and iron pipe, thus limiting iron corrosion; On the other hand, the increase of CO_3^- concentration in water is conducive to the formation of insoluble $FeCO_3$, which is then oxidized to form α-FeOOH and Fe_3O_4 to cover the surface of iron tubes, thus limiting the corrosion of iron.

Inorganic ions: SO_4^{2-} and Cl^- are the main anions in water. Shi and Taylor[40] found that high concentration of SO_4^{2-} (124−237 mg L^{-1}) could lead to the release of high concentration of Fe^{2+}, and similar studies showed that high concentration of Cl^- (100 mg L^{-1}) could increase the release of Fe^{2+} [41, 42].This is because the existence of these anions can improve the conductivity of water and promote iron corrosion reaction on the one hand; on the other hand, they can react with the released Fe^{2+} to form complexes and further promote iron corrosion reaction.

1.3 Reactive precursor in pipe network

Drinking water pipe network system is the last link to provide users with healthy drinking water, but also an essential step. However, biological processes may occur during drinking water distribution, such as natural organic matter in water bodies, formation and separation of biofilms, microbial growth, and formation of loose sediments. These processes will lead to deterioration of water quality during distribution. When these biological substances are used as reaction precursors, they will react with metal corrosives in the pipe network, thus generating disinfection by-products

and endangering the health of users [5].Therefore, it is necessary to understand the structure and properties of microorganisms in pipe networks so that effective strategies can be developed to ensure consumer water safety.

1.3.1 Humus

Natural organic matter (NOM) is a complex mixture of organic compounds that interact with many inorganic and organic pollutants and can reduce the toxicity of some chemical pollutants in water [43, 44].At the same time, NOM is also an important precursor of disinfection by-products (DBPs) [45].It is well known that the production of DBPs depends on the concentration of NOM, and the concentration of NOM depends primarily on the primary contributor of NOM, but there are many other factors, such as NOM composition and water treatment methods [46].

Humus (HS), an important component of NOM, is a heterogeneous multifunctional polymer synthesized by decomposition of plant and animal tissues or chemical and biological processes. Among natural organic components, HS represents the most extensive natural organic carbon in the biosphere and is the most stable organic component in soil, sediment and water [47]. HS typically accounts for a third or more of dissolved organic carbon (DOC) in natural water bodies. In addition, the properties and functions of HS also play an important role in natural water systems. In particular, the polymer molecular structure of HS has a significant influence on the formation of DBPs during the reaction with disinfectants [48].Therefore, while studying DBPs, it is also very important to study the molecular structure of HS.

Humic acid (HA) is one of the most important components of HS. The HA study is fascinating because of the many physicochemical processes they have discovered that play a crucial role in ecosystems around the world. Their research fields are very wide and have very important research significance for the environmental processes of land, ocean and river [49, 50]. The origins of HA in soil and water have been around for decades. HA is a kind of macromolecular mixture with complex composition and its structure is not specific. Because the structure of HA will change with climate and environment, it is very difficult to identify its structure. However, the composition of HA is non-specific, so the elemental composition of HA mainly includes carbon, hydrogen, oxygen, nitrogen and a small amount of sulfur, phosphorus and other elements. Structurally, in previous

studies, the molecular weight of HA ranged from thousands to hundreds of thousands of Daltons. In complex systems, biological structures with smaller molecular weight formed complex supramolecular structures interacting with hydrophobicity through hydrogen bonding [51-54]. In addition, both hydrophobic and hydrophilic parts exist in HA supramolecular structure. The hydrophobic part is mainly composed of hydrocarbon chains from relatively unchanging segments of the plant polymer, while the hydrophilic part is mainly composed of ionic groups (such as carboxylic acids) and non-ionic polar parts, such as phenols, alcohols, aldehydes, ketones, amides and amines. These characteristics indicate that HA has amphiphilic properties and can act as a natural surfactant [57].

1.3.2 Biofilm

In DWDS, more than 90% of biomass exists in microbial colonies, which are called biofilms and grow on the walls of water supply pipes. Only about 5% of biomass exists free in water. Biofilms are communities of bacteria that adhere to each other's surfaces, including microbial communities, flocs, and communities in the pore spaces of porous media.

Mature biofilms mainly include fungi, bacteria, invertebrates and protozoa, among which the microbial community is mainly composed of eukaryotes and bacteria, and about 90% of the bacterial community is composed of denatured bacteria, Bacteroidetes and actinomycetes. Eukaryotes are mainly amoeba [56-58].The existence of amoeba can provide a place for the growth and proliferation of *AvianTuberculosis* and *Legionella pneumophila* in biofilms [59].According to the pipe network, biofilm microbial community composition will also be different, for example, the biofilm composition of cast iron tube is mainly cocci, while polyethylene (PE) tube is mainly bacillus.

1.3.2.1 Extracellular polymeric substances (EPS)

In most biofilms, the substrate makes up more than 90% of the mass, and the microorganism itself does not make up as much as 10%. These matrices are extracellular substances produced by the microbes themselves and are called EPS. In previous studies, the existence of EPS was often ignored, but EPS is an inevitable secretion in the process of biofilm formation. The existence of EPS not only provides a stable environment for the formation of biofilms, but also is closely related

to the physical and chemical properties of microbial aggregates (structure, surface charge, flocculation, sedimentation and adsorption capacity) [60].In addition, EPS binds with cells through interaction and forms a water-bearing network structure, which can not only protect cells from dehydration but also resist the damage of toxic substances [61].In the case of nutrient deficiency, EPS can not only serve as a carbon source [62], but also accelerate the formation of microbial aggregates by tightly binding cells [63].

The main components of EPS are protein, polysaccharide, nucleic acid and lipids. It has previously been reported that EPS is a amphoteric group (hydrophilic and hydrophobic group), and its ratio is related to the composition of EPS [64]. In addition, the combination of EPS with the active part of organic matter mainly depends on the hydrophobic part of EPS [65]. Jorand et al. [66] used resin to separate EPS groups and found that about 7% of the components were hydrophobic groups and mainly composed of proteins. The hydrophilic group is mainly composed of carbohydrates. Further analysis of the properties of amino acids and monosaccharide groups in EPS shows that about 25% of amino acids are negatively charged and about 24% are hydrophobic [67].In addition, EPS consists of non-polar groups (e.g., aliphatic compounds, aromatic compounds, and hydrophobic regions in carbohydrates) and charged groups (e.g., carboxyl, phosphate, sulfhydryl, phenolic, and hydroxyl groups) [68].The non-polar groups of EPS have the ability to compound with heavy metals [69, 70], and the charged groups can complex with heavy metals [71-73].It is known that EPS has strong binding ability with heavy metals, and the adsorption follows Langmuir or Freundlich equation [70, 74, 75].Moreover, soluble EPS has a stronger adsorption capacity for heavy metals than EPS combined with sludge [76].In summary, the hydrophilicity and hydrophobicity of EPS may significantly affect the nature and structure of EPS [77], which also proves the importance of the site of EPS when adsorbing organic pollutants.

EPS can also form a large number of DBPs. In addition, according to the characteristics introduced above, the composition and structure of EPS significantly affect the formation and morphology of DBPs [78-80]. For example, n-DBPs formed by biofilms are related to amino acids containing unsaturated organic carbon or conjugated bonds in r-groups. Li et al. [81] previously reported that nitrogen components (tryptophan substances) in biofilms can promote DBPs formation compared with other detected components in EPS. Xu et al. [82] compared the effects of EPS on

chlorine and monochloramine disinfection, and found that EPS can both act as a consumer of disinfectants (for chlorine inactivation) and limit the entry of reaction sites on cell membranes (for monochloramine inactivation). Wang et al. [83] studied the effect of biofilms on DBPs generation and attenuation during chlorine (Cl_2) or monochloramine (NH_2Cl) disinfection in pipe network. It was found that DBPs concentration increased sharply when Cl_2 residue reached 2 mg L^{-1}. For NH2Cl disinfection, the content of DBPs is low, and for different residues of NH_2Cl, the formation difference of DBPs is very small.

1.3.2.2 Formation Mechanism of Biofilm

Biofilm generation can be divided into the following five stages: reversible microbial adhesion stage, irreversible microbial adhesion stage, surface community generation stage, biofilm emergence and maturity stage, and biofilm shedding and diffusion stage [62,84,85]. As shown in Figure 1.1:

(1) Microbial reversible adhesion stage: in this stage, microorganisms use their extracellular organelles and various proteins to sense and attach to the surface of the medium (tube wall). Microorganisms immerse themselves in a fluid or matrix containing macromolecules (e.g., proteins, humic acids, etc.) and electrolytes. Soluble components adhere to the surface and are reshaped by matrix proteins and cell-secreted DNA. In this stage, microorganisms adhere to the surface of the medium mainly through van der Waals force, electrostatic force and other physical and chemical effects, and the impact of water flow may make these microorganisms that have adhered to the medium desorbed, that is, they are still in an unstable reversible adhesion state.

(2) Microbial irreversible adhesion stage: after the reversible adhesion stage, microorganisms secrete EPS.EPS has a bonding effect and can make microbes adhere closely to the surface of the carrier, so that the adhesion becomes more stable and irreversible. The irreversible adhesion stage is the key stage for the development of biofilms. These microorganisms that can withstand hydraulic shock will gradually form biofilms with complex structure and complete function.

(3) Surface community formation stage: the microorganisms adhering to the surface of the medium proliferate and grow continuously, forming microbial community, which is the initial stage of biofilm formation. In this process, because there is no competition for living space and nutrition

among the microorganisms in the biofilm, the growth and proliferation rate of microorganisms is fast, and the generated microbiome will uniformly cover the surface of the medium.

(4) Biofilm emergence and maturation stage：with the proliferation of microorganisms and the accumulation of EPS, the microbial community gradually generates mature biofilms. In this process, the adhesion rate of microorganisms exceeds the desorption rate, so the structure of the biofilm is gradually complex, and the biomass in the biofilm keeps accumulating.

(5) Biofilm shedding and diffusion stage: when the biofilm grows to a certain thickness, the diffusion of oxygen and nutrients necessary for survival from the outer layer to the inner layer is blocked, which makes the microorganisms at the bottom of the biofilm unable to replenish in time and die, leading to the mass falling off of the biofilm. After shedding, some cells in the biofilm will diffuse into the water and reattach to the surface of other media to generate new biofilms, which is crucial for the propagation and self-renewal of biofilms.
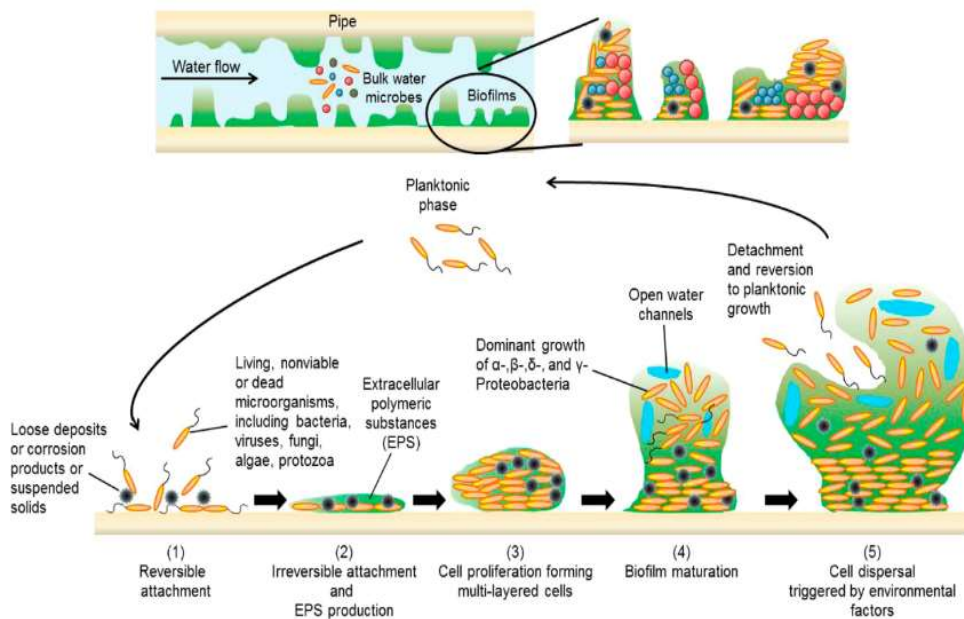
Fig 1.1 The process of biofilm formation in drinking water supply systems[86]

1.3.2.3 Influencing Factors of Biofilm

Biofilm community succession in DWDS is a very complex process, in which a variety of factors, such as nutrients, water temperature, pipe material, disinfectant dosage, etc., can affect the formation and shedding of biofilms to varying degrees.

(1) Nutrients: most of the microorganisms in DWDS are heterotrophic bacteria, which need to consume organic matter for growth and reproduction and other life activities. Organic matter in pipe network is one of the main factors limiting the growth and proliferation of microorganisms. assimilable organic carbon (AOC) and biodegradable dissolved organic carbon (BDOC) are usually used to measure the impact of organic carbon on microbial growth [87]. At the same time, phosphorus and nitrogen in the pipe network also play an extremely important role in the growth and reproduction of microorganisms. Phosphorus is an irreplaceable element in the metabolic activities of biological cells, for example, it is used to produce adenosine triphosphate (ATP), a high-energy compound. Nitrogen is a necessary component element of genetic material and protein. Meanwhile, the autotrophic nitrifying bacteria or nitrifying bacteria in biofilms use nitrogen as energy to synthesize biomass and carry out life activities.

(2) Water temperature: drinking water distribution pipes, although usually buried underground, are still subject to temperature changes, especially in countries and regions with distinct seasons. Changes in temperature can alter the behavior and physiological activity of microorganisms by affecting their internal mechanisms. For example, temperature can affect gene expression, which may affect the ability of microorganisms to secrete EPS and change the hydrophobicity of their cell surface [88, 89].Generally speaking, microorganisms cannot generate more biofilms in a lower temperature environment, which is caused by the delayed time of microbial cell proliferation and the slow growth rate at sub-room temperature [90].Although it is impractical to change the temperature in the water supply network, it is necessary to deeply understand the influence of water temperature on the physicochemical reaction of microorganisms in the water supply network, which can provide relevant scientific basis for the control and prevention policies of the water supply department.

(3) Pipe material: drinking water is transported to users through pipe network, and a series of different pipes are used for drinking water distribution. Generally, the water supply pipe network uses metal pipes, such as cast iron pipes and copper pipes, or polymer pipes, such as polyvinyl chloride (PVC) and PE pipes. Different pipe materials have different effects on biofilm in pipe network. For example, in plastic pipes, the polymer additives will leach or degrade to generate some by-products, which may become carbon sources for the microorganisms in the pipe network and

promote the formation and growth of biofilms in the pipe network [91, 92]. Those that are prone to corrosion have a more significant effect on the growth and diversity of biofilms. For example, the corroded surface of corroded iron tubes can protect the biofilm from physical or chemical interference (or both) and provide a larger surface area for the biofilm to attach and multiply. The corrosion products can also react with disinfectants to promote the decay of disinfectants and thus protect the biofilm [93, 97].

(4) disinfectant dosage: the national drinking water sanitation standard stipulates that the residual chlorine content in the end of water supply network shall not be less than 0.05 mg L^{-1}.In general, the amount of biofilm generation in pipe network decreases with the increase of disinfectant dose, but the formation of biofilm cannot be completely restricted even with residual chlorine concentration as high as 5 mg L^{-1}.In addition, different disinfectants have different inhibitory abilities on biofilm, such as chloramine and free chlorine. Although the bactericidal ability of free chlorine is stronger than that of chloramine, chloramine shows stronger inhibitory ability on biofilm formation. This is because free chlorine has stronger reactivity, and it is often consumed in a large amount within the biofilm, while chloramine, with weak reactivity, is more likely to diffuse to the bottom of the biofilm and inactivate the microorganisms at the bottom, thus inhibiting the formation of the biofilm.

1.4 Disinfection byproducts

Disinfection is an essential part of drinking water treatment process and an important step to ensure drinking water clean and safe. Since the birth of chlorine disinfection more than 100 years ago, it has been widely used because of its advantages of low cost, convenient operation, good sterilization effect, and ability to inhibit microbial contamination. Nowadays, it is also the most commonly used disinfection method in waterworks at home and abroad. In the disinfection efficacy dosing guidelines established by the World Health Organization, they recommend a minimum residual chlorine content of 0.2 mg L^{-1} and a maximum of 5.0 mg L^{-1}[95].According to China's Drinking Water Hygiene Standards (GB5749−2006), a certain amount of disinfectant must be kept at the end of pipe network to prevent secondary contamination by microorganisms in the pipe network. For example, when chlorine dioxide is used as a disinfectant, the content of pipe network

end should not be less than 0.02 mg L^{-1} (Table 1.1)

Table 1.1 The indexes of disinfectants in drinking water

Type of disinfectant	Contact time（min）	Finished water limit（mg L^{-1}）	Finished water allowance（mg L^{-1}）	Network end allowance（mg L^{-1}）
Chlorine	≥ 30	4	≥ 0.3	≥ 0.05
Chloramine	≥ 120	3	≥ 0.5	≥ 0.05
ClO$_2$	≥ 30	0.8	≥ 0.1	≥ 0.02
O$_3$	≥ 12	0.3		≥ 0.02

While drinking water disinfection has brought convenience to common people's life, an unexpected result—DBPs discovery. Disinfectants (e.g., free chlorine) react with organic substances (e.g., natural organic matter (NOM)) in water to produce DBPs, which are harmful to human health. Since 1974, when Dutch scientist Rook[96] discovered the first DBPs—THMs in us water plants, more than 700 disinfection byproducts have been detected, but this still probably accounts for only about 50% of the total disinfection byproducts in water [97].DBPs generated by different raw water quality, different disinfectants and different disinfection methods are different. The organic by-products produced by chlorination disinfection are mainly THMs, HAAs and HANs. If the raw water contains Bromine ions (Br$^-$) or iodide ions (I$^-$), brominated byproducts (Br−DBPs) or I−DBPs will also be generated. When chloramine is used as a disinfectant, some new and more toxic N−DBPs can be generated, such as Cyanogen chloride (CNCl), HAcAms, halogenated nitromethane (HNMs), etc. [98]. At present, the types of disinfection by-products commonly found in drinking water are shown in Table 1.2.

Table 1.2 Common disinfection byproducts in drinking water

Species	Chemical formula
THMs	$CHCl_3$、$CHBrCl_2$、$CHBr_2Cl$、$CHBr_3$
HAAs	$ClCH_2COOH$、$C_2H_2Cl_2O_2$、$C_2HCl_3O_2$、$C_2H_3O_2Br$、$C_2H_2Br_2O_2$、$C_2HBr_3O_2$、$C_2HBrCl_2O_2$、$C_2HBr_2ClO_2$、$C_2H_2BrClO_2$
HANs	C_2H_2ClN、C_2HCl_2N、C_2Cl_3N、C_2H_2BrN、C_2HBr_2N、C_2Br_3N、C_2BrCl_2N、C_2Br_2ClN、$C_2HBrClN$
HAcAms	C_2H_4ClNO、$C_2H_3Cl_2NO$、$C_2H_2Cl_3NO$、C_2H_4BrNO、$C_2H_3Br_2NO$、$C_2H_2Br_3NO$、$C_2H_2BrCl_2NO$、$C_2H_2Br_2ClNO$、$C_2H_3BrClNO$
HCNs	$CNCl$、HBr
HNMs	CH_2ClNO_2、$CHCl_2NO_2$、CCl_3NO_2、CH_2BrNO_2、$CHBr_2NO_2$、CBr_3NO_2、$CBrCl_2NO_2$、CNO_2ClBr_2、$CHBrClNO_2$

1.4.1 Iodine disinfection byproducts

Disinfection of drinking water is one of the most successful technological inventions of the last century. According to statistics, in the United States, its introduction has reduced the incidence of cholera by 90%, typhoid by 80%, and amebic dysentery by 50% [99]. Chemical disinfectants are effective in killing harmful microorganisms in drinking water, but they are also strong oxidants that oxidize most natural organic and man-made pollutants to form bromides and iodides.

Scientists first realized the existence of DBPs in the early 1970s. In 1974, Rook et al. [96] reported the discovery of the first disinfection by-products in chlorinated drinking water: chloroform (CCl_3) and other trihalomethanes (THMs). In 1976, the US Environmental Protection Agency (US EPA) published the results of a national survey showing that CCl_3 and THMs are ubiquitous in chlorinated drinking water. In the same year, the results published by the US National

Cancer Institute showed that CCl_3 was carcinogenic [99]. In addition, in late 1970, Loper et al. [100] found mutagenicity of organic extracts from drinking water in salmonella mutagenesis tests. As a result of these findings, the existence of DBPs is gradually recognized as an important public health safety problem.

Since the detection of CCl_3 in 1974, more than 700 DBPs have been chemically characterized. The discovery of DBPs has forced regulators and the drinking water industry to strike a balance between the risks associated with pathogen exposure and those associated with toxic DBPs. Although a lot of work has been done on the study of disinfection by-products, the discovered DBPs only account for about 50% of the total amount [101]. DBPs generated by different raw water quality, disinfectants and disinfection methods are different. If the raw water contains bromine ion (Br^-) or iodide ion (I^-), bromine disinfection by-products (Br-DBPs) and iodide disinfection by-products (I-DBPs) will also be generated [98].

In 2000, Cancho et al. [102] synthesized five iodimethanes (I-THMs) and quantitatively analyzed them in chlorinated drinking water in Spain. I-thms is associated with taste and odor problems in drinking water, and its minimum threshold level is 0.02-0.5 μg L^{-1}[103].Despite the lack of evidence of toxicity from intracellular tests and molecular epidemiological studies of I-DBPs, extracellular toxicity studies of 103 DBPs showed that I-DBPs were more cytotoxic and genotoxic than bromine and chlorine disinfection byproducts [104-108].Since its discovery, I-DBPs have been widely detected in drinking water, so more and more attention has been paid to the study of more toxic I-DBPs in recent years. At present, types of iodine disinfection by-products commonly found in drinking water are shown in Table 1.3.

Table 1.3 Common iodine disinfection byproducts in drinking water

Species	Chemical formula
I-THMs	$CHCl_2I$、$CHBrClI$、$CHBr_2I$、$CHClI_2$、$CHBrI_2$、CHI_3、CH_2ClI、CCl_3I
I-HAAs	$C_2H_3IO_2$、$C_2H_2BrIO_2$、$C_2H_2ClIO_2$、$C_2H_2I_2O_2$、$C_2HI_3O_2$
I-HANs	C_2H_2IN、C_2HClIN
I-HAcAms	C_2H_3ClINO、$C_2H_3I_2NO$、C_2H_4INO、C_2H_3BrINO
I-HAs	ICH_2CHO、C_6H_5IO

1.4.2 Hazards of disinfection byproducts

The harms of disinfection by-products mainly include carcinogenesis, teratogenesis, mutagenesis, etc. Meanwhile, most of the identified DBPs are cytotoxic and genotoxic [109-111],and these DBPs can enter the human body through showers, drinking water and breathing and be rapidly absorbed [112-115] .The thiogenic effects and health threats caused by toxicity of DBPs have attracted extensive attention and research from the government and scientists.

1.4.2.1 Hazards of common DBPs

(1) THMs: THMs is the DBPs with the largest amount generated in the chlorination disinfection process of drinking water. Studies have shown that THMs has strong carcinogenic effect. Gottlieb et al. [116] found that the concentration of THMs in drinking water was correlated with the occurrence of bladder cancer, rectal cancer and other cancers. Meanwhile, he found that chlorinated surface water could significantly increase the probability of cancer occurrence by comparing cases and mortality. In addition, epidemiological data showed that when pregnant women drank drinking water containing chloroform (CF) at a concentration of more than 10 PPB for a long time, the risk add-factor for fetal underweight was 1.3, and that for premature delivery was 0.8−1.2[117] .According to the report on carcinogenic risk of DBPs released by American Water Works Association (AWWA), the physical and chemical characteristics and carcinogenic risk of

THMs were sorted out (Table 1.4).

Table 1.4 Physical chemical characters and caner hazard

THMs	Molecular weight	Boiling point（℃）	Unit carcinogenic risk （$\times 10^{-6}$）
$CHCl_3$	119	61	0.056
$BrCHCl_2$	164	90	0.35
$CHBr_2Cl$	208	120	−
$CHBr_3$	253	151	0.10

(2) HAAs: according to AWWA's cancer risk report on DBPs, the cancer risk of Trichloroacetic acid (TCAA) is about 100 times higher than that of CF. At the same time, HAAs is non-volatile and does not evaporate after boiling like THMs, so it poses a greater health threat than THMs. In animal experiments, scientists have found that HAAs has multiple toxic effects, affecting animal reproductive development, resulting in slow and defective embryo development, and a high risk of cancer. Herren et al. [118] found that dichloroacetic acid (DCAA) and TCAA can cause liver tumors in rats and mice. Law et al. [119] also obtained similar results with Japanese killifish as experimental object, and they found that short-term exposure of Japanese killifish to DCAA would cause changes in liver cells and induce tumor formation. Yang Yuan et al. [120] found through DNA loss experiments that DCAA could lead to DNA loss of liver cells in both in vitro and in vivo experiments, and the loss degree increased with the increasing number of experiments.

(3) HANs: with the discovery of C−DBPs in THMs and HAAs, researchers began to try new disinfection methods to avoid the generation of DBPs, such as using chloramine as a disinfectant to replace chlorine disinfection. However, when chloramine was used as a disinfectant, although the production of C−DBPs decreased, the production of N−DBPs increased significantly. In general, the

production of N−DBPs is lower than that of C−DBPs, but its triple effect and toxicity are stronger [121]. HANs was the first discovered N−DBPs. Scientists found that the cytotoxicity and genotoxicity of HANs were nearly 100 and 10 times higher than HAAs in Chinese hamster ovarian cell toxicology experiments [105,122]. In addition, HANs has embryonic toxicity, and it was found in teratogenic experiments in young mice that HANs would make the growth and development of young mice stop, seriously affecting their survival rate [97].

1.4.2.2 Hazards of Iodine Disinfection Byproducts

The formation of disinfection byproducts has teratogenic, carcinogenic and mutagenic risks to human health. Concentrations of I-DBPs in drinking water range from microgram to nanogram. The presence of iodide methane and iodide acetic acid in drinking water was detected in 23 cities in Canada and the United States, respectively. The mean concentrations of iodide methane and iodide acetic acid in 12 networks were 10.2 μg L^{-1} and 1.7 μg L^{-1}, respectively, although the concentration of I-DBPs was lower than that of chlorination and bromination disinfection byproducts. But they are much more cytotoxic and genotoxic. In daily life, these I-DBPs enter the human body through drinking water and daily water and are rapidly absorbed by the human body [112,115]. Therefore, I-DBPs is getting more and more attention. The following is a brief description of the common hazards of I-DBPs:

(1) I-THMs: at present, I-THMS is the most detected I-DBPs in the detection process of drinking water. The results showed that I$^-$ and Br$^-$ in source water significantly affected the formation of I-DBPs. THMs was found to increase sister chromatids of mouse cells and human lymphocytes in vivo. Congenital malformations such as cleft lip and palate, damage of nervous system, and cancers such as breast cancer, bladder cancer and colon cancer are all related to THMs concentration in drinking water [123].

(2) I-HAAs: Their concentrations are generally lower than I-THMs, ranging from micrograms to nanograms, but they are not volatile and cannot be removed by boiling in drinking water, and I-HAAs is significantly more toxic than chlorine and bromoacetic acid, making I-HAAs a greater health threat. Plewa et al. [104] demonstrated that iodoacetic acid (IAA) was more mutagenic, genotoxic and cytotoxic than bromoacetic acid or chloroacetic acid in salmonella typhimurium and

mammalian cells. Wei et al. [124] studied the generation of IAA and iodoform (IF) in drinking water in Shanghai and found that IAA was more cytotoxic to mammalian cells and low concentration of IAA could induce malignant transformation of NIH_3T_3 mouse cell lines.

(3) I-HANs: The nitrogenous disinfection byproducts of I-HANs and I-HAcAms are constantly being discovered, among which I-HANs is the first discovered N−DBPs. Previous studies have found that HANs is 100 and 10 times more cytotoxic and genotoxic than HAAs, respectively [105,122]. In addition, HANs also has embryonic toxicity, resulting in growth retardation and malformed development in the growth and development of mouse pups [101].

(4) I-HAcAms: Haloacetamide is a newly developed disinfection by-product of nitrogenous drinking water. Its chronic cytotoxicity and ability to induce genomic DNA damage in Chinese hamster ovary cells were analyzed. The cytotoxicity and genotoxicity of C_2H_4ClNO, $C_2H_3Cl_2NO$, $C_2H_2Cl_3NO$, $C_2H_3BrClNO$, $C_2H_2BrCl_2NO$, C_2H_3ClINO, $C_2H_2Br_2ClNO$, C_2H_4BrNO, $C_2H_3Br_2NO$, $C_2H_2Br_3NO$, C_2H_3BrINO, C_2H_4INO and $C_2H_3I_2NO$ have been studied in previous studies. Among the 13 kinds of haloacetamide, diiodoacetamide has the highest cytotoxicity, iodic haloacetamide has the highest cytotoxicity, and chloroacetamide has the lowest cytotoxicity. The genotoxicity of tribromoacetamide was the highest, followed by diiodoacetamide and trichloroacetamide was the lowest. Thus, the cytotoxicity and genotoxicity were determined by the tendency of halogen, and followed the order I > Br > Cl.

1.4.3 Generation of disinfection byproducts in pipe network

After drinking water leaves the waterworks, a certain amount of disinfectant is usually added to prevent secondary contamination in the pipe network. These disinfectants can produce DBPs through a series of side reactions such as substitution, decarboxylation and hydrolysis with NOMs that are difficult to remove in water. For example, organic compounds with methyl ketone functional groups will form CF after enolization, chlorine substitution, and hydrolysis (Fig.1.2). However, due to the complex environment and the interaction between substances in the pipe network, the generation mechanism and pathway of DBPs in the pipe network are more complicated. Corrosion products of pipe network play a decisive role in the generation of disinfection by-products. As shown in Figure 1.3, corrosion products can not only play a catalytic

role, but also generate free radicals through oxidation, which will react with organic matter. Latchley et al. [125] found that corrosion pipe network can promote the generation of chloroform by promoting catalysis (enolization).Zhang and Andrews[126,127] reported that HAAs and nitroso dimethylanilines (NDMAs) increased significantly in the presence of Cu^{2+}.Lin et al. found that I^- can be oxidized by PbO_2 to form I_3^-, and I_3^- can react with NOM to form iodoform (TIM).Allard et al. found in their study that manganese dioxide (MnO_2) has oxidation capacity, which can oxidize I^- in water to form HOI/I_2, and then react with natural organic matter in water to produce more toxic I-DBPs and IO_3^-[20,128].
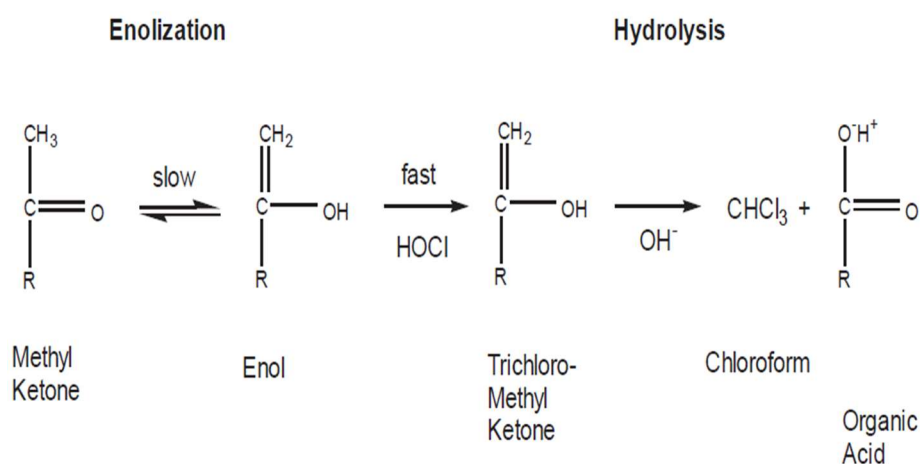
Fig 1.2 Chloroform formation from methyl ketone by the haloform reaction
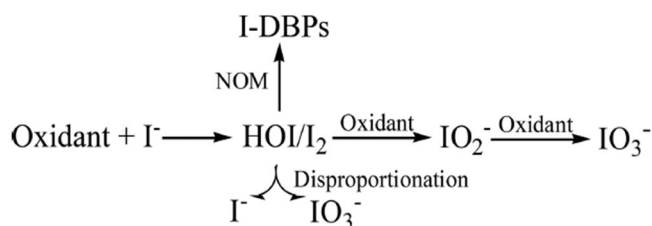
Figure 1.3 Formation pathways of I-DBPs during oxidation and disinfection

NOMs, which are widely present in DWDS, are not easy to be removed by common drinking water treatment technology [129], they can react with disinfectants as precursors to generate DBPs. In addition, other substances in the distribution system water can also be oxidized by disinfectants to form new DBPs. Under the action of residual chlorine, microorganisms themselves, secreted EPS

and metabolites of life activities in the pipe network can all become the precursors of DBPs. Meanwhile, because of their different components, higher concentration or more toxic DBPs may be generated. Wang et al. [130] found that when a biofilm dominated by Pseudomonas Aeruginosa interacts with residual chlorine, DBPs generated are rich in diversity and contain a large number of N-DBPs. This indicates that biofilms and other substances in the pipe network are also one of the important precursors of DBPs. In addition to NOMs, more attention and research should also be paid to other organics in the pipe network.

1.5 Research contents and innovations

1.5.1 Research contents

Drinking water safety is one of the basic conditions to guarantee people's life quality and health. Water supply pipe network is the key part connecting water plant and users. It is of great scientific and practical significance to ensure the clean and safe drinking water in water supply pipe network. This paper studies the generation and transformation mechanism of DBPs in the pipe network when EPS is used as the precursor, discusses the influence of different PCPs on DBPs generation, and evaluates the comprehensive effect of PCPs in the water supply pipe network system.

(1) The formation and transformation of DBPs were observed when EPS was used as precursor. The species and concentration of DBPs were analyzed by Gas chromatography (GC).

(2) The catalytic effect of two kinds of CCPs (CuO and Cu^{2+}) on DBPs formation of EPS under chlorination disinfection was studied. The influence of water quality factors such as pH and inorganic ion (Br^-) on CCPs catalysis was studied. Protein and polysaccharide components in EPS were separated and extracted as precursors for reaction, so as to analyze the influence of precursor components and structure on CCPs catalysis. Amino acids were used as model molecules to reasonably predict the catalytic mechanism of CCPs.

(3) In the $I^-/PbO_2/EPS$ system, the oxidation of PbO_2 generates I-DBPs. The effects of pH, PbO_2 dose and I^- concentration on I-DBPs production were studied. The effects of PbO_2 oxidation and I-DBPs production were studied when EPS protein components, polysaccharides and amino acids were used as precursors.

(4) In the I^-/MnO$_2$/EPS system, the oxidation of MnO$_2$ generates I-DBPs. The influence of pH, MnO$_2$ dose and I^- on I-DBPs formation was studied. Protein components of EPS, polysaccharides and amino acids were used as precursors to study the influence on MnO$_2$ oxidation and I-DBPs formation, as well as the control strategy for I-DBPs formation.

1.5.2 Innovations

Different from previous studies that focused on DBPs generation by NOM in DWDS, this paper focused on the generation and transformation of I-DBPs when EPS was used as the precursor under the catalytic or oxidative action of PCPs in DWDS, and elaborated the action pathways and mechanisms of different PCPs affecting EPS transformation and I-DBPs generation. The toxicity of EPS as precursor was studied. And control strategies to control I-DBPs generation when biofilms erupt.

Reference

[1]   Liao W.L. The Effect of Water-supply Pipeline Materials on Water Quality and Their Corrosion-prevention Measures [J]. Journal of Chongqing Technology and Business University (Natural Science Edition),2012, 29 (11):93-98.

[2]   Ruan L.H. The interaction between disinfectants and pipes and its influence on water quality [D]. Hunan University, 2014.

[3]   Lu P.P, Tong Z.G. Analysis of the Pipeline Material on Influence of Water Quality in the Water Distribution Network [J]. Journal of East China Jiaotong University, 2006, 23(04):27-29.

[4]   Hu J, Wang C, Shao B.J, et al. Enhanced formation of carbonaceous and nitrogenous disinfection byproducts from biofilm extracellular polymeric substances undercatalysis of copper corrosion products [J]. Science of the Total Environment, 2020, 723: 138–160.

[5]   Liu G, Verberk J.Q.J.C, Van Dijk J C. Bacteriology of drinking water distribution systems: an integral and multidimensional review [J]. Applied Microbiology and Biotechnology, 2013, 97(21): 9265-76.

[6]   Sarin P, Snoeyink VL, Bebee J, et al. Physico-chemical characteristics of corrosion scales in

old iron pipes [J]. Water Research, 2001, 35(12): 2961-9.

[7]   Camper A K. Involvement of humic substances in regrowth [J]. International Journal of Food Microbiology, 2004, 92(3): 355-64.

[8]   Schwartz T, Hoffmann S, Obst U. Formation of natural biofilms during chlorine dioxide and u.v. disinfection in a public drinking water distribution system [J]. Journal of Applied Microbiology, 2003, 95(3): 591-601.

[9]   Regan J M, Harrington G W, Baribeau H, et al. Diversity of nitrifying bacteria in full-scale chloraminated distribution systems [J]. Water Research, 2003, 37(1): 197-205.

[10]   Schwartz T, Hoffmann S, Obst U. Formation and bacterial composition of young, natural biofilms obtained from public bank-filtered drinking water systems [J]. Water Research, 1998, 32(9): 2787-97.

[11]   Lin Y-P, Valentine R L. Reduction of Lead Oxide (PbO2) and Release of Pb(II) in Mixtures of Natural Organic Matter, Free Chlorine and Monochloramine [J]. Environmental Science & Technology, 2009, 43(10): 3872-7.

[12]   Xie Y, Wang Y, Singhal V, et al. Effects of pH and Carbonate Concentration on Dissolution Rates of the Lead Corrosion Product PbO2 [J]. Environmental Science & Technology, 2010, 44(3): 1093-9.

[13]   Li B, Qu J, Liu H, et al. Effects of copper (II) and copper oxides on THMs formation in copper pipe [J]. Chemosphere, 2007, 68(11): 2153-60.

[14]   Feng Y, Teo W K, Siow K S, et al. The corrosion behaviour of copper in neutral tap water. Part I: Corrosion mechanisms [J]. Corrosion Science, 1996, 38(3): 369-85.

[15]   Xu B.J, An D.N. Water Treatment Theory and Technology [M]. BeiJing: China Architecture & Building Press, 1993.

[16]   Hukovic M.M., Babic R., Paic I. Copper corrosion at various pH values with and without the inhibitor [J]. Journal of Applied Electrochemistry, 2000, 30: 617–624.

[17]   Merkel T.H., Groß H.J., Werner W., et al. Copper corrosion by-product release in long-term stagnation experiments [J]. Water Research, 2002, 36: 1547–1555.

[18]   Li B, Qu J.H, Liu H.J, Lei P.J, Gu J.N. Study on catalytic effects of copper homogeneous

and heterogeneous system on chlorinated disinfection reaction [J]. Acta Scientiae Circumstantiae, 2007, (12):1962–1967.

[19]   Ding S.K., Deng Y., Bond T., et al. Disinfection byproduct formation during drinking water treatment and distribution: A review of unintended effects of engineering agents and materials [J]. Water Research, 2019, 160: 313−329.

[20]   Lin Y.P., Washburn M.P., Valentine R.L. Reduction of lead oxide (PbO2) by iodide and formation of iodoform in the PbO2/I−/NOM System [J]. Environmental Science & Technology, 2008, 42 (8): 2919–2924.

[21]   Cerrato J.M., Reyes L.P., Alvarado C.N., et al. Effect of PVC and iron materials on Mn(II) deposition in drinking water distribution systems [J]. Water Research, 2006, 40 (14): 2720–2726.

[22]   Allard S., von Gunten U., Sahli E., et al. Oxidation of iodide and iodine on birnessite (δ-MnO2) in the pH range 4–8 [J]. Water Research, 2009, 43 (14): 3417−3426.

[23]   Cook D.C. Spectroscopic identification of protective and non-protective corrosion coatings on steel structures in marine environments [J]. Corrosion Science, 2005, 47 (10): 2550–2570.

[24]   Benjamin M.M., Sontheimer H., Leroy P. Corrosion of iron and steel [J]. Denver, CO: AWWA Research Foundation, 1996, 2970.

[25]   Sarin P., Snoeyink V.L., Bebee J., et al. Iron release from corroded iron pipes in drinking water distribution systems: effect of dissolved oxygen [J]. Water Research, 2004, 38: 1259−1269.

[26]   Chu W.H., Ding S.K., Bond T., et al. Zero valent iron produces dichloroacetamide from chloramphenicol antibiotics in the absence of chlorine and chloramines [J]. Water Research, 2016, 104: 254−261.

[27]   Xia Y., Lin Y.L., Xu B., et al. Iodinated trihalomethane formation during chloramination of iodate-containing waters in the presence of zero valent iron [J]. Water Research, 2017, 124: 219−226.

[28]   Wang W. The Effect and Mechanism of Galvanized Pipe to Haloacetic Acids Transformation

in Drinking Water [D]. Zhejiang University, 2010.

[29]   Benson A S, Dietrich AM, Gallagher DL. Evaluation of Iron Release Models for Water Distribution Systems [J]. Critical Reviews in Environmental Science and Technology, 2012, 42(1): 44-97.

[30]   Sarin P, Snoeyink VL, Lytle DA, et al. Iron Corrosion Scales: Model for Scale Growth, Iron Release, and Colored Water Formation [J]. Journal of Environmental Engineering, 2004, 130(4): 364-73.

[31]   Peng CY, Korshin GV, Valentine RL, et al. Characterization of elemental and structural composition of corrosion scales and deposits formed in drinking water distribution systems [J]. Water Research, 2010, 44(15): 4570-80.

[32]   Cornell R M, Schwertmann U. The Iron Oxides: Structure, Properties, Reactions, Occurrences and Uses [M]. Wiley, 2003.

[33]   Ishikawa T, Kondo Y, Yasukawa A, et al. Formation of magnetite in the presence of ferric oxyhydroxides [J]. Corrosion Science, 1998, 40(7): 1239-51.

[34]   Sontheimer H, Kolle W, Snoeyink V L. The siderite model of the formation of corrosion-resistant scales [J]. Journal - AWWA, 1981, 73(11): 572-9.

[35]   Lytle D A, Gerke T L, Maynard D J B. Effect of bacterial sulfate reduction on iron-corrosion scales [J]. Journal - AWWA, 2005, 97(10): 109-20.

[36]   Iino T, Ito K, Wakai S, et al. Iron Corrosion Induced by Nonhydrogenotrophic Nitrate-Reducing & lt;span class = & quot;named-content genus-species & quot; id = & quot ; named-content-1 & quot ; & gt;Prolixibacter & lt ;/span & gt ; sp. Strain MIC1-1 [J]. Appl Environ Microbiol, 2015, 81(5): 1839.

[37]   Zhang Y, Griffin A, Edwards M. Nitrification in Premise Plumbing: Role of Phosphate, pH and Pipe Corrosion [J]. Environmental Science & Technology, 2008, 42(12): 4280-4.

[38]   Kuch A. Investigations of the reduction and re-oxidation kinetics of iron(III) oxide scales formed in waters [J]. Corrosion Science, 1988, 28(3): 221-31.

[39]   Mckernan S, Carter C B, Ricoult D, et al. High-Resolution Electron Microscopy of Olivine-Magnetite Interfaces [J]. MRS Proceedings, 2011, 159(407.

[40]   Shi B, Taylor J S. Iron and Copper Release in Drinking-Water Distribution Systems [J]. Journal of Environmental Health, 2007, 70(2): 29-36.

[41]   Lytle D A, Sarin P, Snoeyink V L. The effect of chloride and orthophosphate on the release of iron from a cast iron pipe section [J]. Journal of Water Supply: Research and Technology-Aqua, 2005, 54(5): 267-81.

[42]   Sarin P, Clement J A, Snoeyink V L, et al. Iron Release from corroded, unlined cast-iron pipe [J]. Journal - AWWA, 2003, 95(11): 85-96.

[43]   Cabaniss S.E., Shuman M.S. Copper binding by dissolved organic matter: I. Suwannee river fulvic acid equilibria [J]. Geochimica et Cosmochimica Acta, 1988, 52: 185–193.

[44]   Ma H.Z., Allen H.E., Yin Y.J. Characterization of isolated fractions of dissolved organic matter from natural waters and a wastewater effluent [J]. Water Research, 2001, 35 (4): 985–996.

[45]   Khan E., Babcock R.W., Suffet I.H., Stenstorm M.K. Biodegradable dissolved organic carbon for indication wastewater reclamation plant performance and treated wastewater quality [J]. Water Environ Research, 1998, 70: 1033–1040.

[46]   Kim H.C, Yu M.J. Characterization of natural organic matter in conventional water treatment processes for selection of treatment processes focused on DBPs control [J]. Water Research, 2005, 39 (19) : 4779–4789.

[47]   Kelleher B.P., Simpson A.J. Humic substances in soils: Are they really chemically distinct? [J]. Environmental Science & Technology, 2006, 40 (15): 4605–4611.

[48]   Salati S., Papa G., Adani F. Perspective on the use of humic acids from biomass as natural surfactants for industrial applications [J]. Biotechnology Advances, 2011, 29 (6): 913–922.

[49]   Senesi N., Loffredo E. The chemistry of soil organic matter [M]. 1999.

[50]   Wershaw R. Model for humus in soils and sediment [J]. Environmental Science & Technology, 1993, 27: 814–816.

[51]   Buurman P, van Lagen B, Piccolo A. Increase in stability against thermal oxidation of soil humic substances as a result of self association [J]. Organic Geochemistry, 2002, 33 (3): 367−381.

[52]   Piccolo A. The supramolecular structure of humic substances: A novel understanding of humus chemistry and implications in soil science [M]. Sparks D.L. Advances in Agronomy. 2002: 57–134.

[53]   Singh R.P., Gupta N., Singh A., et al. Toxicity of ionic and non-ionic surfactants to six microbes found in Agra, India. [J]. Bull Environ Contam Toxicol, 2002, 69: 265–270.

[54]   Sutton R., Sposito G. Molecular structure in soil humic substances: The new view [J]. Environmental Science & Technology, 2005, 39 (23) : 9009–9015.

[55]   Kleber M., Sollins P., Sutton R. A conceptual model of organo-mineral interactions in soils: self-assembly of organic molecular fragments into zonal structures on mineral surfaces [J]. Biogeochemistry, 2007, 85 (1): 9–24.

[56]   Revetta R P, Gomez-Alvarez V, Gerke T L, et al. Establishment and early succession of bacterial communities in monochloramine-treated drinking water biofilms [J]. FEMS Microbiology Ecology, 2013, 86(3): 404-14.

[57]   Liu R, Yu Z, Guo H, et al. Pyrosequencing analysis of eukaryotic and bacterial communities in faucet biofilms [J]. Science of The Total Environment, 2012, 435-436(124-31.

[58]   Hunt A P, Parry J D. The effect of substratum roughness and river flow rate on the development of a freshwater biofilm community [J]. Biofouling, 1998, 12(4): 287-303.

[59]   Siqueira V M, Oliveira H M B, Santos C, et al. Filamentous Fungi in Drinking Water, Particularly in Relation to Biofilm Formation [J]. International Journal of Environmental Research and Public Health, 2011, 8(2): 456-69.

[60]   Flemming H.C., Percival S.L., Walker J.T. Contamination potential of biofilms in water distribution systems [J]. Water Supply, 2002, 2 (1): 271–280.

[61]   Zhang X., Bishop P. Biodegradability of biofilm extracellular polymeric substances [J]. Chemosphere, 2003, 50: 63–69.

[62]   Sutherland I.W. The biofilm matrix – an immobilized but dynamic microbial environment [J]. Trends Microbiol, 2001, 9: 222–227.

[63]   Lux R., Li Y., Lu A., Shi W. Detailed threedimensional analysis of structural features of Myxococcus xanthus fruiting bodies using confocal laser scanning microscopy [J]. Biofilms,

2004, 1: 293–303.

[64]   Guo P.S., Han Q.Y., Xiao Y.L. Extracellular polymeric substances (EPS) of microbial aggregates in biological wastewater treatment systems: A review [J]. Biotechnology Advances, 2010: 882–894.

[65]   Spath R., Flemming H.C., Wuertz S. Sorption properties of biofilms [J]. Water Science and Technology, 1998, 37 (4–5): 207–210.

[66]   Jorand F., F. Z., Thomas F., et al. Chemical and structural (2D) linkage between bacteria within activated sludge flocs [J]. Water Research, 1995: 1639–1647.

[67]   Dignac M.F., V. U., Rybacki D., et al. Chemical description of extracellular polymeric substances: Implication on activated sludge floc structure [J]. Applied Microbiology and Biotechnology, 1998, 46: 197–201.

[68]   Flemming H.C., Wingender J. in Encyclopedia of Environmental Microbiology [M]. Wiley, New York, 2002.

[69]   Priester J.H., Olson S.G., Webb S.M., et al. Enhanced exopolymer production and chromium stabilization in pseudomonas putida unsaturated biofilms [J]. Applied and Environmental Microbiology, 2006, 72: 1988–1996.

[70]   Zhang D.Y., Wang J.L., Pan X.L. Cadmium sorption by EPSs produced by anaerobic sludge under sulfate-reducing conditions [J]. Journal of Hazardous Materials, 2006, 138: 589–593.

[71]   Liu H., Fang H.H.P. Characterization of electrostatic binging sites of extracellular polymers by linear programming analysis of titration data [J]. Biotechnology and bioengineering, 2002, 80: 806–811.

[72]   Joshi R.M., Juwarkar A.A. In vivo studies to elucidate the role of extracellular polymeric substances from Azotobacter in immobilization of heavy metals [J]. Environmental Science & Technology, 2009, 43: 5884–5889.

[73]   Ha J., Gelabert A., Spormann A.M., Brown G.E. Role of extracellular polymeric substances in metal ion complexation on Shewannella oneidensis: Batch uptake, thermodynamic modeling, ATR-FTIR, and EXAFS study [J]. Geochimica et Cosmochimica Acta, 2010, 74: 1–15.

[74] Bhaskar P.V., Bhosle N.B. Bacterial extracellular polymeric substances (EPS): A carrier of heavy metals in the marine food-chain [J]. Environment International, 2006, 32: 191–198.

[75] Moon S.H., Park C.S., Kim Y.J., et al. Biosorption isotherms of Pb (II) and Zn (II) on Pestan, an extracellular polysaccharide, of Pestalotiopsis sp. KCTC 8637P. [J]. Process Biochemistry, 2006, 41:312–316.

[76] Comte S., Guibaud G., Baudu M. Biosorption properties of extracellular polymeric substances (EPS) resulting from activated sludge according to their type: Soluble or bound [J]. Process Biochemistry, 2006, 41: 815−823.

[77] Liu Y., Fang H.H.P. Influence of extracellular polymeric substances (EPS) on flocculation, settling, and dewatering of activated sludge [J]. Critical Reviews in Environmental Science and Technology, 2003, 33: 237–273.

[78] Wang J.J., Liu X., Ng T.W., et al. Disinfection byproduct formation from chlorination of pure bacterial cells and pipeline biofilms [J]. Water Research, 2013, 47: 2701–2709.

[79] Wang Z.K., Choi O.K., Seo Y.W. Relative contribution of biomolecules in bacterial extracellular polymeric substances to disinfection byproduct formation [J]. Environmental Science & Technology, 2013, 47: 9764–9773.

[80] Wang Z.K., Kim J., Seo Y. Influence of bacterial extracellular polymeric substances on the formation of carbonaceous and nitrogenous disinfection byproducts. [J]. Environmental Science & Technology, 2012, 46: 11361–11369.

[81] Li L., Jeon Y., Ryu H., et al. Assessing the chemical compositions and disinfection byproduct formation of biofilms: Application of fluorescence excitation-emission spectroscopy coupled with parallel factor analysis. [J]. Chemosphere,2020, 246: 125745.

[82] Xue Z., Hessler C.M., Panmanee W., et al. Pseudomonas aeruginosa inactivation mechanismis affected by capsular extracellular polymeric substances reactivity with chlorine and monochloramine. [J]. FEMS Microbiology Ecology, 2012, 83: 101–111.

[83] Wang Z.K., Li. L., Arissd R.W., et al. The role of biofilms on the formation and decay of disinfection by-products in chlor(am)inated water distribution systems [J]. Science of the Total Environment, 2021, 753: 141606.

[84]   Characklis W G. Bioengineering report: Fouling biofilm development: A process analysis [J]. Biotechnology and Bioengineering, 1981, 23(9): 1923-60.

[85]   Zobell C E. The Effect of Solid Surfaces upon Bacterial Activity [J]. J Bacteriol, 1943, 46(1): 39-56.

[86]   Liu S, Gunawan C, Barraud N, et al. Understanding, Monitoring, and Controlling Biofilm Growth in Drinking Water Distribution Systems [J]. Environmental Science & Technology, 2016, 50(17): 8954-76.

[87]   Ndiongue S, Huck P M, Slawson R M. Effects of temperature and biodegradable organic matter on control of biofilms by free chlorine in a model drinking water distribution system [J]. Water Research, 2005, 39(6): 953-64.

[88]   Liu S, Graham J E, Bigelow L, et al. Identification of Listeria monocytogenes genes expressed in response to growth at low temperature [J]. Appl Environ Microbiol, 2002, 68(4): 1697-705.

[89]   Kannan A, Gautam P. A quantitative study on the formation of Pseudomonas aeruginosa biofilm [J]. SpringerPlus, 2015, 4(1): 379.

[90]   Pintar K D M, Slawson R M. Effect of temperature and disinfection strategies on ammonia-oxidizing bacteria in a bench-scale drinking water distribution system [J]. Water Research, 2003, 37(8): 1805-17.

[91]   Kilb B, Lange B, Schaule G, et al. Contamination of drinking water by coliforms from biofilms grown on rubber-coated valves [J]. International Journal of Hygiene and Environmental Health, 2003, 206(6): 563-73.

[92]   Skjevrak I, Due A, Gjerstad K O, et al. Volatile organic components migrating from plastic pipes (HDPE, PEX and PVC) into drinking water [J]. Water Research, 2003, 37(8): 1912-20.

[93]   Niquette P, Servai P, Savoir R. Impacts of pipe materials on densities of fixed bacterial biomass in a drinking water distribution system [J]. Water Research, 2000, 34(6): 1952-6.

[94]   Zhang Z, Stout J E, Yu V L, et al. Effect of pipe corrosion scales on chlorine dioxide consumption in drinking water distribution systems [J]. Water Research, 2008, 42(1):

129-36.

[95]   Organization W H. Guidelines for Drinking-water Quality 4th Ed [J]. 2011,

[96]   Rook J J. Formation of haloforms during chlorination of natural waters [J]. 1974,

[97]   Krasner S W, Weinber H S, Richardson S D, et al. Occurrence of a New Generation of Disinfection Byproducts [J]. Environmental Science & Technology, 2006, 40(23): 7175-85.

[98]   Zhao Y.L, Li J.F. Drinking water disinfection by prodoucts: Chemical characterization and toxicity [J]. Environmental Chemistry, 2011, 30(01): 20-33.

[99]   Richardson S.D., Plewa M.J., Wagner E.D., et al. Occurrence, genotoxicity, and carcinogenicity of regulated and emerging disinfection by-products in drinking water: A review and roadmap for research [J]. Mutation Research-Reviews in Mutation Research, 2007, 636: 178–242.

[100]   Loper J.C. Mutagenic effects of organic compounds in drinking water [J]. Mutat Resxs-Fund 1980, 76: 241–268.

[101]   Krasner S.W., Weinberg H.S., Richardson S.D., et al. Thruston A.D. Occurrence of a new generation of disinfection byproducts [J]. Environmental Science & Technology, 2006, 40(23): 7175–7185.

[102]   Cerrato J.M., Falkinham J.O., III, Dietrich A.M., et al. Manganese-oxidizing and -reducing microorganisms isolated from biofilms in chlorinated drinking water systems [J]. Water Research, 2010, 44 (13): 3935–3945.

[103]   Dong H.Y., Qiang Z.M., Richardson S.D. Formation of iodinated disinfection byproducts (I-DBPs) in drinking water: Emerging concerns and current issues [J]. Accounts of Chemical Research, 2019, 52 (4): 896−905.

[104]   Plewa M.J., Wagner E.D., Richardson S.D., et al. Chemical and biological characterization of newly discovered lodoacid drinking water disinfection byproducts [J]. Environmental Science & Technology, 2004, 38 (18): 4713–4722.

[105]   Plewa M.J., Muellner M.G., Richardson S.D., et al. Occurrence, synthesis, and mammalian cell cytotoxicity and genotoxicity of haloacetamides: An emerging class of nitrogenous drinking water disinfection byproducts [J]. Environmental Science & Technology, 2008, 42

(3): 955–961.

[106] Plewa M.J., Simmons J.E., Richardson S.D., et al. Mammalian cell cytotoxicity and genotoxicity of the haloacetic acids, a major class of drinking water disinfectionby-Products [J]. Environmental and Molecular Mutagenesis, 2010, 51 (8–9) : 871–878.

[107] Richardson S.D., Fasano F., Ellington J.J., et al. Occurrence and mammalian cell toxicity of iodinated disinfection byproducts in drinking water [J]. Environmental Science & Technology, 2008, 42 (22) : 8330–8338.

[108] Wagner E.D., Plewa M.J. CHO cell cytotoxicity and genotoxicity analyses of disinfection by-products: An updated review [J]. Journal of Environmental Sciences, 2017, 58: 64−76.

[109] Plewa M, Kargalioglu Y, Vankerk D, et al. Mammalian cell cytotoxicity analysis of drinking water disinfection by-products [J]. Environmental and molecular mutagenesis, 2002, 40(134-42.

[110] Plewa M J, Wanger E D, Jazwiersk P, et al. Halonitromethane Drinking Water Disinfection Byproducts: Chemical Characterization and Mammalian Cell Cytotoxicity and Genotoxicity [J]. Environmental Science & Technology, 2004, 38(1): 62-8.

[111] Erdinger L, Kuhn K P, Kirsch F, et al. Pathways of trihalomethane uptake in swimming pools [J]. International Journal of Hygiene and Environmental Health, 2004, 207(6): 571-5.

[112] Miles A M, Singer P C, Ashley D L, et al. Comparison of Trihalomethanes in Tap Water and Blood [J]. Environmental Science & Technology, 2002, 36(8): 1692-8.

[113] Xu X, Weisel C. Dermal uptake of chloroform and haloketones during bathing [J]. Journal of exposure analysis and environmental epidemiology, 2005, 15(289-96.

[114] Zwiener C, Richardson S D, Demarini D M, et al. Drowning in Disinfection Byproducts? Assessing Swimming Pool Water [J]. Environmental Science & Technology, 2008, 42(5): 1812-.

[115] Sadiq R, Rodriguez M J. Fuzzy synthetic evaluation of disinfection by-products—a risk-based indexing system [J]. Journal of Environmental Management, 2004, 73(1): 1-13.

[116] Gottlieb M, Carr J. Case-Control Cancer Mortality Study and Chlorination of Drinking Water in Louisiana [J]. Environmental health perspectives, 1983, 46(169-77.

[117] Wu Y. Research on Disinfection by-products in water distribution system [D]. Harbin Institute of Technology, 2006.

[118] Herren-Freund S L, Pereira M A, Khoury M D, et al. The carcinogenicity of trichloroethylene and its metabolites, trichloroacetic acid and dichloroacetic acid, in mouse liver [J]. Toxicology and Applied Pharmacology, 1987, 90(2): 183-189.

[119] Mchugh L J, Lopez L, Deangelo A B. Hepatotoxity of the drinking water disinfection by-product, dichloroacetic acid, in the medaka small fish model [J]. Toxicology Letters, 1998, 94(1): 19-27.

[120] Yang Y, Heng Z.C. Studies on DNA damage of mice hepatocytes induced by dichloroacetic acid [J]. Modern Preventive Medicine, 2004, 31(03): 324-335.

[121] Krasner S. The Formation and Control of Emerging Disinfection By-Products of Health Concern [J]. Philosophical transactions Series A, Mathematical, physical, and engineering sciences, 2009, 367(40)77-95.

[122] Muellner M G, Wagner E D, Mccalla K, et al. Haloacetonitriles vs. Regulated Haloacetic Acids: Are Nitrogen-Containing DBPs More Toxic? [J]. Environmental Science & Technology, 2007, 41(2): 645-51.

[123] Wei X., Wang S., Zheng W.W., et al. Drinking sater disinfection byproduct iodoacetic acid induces tumorigenic transformation of NIH3T3 cells [J]. Environmental Science & Technology, 2013, 47 (11): 5913–5920.

[124] Muellner M.G., Wagner E.D., McCalla K., et al. Haloacetonitriles vs. rregulated haloacetic a acids: Are nitrogen-containing DBPs more toxic? [J]. Environmental Science & Technology, 2007, 41 (2) : 645–651.

[125] Zhang H, Andrews S A. Catalysis of copper corrosion products on chlorine decay and HAA formation in simulated distribution systems [J]. Water Research, 2012, 46(8): 2665-73.

[126] Zhang H, Andrews S A. Factors affecting catalysis of copper corrosion products in NDMA formation from DMA in simulated premise plumbing [J]. Chemosphere, 2013, 93(11): 2683-9.

[127] Lin Y.P., Washburn M.P., Valentine R.L. Reduction of lead oxide (PbO2) by iodide and

formation of iodoform in the PbO2/I−/NOM System [J]. Environmental Science & Technology, 2008, 42 (8): 2919–2924.

[128] HEEB M B, CRIQUET J, ZIMMERMANN-STEFFENS S G, et al. Oxidative treatment of bromide-containing waters: Formation of bromine and its reactions with inorganic and organic compounds — A critical review [J]. Water Research, 2014, 48:15-42.

[129] Wang Z, Kim J, Seo Y. Influence of Bacterial Extracellular Polymeric Substances on the Formation of Carbonaceous and Nitrogenous Disinfection Byproducts [J]. Environmental Science & Technology, 2012, 46(20): 11361-9.

[130] Bougeard C M M, Goslan E H, Jeffersin B, et al. Comparison of the disinfection by-product formation potential of treated waters exposed to chlorine and monochloramine [J]. Water Research, 2010, 44(3): 729-40.

Chapter 2

MATERIALS AND ANALYTICAL METHODS

2.1 Materials

2.1.1 Experimental chemicals

The purity of experimental chemicals was analytical pure (AR) or above: Sodium sulfate (Na_2SO_4), sodium chloride (NaCl), sodium hydroxide (NaOH), disodium hydrogen phosphate dodecahydrate ($Na_2HPO_4 \cdot 12H_2O$) and potassium dihydrogen phosphate (KH_2PO_4) were purchased from Sinopharm Chemical Reagent Co., Ltd. Sodium borate ($Na_2B_4O_7 \cdot 10H_2O$), boric acid (H_3BO_3), nitric acid (HNO_3), sulfuric acid (H_2SO_4), hydrochloric acid (HCl) were purchased from Shanghai Aladdin Biochemical Technology Co., LTD. Potassium bromide (KBr), potassium iodide (KI), potassium iodate (KIO_3), copper nitrate ($Cu(NO_3)_2$), lead nitrate ($Pb(NO_3)_2$), potassium permanganate ($KMnO_4$), manganese chloride ($MnCl_2$) were purchased from Shanghai Maclin Biochemical Technology Co., Ltd.

All organic reagents in the experiment are shown in Table 2.1:

Table 2.1.   Organic chemicals

Chemicals	Purity	Manufacturer
Methyl tert-butyl ether	GR	Shanghai Aladdin Biochemical Technology
Benzene	AR	Shanghai Lingfeng Chemical Reagent Co.,
Phenol	AR	Shanghai Aladdin Biochemical Technology
Acetone	AR	Hangzhou Shuanglin Chemical Reagent Co.,
Trichloroacetic acid	AR	Shanghai Aladdin Biochemical Technology
Ethyl acetate	AR	Shanghai Lingfeng Chemical Reagent Co.,
Acetic Acid	GR	Shanghai Aladdin Biochemical Technology
Methanol	GR	Tianjin Siyou Fine Chemicals Co., Ltd.
Amino acid	AR	Shanghai Sangon Biotech Co., Ltd.

Humic acid	AR	Shanghai Aladdin Biochemical Technology
Iodophenol	AR	Shanghai Aladdin Biochemical Technology
Chloroform	AR	Shanghai Aladdin Biochemical Technology
Bromodichloromethane	97%	J&K Scientific
Dibromochloromethane	97%	J&K Scientific
Tribromomethane	AR	Shanghai Aladdin Biochemical Technology
Chloroacetic acid	AR	Shanghai Aladdin Biochemical Technology
Dichloroacetic acid	AR	Shanghai Macklin Biochemical Co., Ltd.

Table 2.1 Organic chemicals (continued)

Chemicals	Purity	Manufacturer
Bromoacetic acid	AR	Shanghai Aladdin Biochemical Technology
Dibromoacetic acid	97%	J&K Scientific
Tribromoacetic acid	99%	Shanghai Macklin Biochemical Co., Ltd.
Bromochloroacetic acid	97%	J&K Scientific
Chlorodibromoacetic	97%	J&K Scientific
Bromodichloroacetic	97%	J&K Scientific
Chloroacetonitrile	98%	TCI Shanghai Co., Ltd.
Dichloroacetonitrile	98%	Shanghai Macklin Biochemical Co., Ltd.
Trichloroacetonitrile	98%	Shanghai Macklin Biochemical Co., Ltd.
Bromochloroacetonitril	97%	J&K Scientific
dibromoacetonitrile	97%	Shanghai Macklin Biochemical Co., Ltd.
Tribromoacetonitrile	97%	J&K Scientific
Chloroacetamide	99%	Shanghai Aladdin Biochemical Technology

Dichloroacetamide	97%	Shanghai Aladdin Biochemical Technology
Trichloroacetamide	98%	Shanghai Aladdin Biochemical Technology
Bromoacetamide	97%	Shanghai Macklin Biochemical Co., Ltd.
Dibromoacetamide	98%	J&K Scientific
Tribromoacetamide	98%	J&K Scientific
Iodoform	AR	Shanghai Aladdin Biochemical Technology
Iodoacetic acid	AR	Shanghai Aladdin Biochemical Technology
Diiodoacetic acid	98%	Toronto Research Chemicals（TRC）
Triiodoacetic acid	90%	Toronto Research Chemicals（TRC）
Iodoacetonitrile	98%	Shanghai Macklin Biochemical Co., Ltd.
Iodoacetamide	98%	Shanghai Aladdin Biochemical Technology
Diiodoacetamide	99%	Toronto Research Chemicals（TRC）

2.1.2 Experimental instruments

Experimental instruments are shown in Table 2.2:

Table 2.2 List of experimental instruments

Instrument	Model	Manufacturer
Multi-head magnetic heating agitator	HJ−6A	Changzhou Guohua Electric Appliance Co., Ltd.
Multi-pipe mixing device	DMT−2500	Hangzhou Miu Instruments Co., Ltd.
Electronic analytical balance	FA2204B	Sartorius Scientific Instruments Co. Ltd.
Total organic carbon analyzer	TOC V−CPH	Shimadzu Japan Co., Ltd.
Carry-home pH meter	SX−620	Shanghai Sanxin Instruments factory
Vacuum drying box	DZG−6050S	Shanghai Senxin Experimental Instruments Co., Ltd.

Centrifuge	3H12RI	Hunan Husi Instrument Equipment Co., Ltd.
Magnetic stirre	DF−101T	Henan Yuhua Instruments Co., Ltd.
Gas chromatograph	Agilent 6890N	NYSE: A Company
Freeze dryer	TF−FD−1	Shanghai San-Xin Instruments Co., Ltd.
Surface area and pore structure analyzer	ASAP 2100	Micromeritics Instruments Co., Ltd.
HPLC tandem mass spectrometer	Q-Exactive HF	Thermo Fisher Scientific Co., Ltd.
Ion chromatograph	DionexICS2000	DIONEX Company
Liquid chromatograph	Waters 2695	Waters Associates
Muffle furnace	HY1200−40−25	Shanghai Hongyue Technology Co., Ltd.

2.2 Analysis methods

2.2.1 Gas chromatography

Gas chromatography was used to detect THMs, HAAs, HANs and HAcAms. The separation column was DB-5 capillary column (30 m × 0.25 mm, 0.25 μm). The determination method of THMs, HANs and HAcAms is modified from EPA standard method 551[1] . The pretreatment steps of water samples are as follows:20 mL water sample was taken, and 2 mL methyl tert-butyl ether was added for 5 min of eddy shaking. After static stratification, 1 mL upper organic solvent was taken into GC/ECD analysis. For chlorinated and brominated THMs, HANs and HAcAms, GC column temperature is programmed: the initial temperature is 50 ℃; 1 ℃ min^{-1} Heating to 60 ℃; 20 ℃ min^{-1} Heating to 160 ℃; 15 ℃ min^{-1} Temperature rise to 280 ℃. The inlet temperature is 180 ℃, the detector temperature is 300℃, the injection method is non-split injection, the injection volume is 1 μL. The carrier gas is nitrogen, and the flow rate is 2 mL min^{-1}.For iodinated THMs, HANs and HAcAms, the GC column temperature was programmed: the initial temperature was 40 ℃, which was maintained for 5 min; 1 ℃ min^{-1} Heat the temperature to 45 ℃ for 2 minutes.10 ℃ min^{-1} Heat up to 115 ℃ for 1 min.15 ℃ min^{-1} Heating to 160 ℃; 20 ℃ min^{-1} Heat the temperature to 240 ℃ and hold the temperature for 8 minutes. Other conditions are consistent

with the former.

HAAs's measurement method was modified from EPA standard method 552.2[1] . The pre-treatment steps of water samples were as follows: take 20 mL water samples and add them into 40 mL sample bottles; add 1 mL concentrated sulfuric acid; add 3.0g Na_2SO_4 powder, shake until dissolved; add 4 mL MTBE (including internal standard 1,2-dibromopropane), shake for 3 min, stand for 5 min; transfer 2.5 mL of upper organic phase to another sample bottle;2.5ml of 10% sulfuric acid-methanol solution was added and heated in water bath for 2h (50 ± 2 ℃), then cooled at 4℃ for 10 min.7 mL saturated Na_2SO_4 solution was added to shake the two phases completely. Take 1 mL of upper organic solvent into GC/ECD analysis. GC column temperature was programmed: the initial temperature was 40 ℃ and kept for 4 min;2 ℃ min^{-1} Heating to 80 ℃; 5 ℃ min^{-1} Heating to 105 ℃; 5 ℃ min^{-1} heat the temperature to 135 ℃ and hold the temperature for 2 minutes. The inlet temperature is 210 ℃, and the detector temperature is 300 ℃. The injection method is non-split injection, and the injection volume is 1 μL. The carrier gas is nitrogen, and the flow rate is 2 mL min^{-1}.

2.2.2 Liquid chromatography

The free iodine (I_2/HOI) was determined by chromatography method. The ratio of benzene solution to water sample was 1:1, 1 mL in the upper benzene solution was filtered to the brown liquid phase vials by 0.22 μm organic filter, add an excess of phenol solution. The determination of indophenol at 231 nm was performed by high-performance liquid chromatography (HPLC) combined with UV detector and the Atlantis T3 column (4.6 × 250 mm, 5.0 μm). Mobile phase A (100% methanol) and mobile phase B (99.7% ultrapure water and 0.3% glacial acetic acid), the proportion is 70%: 30%.

2.2.3 Determination by ion chromatography

IO_3^- and I^- were determined by ion chromatography. The specific method is as follows: firstly, the water sample is filtered by 0.45 μm water filter, and then filtered by C18 and sodium column in order to remove the influence of organic matter and metal ions on the experimental determination. Finally, the obtained samples were analyzed for IO_3^- and I^- using Ionpac AS19 column (250 mm×4.0 mm, 5.0 μm) with a 0.22 μm stream filter. Parameter Settings: the temperature of detector

is 30 °C, the current of suppressor is 99 mA, the concentration of leachate KOH is 40 mM, and the total working time is 25 min. Ion injection volume is 250 μL.

2.2.4 Specific surface area characterization

The specific surface area of the metal oxides was measured by Brunner Emmet Teller characterization (BET) using an automatic specific surface and aperture distributor: The samples were freeze-dried with a freeze-dryer before detection, and then weighed with 0.1−0.2 g samples and placed in 250 °C for 3 h vacuum degassing, followed by N_2 adsorption − desorption (liquid nitrogen temperature −196 °C) to determine the specific surface area of the samples.

2.2.5 Determination of VSS

Firstly, the quantitative filter paper was placed in an oven of 103−105 °C for drying for 4 h, and then weighed after cooling in the dryer. The weight was denoted as m_0.

Take 100 mL activated sludge (mix well before measuring) and filter with the filter paper obtained in the previous step. The filter paper and sludge were placed on a glassware and dried for 8 hours in an oven at 103−105 °C. After cooling in the dryer, it is weighed and denoted as m_1.

Wash the crucible and put it into the oven for drying for 1 h. Weigh it after cooling in the dryer and write it down as m_2.

Put the sludge and filter paper in the second step into the crucible, and then into the Muffle furnace, heated to 600 °C and burned for 1 h. After cooling in the dryer, it is weighed and recorded as m_3.

$$VSS = [(m_1 + m_2 − m_0) − m_3] / 0.1 \quad （g\ L^{−1}）$$

2.2.6 Protein analysis

The peptide was redissolved with mobile phase A (2% acetonitrile, 0.1% formic acid) and centrifuged at 20000 g for 10 min. Sample the supernatant. The samples were separated by HIGH performance liquid chromatography: the samples were enriched and desalted in a Trap column, and then connected in series with a C18 column (75 μm inner diameter, 3μm column material > particle size, 25 cm column length) at a flow rate of 300 nL min$^{−1}$. The effective gradient separation setup

was as follows:0−5 min, 5% mobile phase B (98% acetonitrile, 0.1% formic acid);5−45 min, the mobile phase B increases linearly from 5% to 25%; At 45−50 min, the mobile phase B increases from 25% to 35%. At 50-52 min, the mobile phase B increases from 35% to 80%.52−54 min, 80% mobile phase B;54−60 min, 5% mobile phase B. High performance liquid chromatography end linked mass spectrometer.

The peptides separated by HIGH performance liquid chromatography were ionized by nanoESI source and then entered into tandem mass spectrometer for DNA (Data-dependent Acquisition) mode detection. Main parameters are set as follows: ion source voltage 1.6 kV; First-order ms scanning range 350−1600 m/z; The resolution is 60000; The initial m/z of secondary ms was fixed at 100; The resolution is 15000.The selection conditions of secondary fragmentation parent ions are as follows: charge 2^+ to 6^+, peak strength over 10000 rank in the top 30 parent ions. The ion fragmentation mode was HCD, and the fragment ions were detected in Orbitrap. The dynamic exclusion time is set to 30 seconds. The AGC is set to level 1 3E6 and Level 2 1E5.

Protein full spectrum identification is mainly through matching experimental tandem mass spectrometry data with theoretical mass spectrometry data obtained from database simulation, so as to obtain protein identification results. The main databases used are: UniProt protein database, gene annotation based protein database and other sources database.

2.2.7 Determination of chronic cytotoxicity

Water sample pretreatment: Organic compounds in water are concentrated by adsorption onto XAD resin.XAD−2 (Amberlite XAD 2) and XAD−8 (Supelite DAX 8) resins, each with a volume of 55 mL, were installed on a glass wool plug of a glass column. The maximum ratio of water to resin is 770:1 to minimize infiltration and maximize adsorption of organic matter. Before adding the water sample to the column for extraction, it is acidified to pH < 2 with sulfuric acid to ensure protonation of carboxylic organic matter. The organic compounds were eluted with 400 mL ethyl acetate. Residual water in the ethyl acetate eluent was removed using a separation funnel, and then the ethyl acetate was passed through an anhydrous sodium sulfate column to further remove residual water. Finally, the ethyl acetate extract was reduced to 1−1.5 mL by rotary evaporator at 50−60 °C. For each sample, dimethyl sulfoxide was used to dissolve the organic extract, thus the

sample was 100 times concentrated.

Cell culture: Chinese hamster ovary cell (CHO) cells were cultured in a medium containing 10% serum (BI) amino acid and glucose, 37 °C, 5% CO_2, saturated humidity incubator.

Cell plate laying and toxicity measurement: CHO cell lines in normal culture at logarithmic stage were washed twice with phosphate buffer solution (PBS), followed by trypsin digestion for 1 min, and complete culture medium was added to terminate digestion. The blow cells were transferred to a 15 mL centrifuge tube, centrifuged for 5 min at 1000 RPM. Lay a 96-well plate with 5 holes for each sample group (3 groups in total). Add 1500 cells to each well and incubate them overnight in an incubator. The experiment was repeated three times to ensure its accuracy.72 h later, the medium was removed, fixed with paraformaldehyde for 5 min, then washed with PBS for 1 to 2 times, stained with crystal violet for 5 min, washed with tap water for 3 times, and added 50 μL dimethyl sulfoxide/methanol (3:1), incubate at dark for 10 min, read the OD value of each well at 595 nm and 650 nm, and the final OD value is 595 nm−650 nm.

The experimental results were calculated as follows:

Cell survival rate (%) = experimental group (OD_{595}−OD_{650}) /CK group (OD_{595}−OD_{650}) ×100%, the survival rate of CK group was 100%.

2.3 Extraction methods

2.3.1 Extraction of EPS

EPS was extracted by cation exchange numerical method (CER, 732 sodium type)[2] .About 200 mL of activated sludge and CER of 70 g/g VSS were mixed in a 500 mL beaker and placed in a magnetic stirrer at 250 rpm min^{-1} for 6 h at 4 °C.The suspension was centrifuged at 10000 g at 4 °C for 20 min and then filtered by 0.45 μm filter membrane. The collected filtrate was refrigerated at −80°C for 2 h, and then placed in a freeze dryer for 48 h to obtain EPS powder, which was sealed and stored at room temperature. Activated sludge came from the Institute of Environmental Water Pollution and Control, Zhejiang University of Technology.

2.3.2 Extraction of protein

Proteins in EPS were extracted by an improved TCA precipitation method [3]. In the first step, TCA (100%, w/v) of trichloroacetic acid was slowly added to EPS filtrate until the final concentration was 13%. The mixture was mixed and placed in an environment of 4 °C overnight for precipitation. On the second day, the mixture was centrifuged at 4 °C for 10000 g for 20 min, and the supernatant was poured out. Appropriate amount of acetone was added to wash the precipitate and centrifuged at 10000 g for 3 min, repeated three times to remove the residual TCA. Finally, the EPS protein components were obtained by freeze-drying the precipitate for 48 h.

2.3.3 Extraction of polysaccharides

Polysaccharides were extracted by precipitation method [4]. Before EPS extraction, the activated sludge was cleaned with methanol for 3 times to remove lipids. For the subsequent extraction methods, please refer to 2.3.1. TCA (80%, w/v) was first added to EPS filtrate to a final concentration of 4% to remove proteins. The mixture was mixed and incubated overnight in 4% environment. On the second day, the mixture was centrifuged at 10000 g in 4 °C centrifuge for 20 min to remove the precipitate. After freeze-drying, the supernatant was re-dissolved in 1 mL deionized water, and 3 mL ethanol (95%, v/v) was added to incubate at 4°C for 24 h to precipitate the polysaccharide. The precipitate was recovered by centrifugation (10000 g, 4 °C, 20 min). After the precipitate was readded to deionized water, the insoluble was removed by centrifugation at 1000 g and 4 °C for 20 min, and the supernatant was transferred to a dialysis bag (3000 Da). After 72 h of dialysis in deionized water at 4°C, the deionized water was replaced regularly. Finally, the supernatant was freeze-dried to obtain EPS polysaccharide components.

2.3.4 Enzymatic hydrolysis of proteins

Take 100 μg protein solution from each sample. Add Trypsin 2.5 μg at the ratio of 40:1 protein: enzyme, and enzymelike at 37 °C for 4 h. Trypsin was added at the original ratio and unsymbolized at 37 °C for 8 h. Strata X column was used to remove salt and drain the peptide.

2.4 Preparation of metal oxides

2.4.1 Preparation of CuO

CuO was prepared by CTAB−Hydrothermal method [5]: Under the condition of magnetic agitation, Cu(NO3)2 solution (500 mL, 0.2 M) was mixed with NaOH solution (500 mL, 0.5 M) and stirred for more than 48 h. The resulting precipitate is rinsed repeatedly with deionized water until the pH does not change significantly. The precipitate was then dried overnight in an oven at 70 °C and finally heated at 200 °C for 12 h.

2.4.2 Preparation of PbO$_2$

Preparation of PbO$_2$ reference [6]:250 mL of 0.1 mol L^{-1} Pb (NO$_3$)$_2$ solution was prepared, and the mole ratio of NaClO solution to Pb^{2+} was 1:1.After standing at room temperature for 24 h, the brownish red solution was transferred to a centrifugal tube. The precipitate was obtained by centrifugation (6000 rpm, 6 min) and cleaned several times with deionized water. The obtained solids were transferred to a dialysis bag and dialyzed in deionized water for 72 h. The deionized water was replaced periodically. Finally, the solids are freeze-dried to obtain PbO$_2$.

2.4.3 Preparation of δ-MnO$_2$

Preparation method of δ-MnO$_2$ Reference [7]: Firstly, anaerobic water was prepared. Fill 900−1000 mL ultra-pure water into a wide-mouth bottle with a volume of 1000 mL, expose nitrogen for 2 h, and quickly close the lid of the wide-mouth bottle. Then the potassium permanganate reserve solution (0.1 mol L^{-1}), sodium hydroxide reserve solution (0.1 mol L^{-1}) and anaerobic manganese chloride reserve solution (0.1 mol L^{-1}) were prepared. Potassium permanganate reserve solution is placed under shading. Anaerobic manganese chloride reserve solution is prepared using anaerobic water. Then prepare a 2 L beaker, add 1230 mL ultra-pure water to stir on a magnetic stirrer, and pre-aerate nitrogen for 1 h. Finally, accurately measure 60 mL potassium permanganate reserve solution and 120 mL sodium hydroxide reserve solution with a measuring cylinder, pour them into the beaker, and expose nitrogen to stir for 30 min. Take 90 mL manganese chloride reserve solution and slowly add anaerobic manganese chloride solution with a rubber head dropper. After 15 minutes of dripping, continue to aerate nitrogen and stir, and fully reaction for 1 h

Reference

[1]   Frølund B, Palmgren R, Keiding K, et al. Extraction of extracellular polymers from activated sludge using a cation exchange resin [J]. Water Research, 1996, 30(8): 1749-58.

[2]   Silva A F, Carvalho G, Soares R, et al. Step-by-step strategy for protein enrichment and proteome characterisation of extracellular polymeric substances in wastewater treatment systems [J]. Applied Microbiology and Biotechnology, 2012, 95(3): 767-76.

[3]   Zhang P, Guo J-S, Shen Y, et al. Microbial communities, extracellular proteomics and polysaccharides: A comparative investigation on biofilm and suspended sludge [J]. Bioresource Technology, 2015, 190(21-8.

[4]   Liu C, Von G U, Croué J-P. Enhanced Bromate Formation during Chlorination of Bromide-Containing Waters in the Presence of CuO: Catalytic Disproportionation of Hypobromous Acid [J]. Environmental Science & Technology, 2012, 46(20): 11054-61.

[5]   Murray J.W. The surface chemistry of hydrous manganese dioxide [J]. Journal of Colloid and Interface Science, 1974, 46 (3): 357−371.

[6]   Lin Y-P, Valentine R L. Reduction of Lead Oxide (PbO_2) and Release of Pb(II) in Mixtures of Natural Organic Matter, Free Chlorine and Monochloramine [J]. Environmental Science & Technology, 2009, 43(10): 3872-7.

[7]   Lechevallier M W, Cawthon C D, Lee R G. Inactivation of Biofilm Bacteria [J]. Appl Environ Microbiol, 1988, 54(10): 2492-9.

STUDY ON THE FORMATION OF CARBON (NITROGEN)-CONTAINING DISINFECTION BY-PRODUCTS FROM EXTRACELLULAR POLYMERS UNDER THE CATALYSIS OF COPPER TUBE CORROSION

Adding a high dose of residual chlorine to the network is a popular method of choice for water utilities to maintain microbial stability in DWDS [1] .though this method can effectively inhibit the growth of microorganisms and ensure the safety of drinking water, it is possible that the water quality will deteriorate by controlling microorganisms through this method. Because a series of complex biochemical reactions will occur between organic compounds, residual chlorine and PCPs in DWDS, resulting in the generation of DBPs. Some studies have reported the effects of various PCPs on DBPs generation, but NOMs is mainly used as a precursor to study, while the research on EPS is still insufficient [2-4].

In DWDS, because NOMs in water is difficult to completely remove, biofilms are generated and widely distributed. Biofilms can produce and secrete EPS, which is mainly composed of nucleic acids, polysaccharides, proteins and lipids [5].Compared with NOMs, these biomolecules are usually richer in nitrogen and have lower molecular weight, which is bound to cause significant changes in the generation rate and species of DBPs [6].A large number of studies have reported that the toxicity of N−DBPs is much higher than that of C−DBPs, so the biomolecules mentioned in the appeal may have great health risks [7-10].Wang et al. [6,11] evaluated the influence of EPS and its composition on the generation of C−DBPs and N−DBPs, and believed that biofilms were a precursor of DBPs that could not be ignored and should be eliminated as far as possible. However, there is still no literature report on the formation of DBPs with EPS as precursor under the catalytic action of PCPs.

Cast iron pipe is the most used pipe material in China, which contains a certain amount of copper element. Copper pipe is also due to its stable nature, recyclable and other advantages from high-end residential gradually to the development of ordinary residential. In DWDS, copper tubes will be corroded to form copper oxide (CuO) on the surface during long-term use and release copper ions (Cu^{2+}) into drinking water [12].

It is well known that DBPs generation is significantly catalyzed in the presence of CCPs. Hu et al. [13] found that Cu^{2+} and CuO increased Br⁻DBPs production by 50.1%

and 7.1%, respectively, in the chlorination process containing Br$^-$ water. Liu and Croue[4].

studied the catalytic effect of CuO on DBPs generation of six soluble organic compounds during chlorination and found that CuO has a better catalytic effect on organics with low SUVA$_{254}$, indicating that there is a complex and important interaction between precursor and CuO.

In this chapter, the catalytic generation of two kinds of CCPs (CuO and Cu^{2+}) on C−DBPs and N−DBPs with EPS as precursor was studied, and the influence of water pH and Br$^-$ on CCPs catalysis was systematically studied. At the same time, the formation of DBPs when the main biomolecules (polysaccharides and proteins) and the model molecules of proteins (amino acids) in EPS were discussed in detail, so as to comprehensively predict the catalytic pathway and mechanism of CCPs.

3.1 Experimental conditions

All experiments were carried out under the conditions of room temperature (25±2℃), dark and magnetic agitation. The reaction bottle is chlorinated before use. Considering the pH change of the reaction system and the complexation of Cu^{2+} and phosphate, the reaction solution adopts boric acid buffer salt solution to ensure no obvious change of pH before and after the reaction. The pH$_{PZC}$ and specific surface area of CuO prepared were 8.3 and 12.8 m^2 g^{-1}, respectively [14].

Considering the concentration range of CCPs in DWDS, the concentration of EPS and humic cid (HA) in water and to ensure the experimental effect [6,15,16] ,the reaction conditions are set as follows:

The initial concentration of free chlorine was set to 9.8 mg L^{-1} (in Cl$_2$); humic acid (HA) and EPS were set to 5.0 mg C L^{-1}. The concentration of Cu^{2+} was set as 2.0 mg L^{-1}. The concentration of CuO was set as 2.0 g L^{-1}. The initial concentration of Br was set to 1.0 mg L^{-1}; The reaction time was 72 h.

After the reaction, the water was filtered with a 0.45 μm membrane and quenched

with ascorbic acid. All experiments were repeated twice and relative percent differences (RPDs) were less than 20%.

3.2 Results and discussion

3.2.1 Catalytic effect of CCPs on EPS

A batch experiment was conducted to evaluate the formation of DBPs using HA and EPS as precursors. The C/N ratios of HA and EPS were 9.4 and 2.6, respectively. Results As shown in Figure 3.1-3.4, when HA and EPS were used as precursors, the yield of DBPs was 181.6 µg L^{-1} and 146.7 µg L^{-1}, respectively. The yield of N−DBPs was 5.8 µg L^{-1} and 22.0 µg L^{-1}, respectively, accounting for 3.2% and 15.0%. These results indicated that HA had a higher potential of DBPs generation, while EPS showed a higher potential of N−DBPs generation, due to the higher nitrogen content of EPS. Experimental results of the toxicity of DBPs on Chinese hamster ovary cells showed that the cytotoxicity and genotoxicity of N−DBPs were about 100 and 10 times higher than HAAs [17,18] .Therefore, although the concentration of Biofilm EPS in water is lower than NOM, the health risk it poses also needs to be paid attention to.
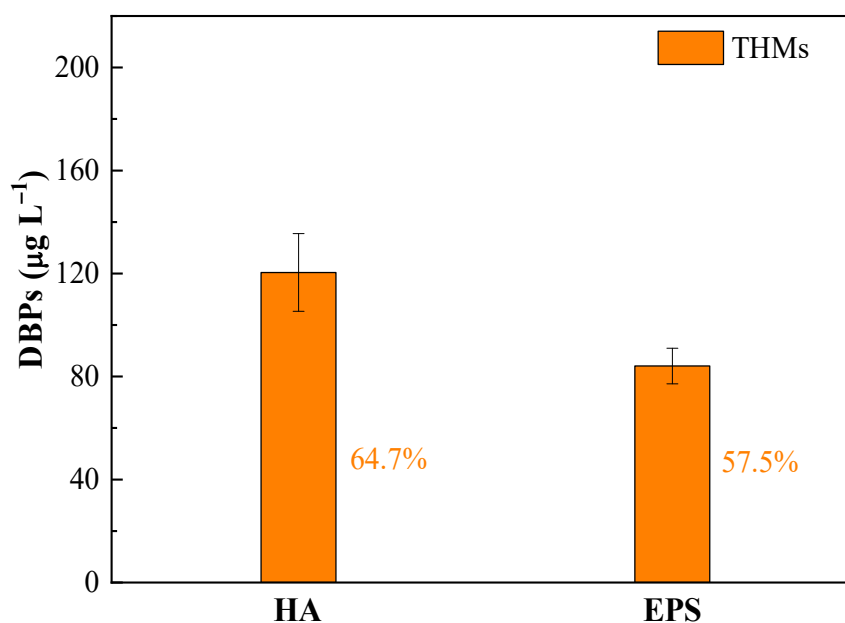
Fig. 3.1 Formation of THMs from HA and EPS
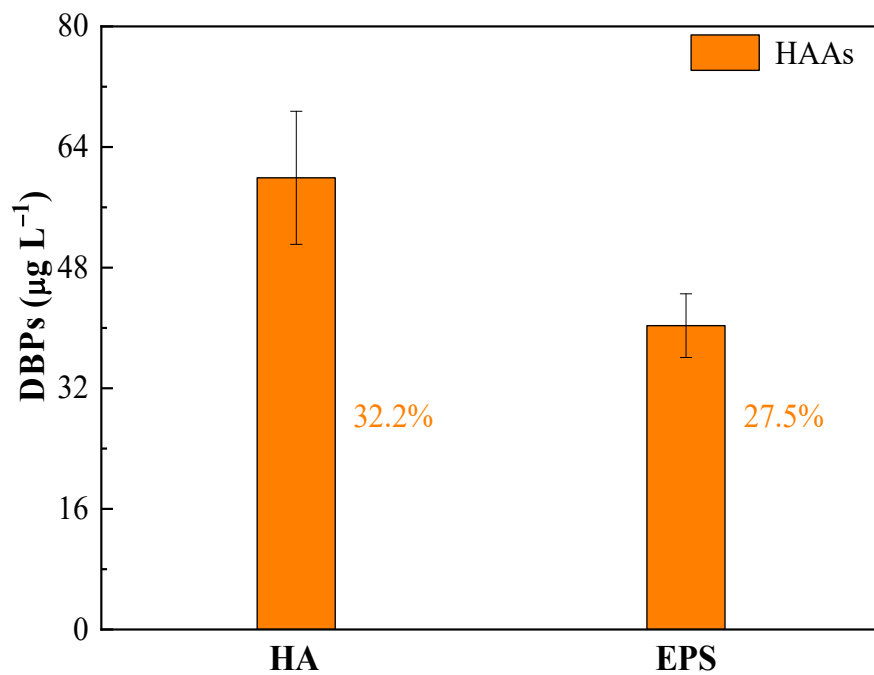
Fig. 3.2 Formation of HAAs from HA and EPS
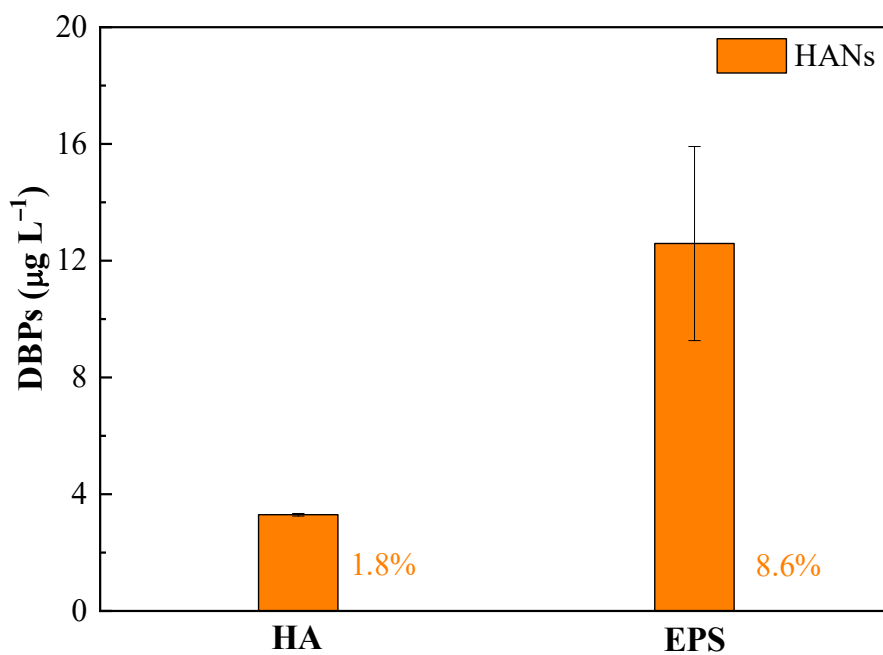
Fig. 3.3 Formation of HANs from HA and EPS
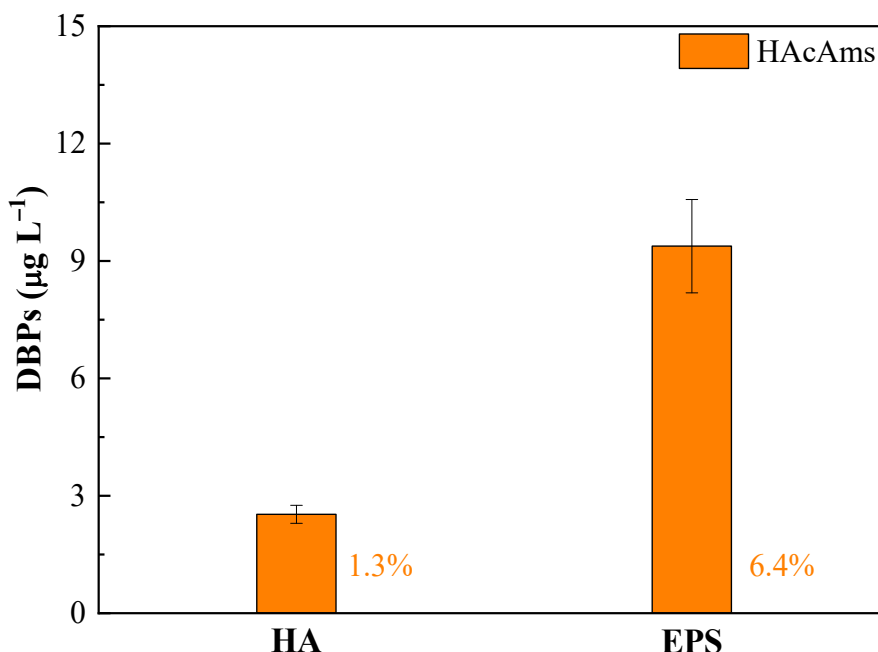
Fig. 4.4 Formation of HAcAms from HA and EPS

As shown in Figure 3.5-3.8, in the presence of CCPs, both Cu^{2+} (2.0 mg L^{-1}) and CuO (2.0 g L^{-1}) have good catalytic enhancement effects. For example, Cu^{2+} and CuO promoted THMs by 77.0% and 17.1%, respectively. Compared with C−DBPs, CCPs has better catalytic promotion effect on N−DBPs. For example, Cu^{2+} promotes the production of THMs, HAAs, HANs and HAcAms by 77.0%, 59.0%, 187.1% and 204.6%, respectively. This result further indicates that EPS as a precursor of DBPs in DWDS should get more attention.

It has been reported that when HA is used as a precursor, the catalytic enhancement effect of Cu^{2+} is achieved by accelerating the ionization of carbonyl and hydroxyl groups through homogeneous catalysis [19] . When EPS is used as a precursor, because it is rich in protein, it can be complexed with Cu^{2+} (CuOX and $CuHOX^+$, X stands for carboxyl group) through spontaneous decarboxylation [6,20].Cuo-dominated heterogeneous catalytic reactions occur through polarization of Cl atoms in HOCl/OCl^-, which has two effects on DBPs generation. On the one hand, CuO polarization of Cl can enhance the electrophilicity of Cl atoms and thus promote the electrophilic substitution reaction of HOCl/OCl^-, which will significantly increase

the production of DBPs [4].On the other hand, CuO polarization of Cl can also promote the attenuation of HOCl/OCl⁻ through disproportionation reaction and oxygen production reaction (as shown in equations 3−1 and 3−2) [14]:

$$2HOCl \xrightarrow{CuO} 2Cl^- + O_2 + 2H^+ \qquad\qquad (3-1)$$

$$3HOCl \xrightarrow{CuO} 2Cl^- + ClO_3^- + 3H^+ \qquad\qquad (3-2)$$

The decay rates of Cl catalyzed by CuO are 10.8, 9.5 and 2.7 M^{-1} s^{-1} at pH 6.6, 7.6 and 8.6, respectively. In general, the reaction rate of HOCl/OCl⁻ and NOM is less than 100 M^{-1} s^{-1}[21,22]. Therefore, Cl attenuation caused by CuO catalysis may delay the reaction of HOCl/OCl⁻ with EPS. In addition, EPS organic groups are attracted to the positively charged CuO surface, thus enhancing the interaction between EPS and HOCl/OCl⁻. Although the presence of CuO has two opposite effects on DBPs generation, the final results show that the presence of CuO significantly promotes DBPs generation.
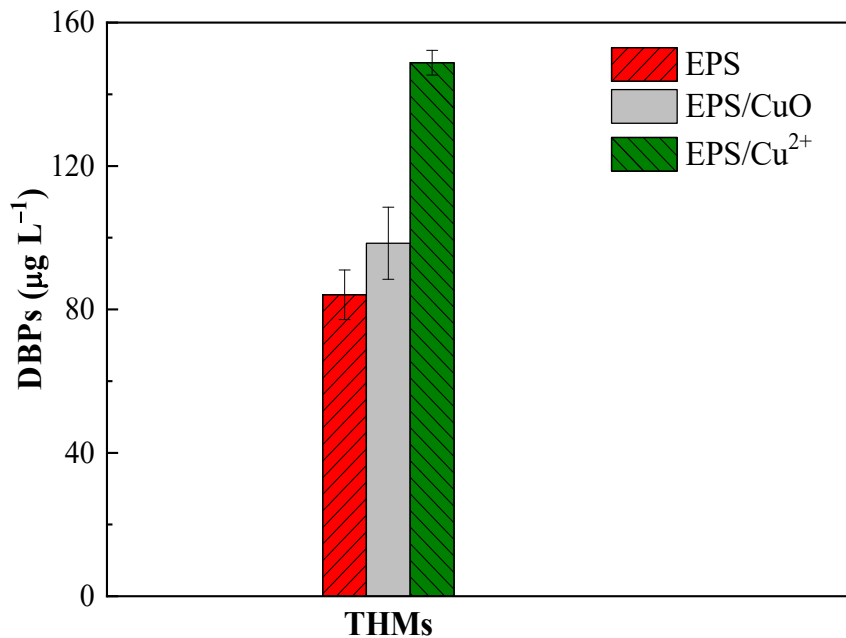
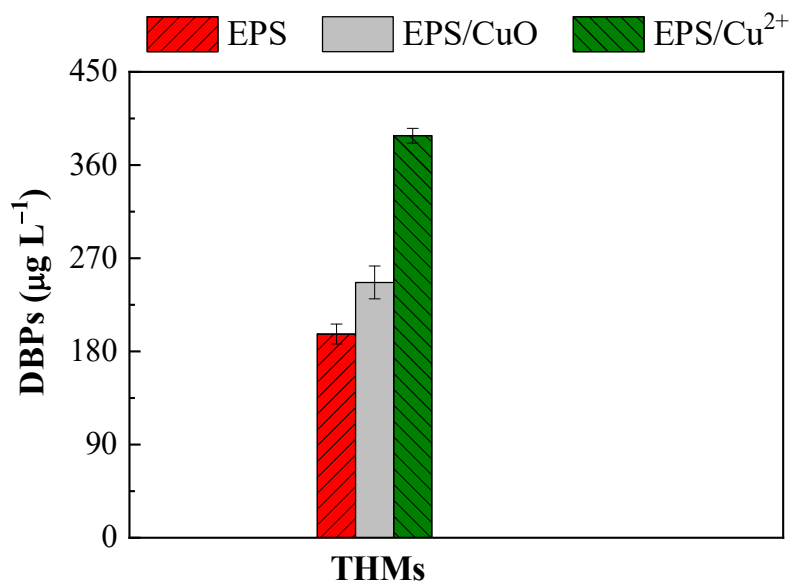**Fig. 3.5 Catalytic formation of THMs from EPS**
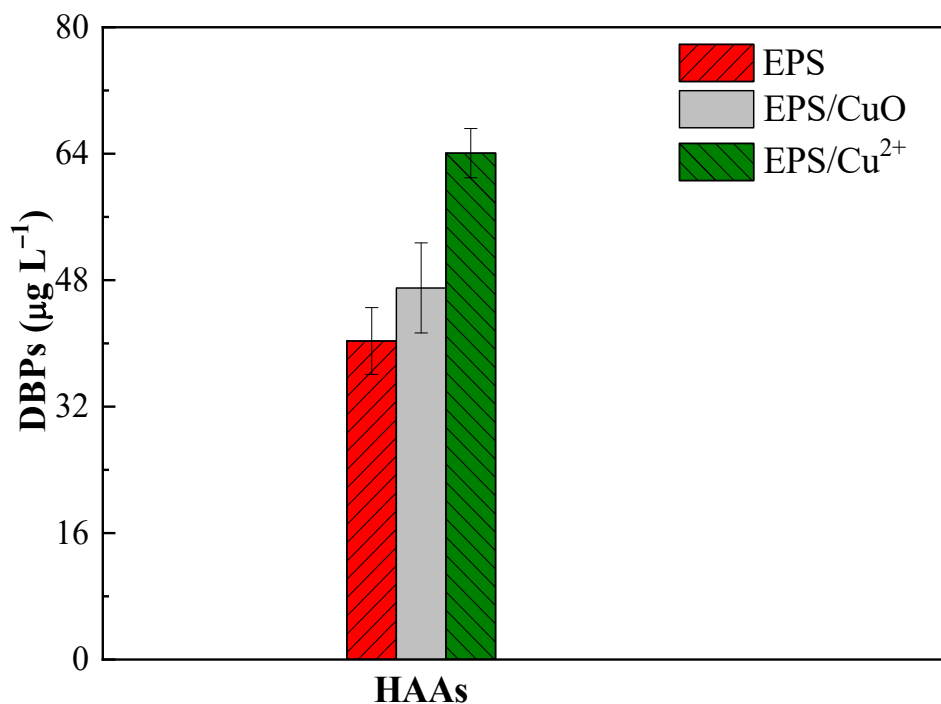
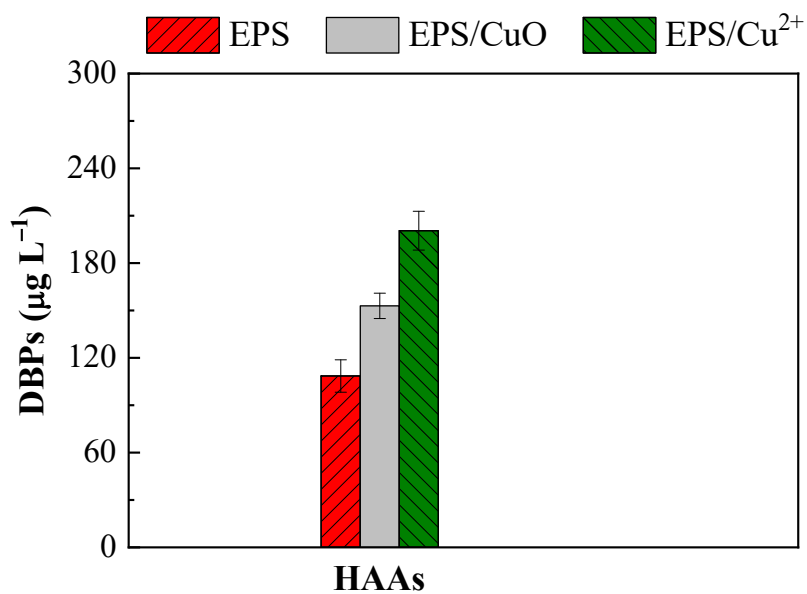**Fig. 3.6 Catalytic formation of HAAs from EPS**
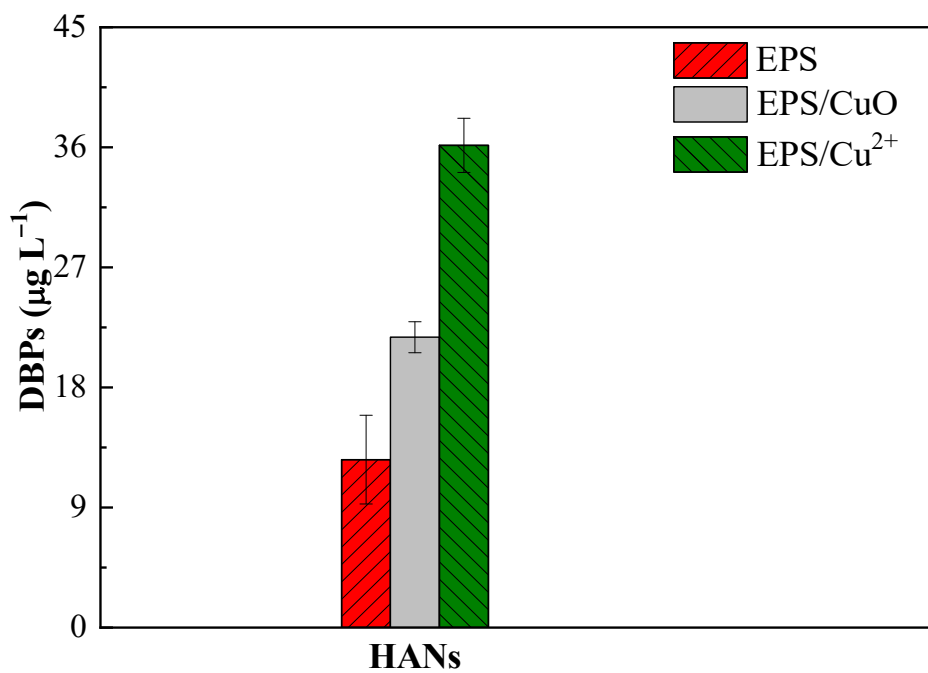
Fig. 3.7 Catalytic formation of HANs from EPS
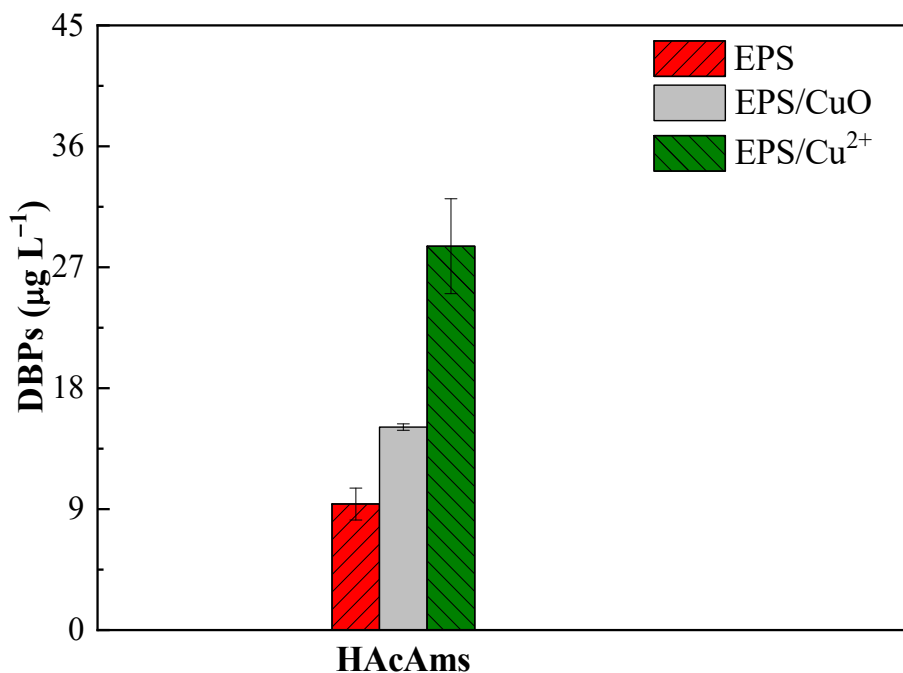
Fig. 3.8 Catalytic formation of HAcAms from EPS

3.2.2 Effects of pH

The reaction process of DBPs catalyzed by EPS was studied in the pH range of 6.6−9.6. As shown in Figure 3.9−3.12, in the absence of CCPs, the production of THMs, HAAs and HANs decreased from 93.2, 46.5 and 11.3 µg L^{-1} to 44.5, 18.9 and 2.2 µg L^{-1}, respectively, when pH increased from 6.6 to 9.6, showing a decreasing trend with increasing pH. The production of HAcAms reached the maximum value when pH=7.6. This is because in the case of higher pH, HOCl/OCl$^-$ mainly exists in the form of OCl$^-$, and the reactivity of OCl$^-$ is weaker than that of HOCl, even though higher pH can promote the occurrence of decarboxylation and hydrolysis [23]. The difference in HAcAms is due to the large difference between the hydrolysis rates of HANs and HAcAms in the pH range of 7−8 [24]. At the same time, it was found that pH significantly affected the catalytic effect of CCPs, the higher the pH, the better the catalytic enhancement effect of CCPs. For example, CuO's promoting effect on HAcAms increased from 28.4% to 72.2% as pH increased from 6.6 to 9.6. On the one hand, higher pH can promote the ionization of carboxyl, carbonyl and hydroxyl

groups in EPS [15,20]. On the other hand, as pH increases from 6.6 to 9.6, Cu^{2+} gradually converts to $Cu(OH)^+$ and $Cu(OH)_2$, weakening the positive charge on the surface. The final results show that higher pH promotes the electrostatic interaction between Cu^{2+} and EPS. The influence of pH on CuO catalysis is similar to that of Cu^{2+}. In addition, alkaline conditions can also promote the deprotonation of HOCl, thus strengthening the electrostatic interaction between OCl^- and the positively charged CuO surface and promoting the formation of CuO−OCl complex, which is conducive to the catalytic effect of CuO on EPS [14].
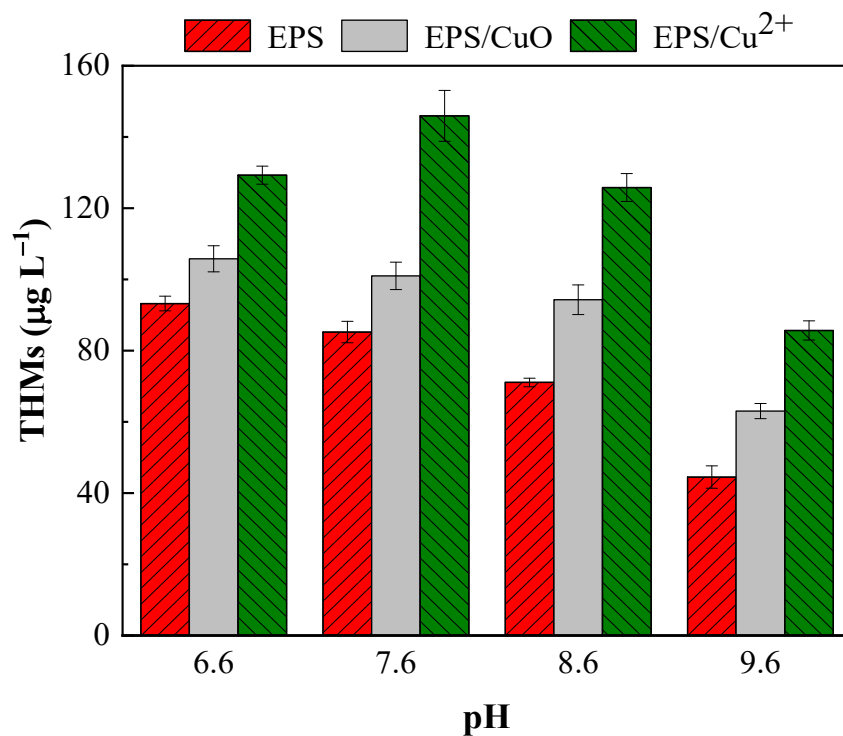
Fig. 3.9 Effect of pH on the catalytic formation of THMs from EPS
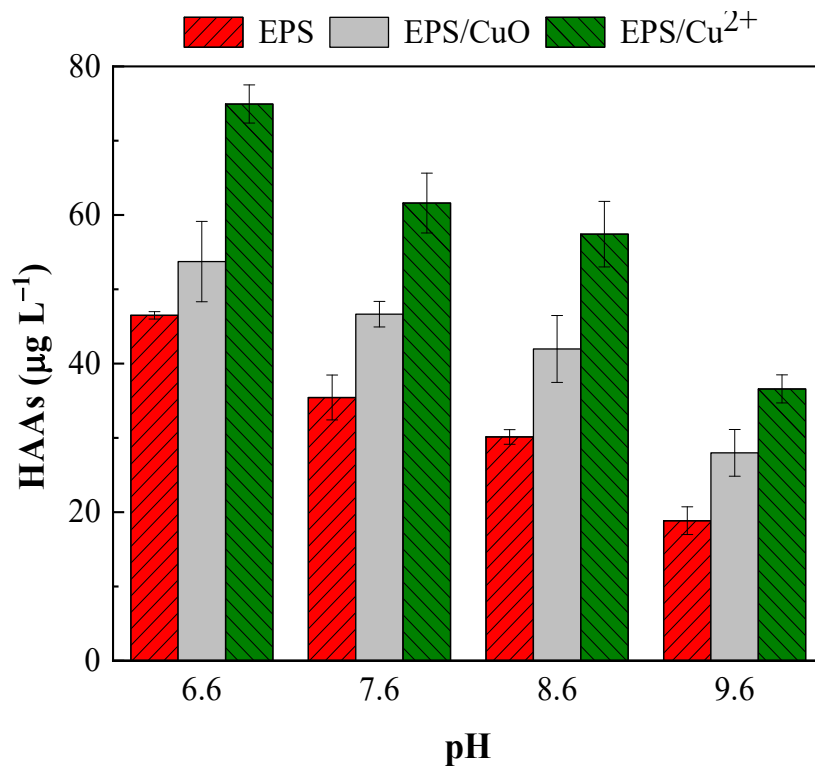
Fig. 3.10 Effect of pH on the catalytic formation of HAAs from EPS
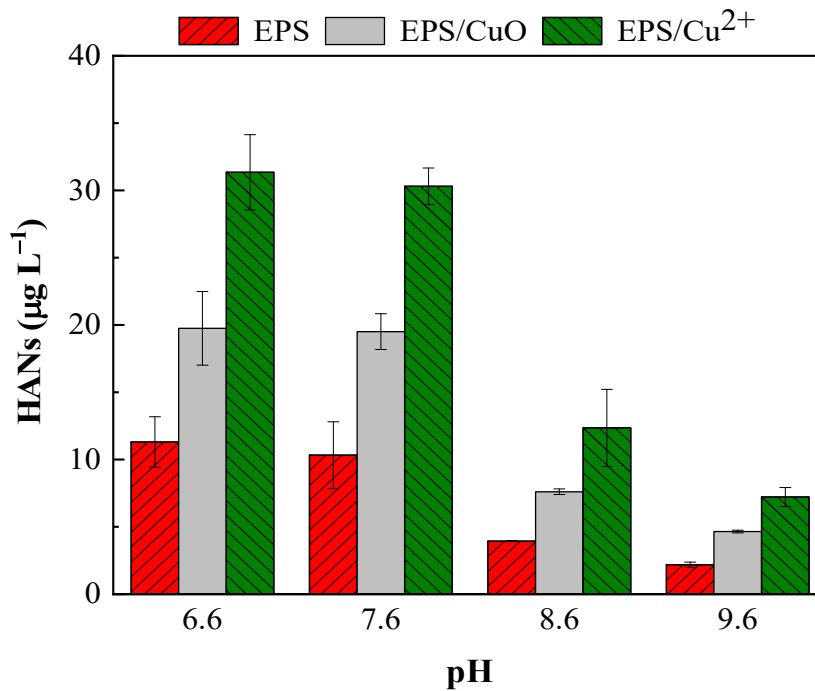
Fig. 3.11 Effect of pH on the catalytic formation of HANs from EPS
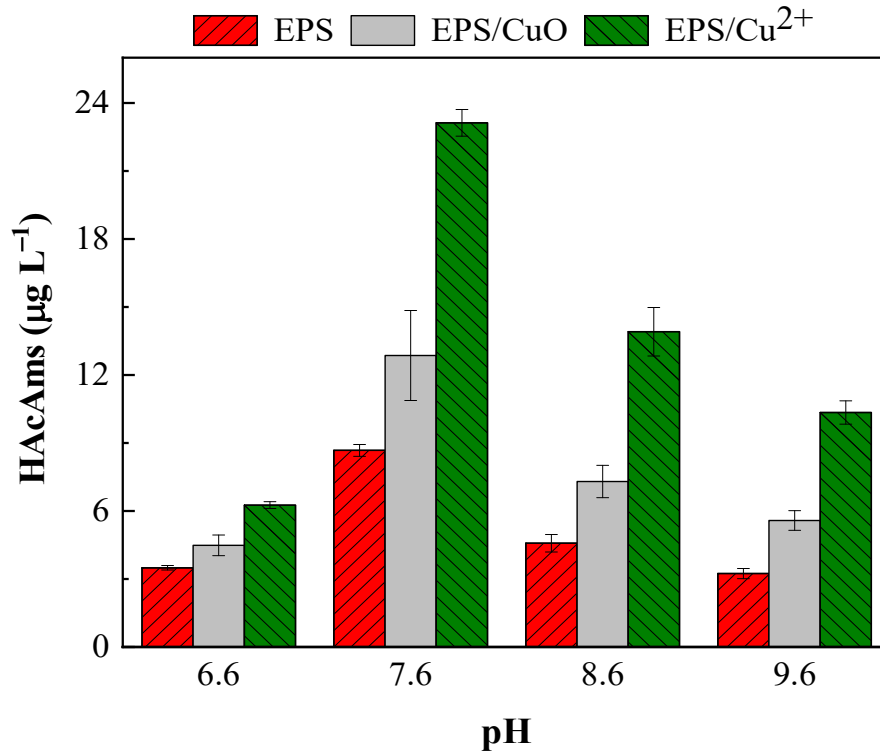
Fig. 3.12 Effect of pH on the catalytic formation of HAcAms from EPS

3.2.3 Effects of Br⁻

In this section, the effect of Br⁻ on CCPs catalytic DBPs generation is measured using bromine Utilization factor (BUF, Bromine Incorporation Factor) and Bromine Incorporation Factor (BIF, Bromine Incorporation Factor) [25]. BUF is the percentage of Br⁻ used to generate Br−DBPs. The BUF value ranges from 0 to 1. BIF refers to the proportion of Br−DBPs partially or completely replaced by Br−DBPs. The value of BIF varies from 0 to 3. BUF and BIF are calculated as follows:

$$BUF(THMs) = \frac{[BDCM] + 2[DBCM] + 3[TBM]}{[Br^-]} \tag{3-3}$$

$$BUF(HAAs) = \frac{[BAA] + [BCAA] + [BDCAA] + 2[DBAA] + 2[DBCAA] + 3[TBAA]}{[Br^-]} \tag{3-4}$$

$$BUF(HANs) = \frac{[BAN] + [BCAN] + [BDCAN] + 2[DBAN] + 2[DBCAN] + 3[TBAN]}{[Br^-]} \tag{3-5}$$

$$BUF(HAcAms) = \frac{[BAcAm]+[BCAcAm]+[BDCAcAm]+2[DBAcAm]+2[DBCAcAm]+3[TBAcAm]}{[Br^-]} \qquad (3-6)$$

$$BIF(THMs) = \frac{[BDCM]+2[DBCM]+3[TBM]}{[THMs]} \qquad (3-7)$$

$$BIF(HAAs) = \frac{[BAA]+[BCAA]+[BDCAA]+2[DBAA]+2[DBCAA]+3[TBAA]}{[HAAs]} \qquad (3-8)$$

$$BIF(HANs) = \frac{[BAN]+[BCAN]+[BDCAN]+2[DBAN]+2[DBCAN]+3[TBAN]}{[HANs]} \qquad (3-9)$$

$$BIF(HAcAms) = \frac{[BAcAm]+[BCAcAm]+[BDCAcAm]+2[DBAcAm]+2[DBCAcAm]+3[TBAcAm]}{[HAcAms]} \qquad (3-10)$$

As shown in Figure 3.13-3.16, in the absence of CCPs, BUF and BIF of C−DBPs are higher than that of N−DBPs, indicating that most Br$^-$ is inserted into the precursor of C−DBPs. As expected, BUF and BIF values showed an upward trend after the addition of CCPs, especially C−DBPs. For example, after adding Cu^{2+}, the BUF and BIF values of THMs increased from 0.11 to 0.15 and from 1.59 to 2.02, respectively. The results show that CCPs can improve the utilization rate of Br$^-$ and promote the transformation of various brominated compounds. However, CCPs had better catalytic enhancement in the absence of Br$^-$. For example, in the presence and absence of Br$^-$, CuO promoted HAcAms by 25.7% and 61.1%, respectively (Figure 1−4 and 13−16). Westerhoff et al. [22] reported that oxidant consumption involves two distinct stages of reaction (rapid initial stage and slow continuous stage). In the slow continuous phase, the second-order rate constants of HOBr/OBr$^-$ for less reactive substances are 20−30 times that of HOCl/OCl$^-$ 15−167 M^{-1} s^{-1} and 0.7−5 M^{-1} s^{-1}, respectively. On the other hand, at pH 7.6, the ratio of OCl$^-$ to HOCl/OCl$^-$ (50%) is higher than that of OBr$^-$ to HOBr/OBr$^-$ (10%). Therefore, in the absence of CCPs, the presence of Br$^-$ can greatly improve DBPs generation. However, CCPs did not achieve better

promotion effect due to the limitation of precursor concentration. In conclusion, CCPs may achieve a relatively higher promotion effect by enhancing the interaction between HOCl/OCl$^-$ and the low active components in EPS.
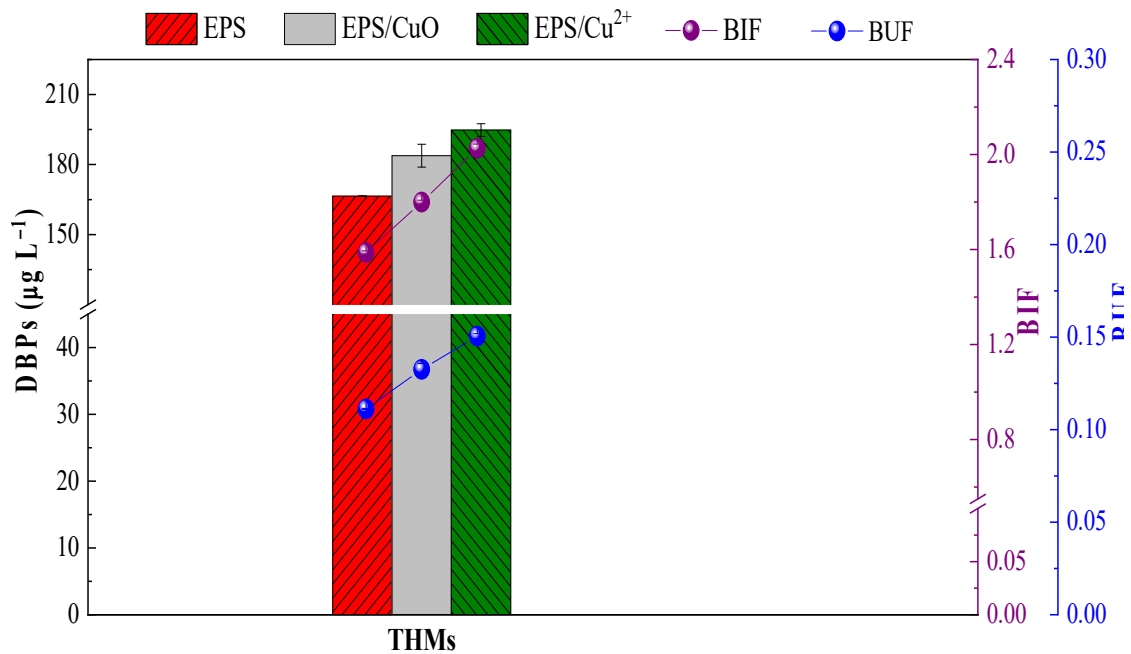
Fig 3.13 Effect of Br$^-$ on the catalytic formation of THMs from EPS
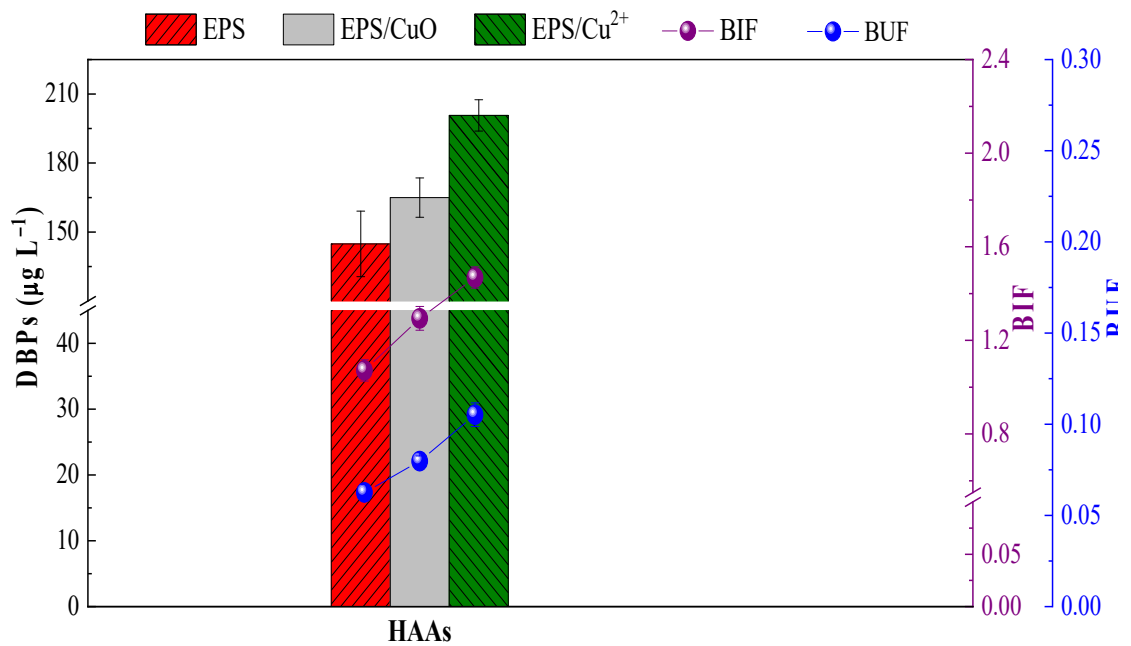
Fig 3.14 Effect of Br$^-$ on the catalytic formation of HAAs from EPS
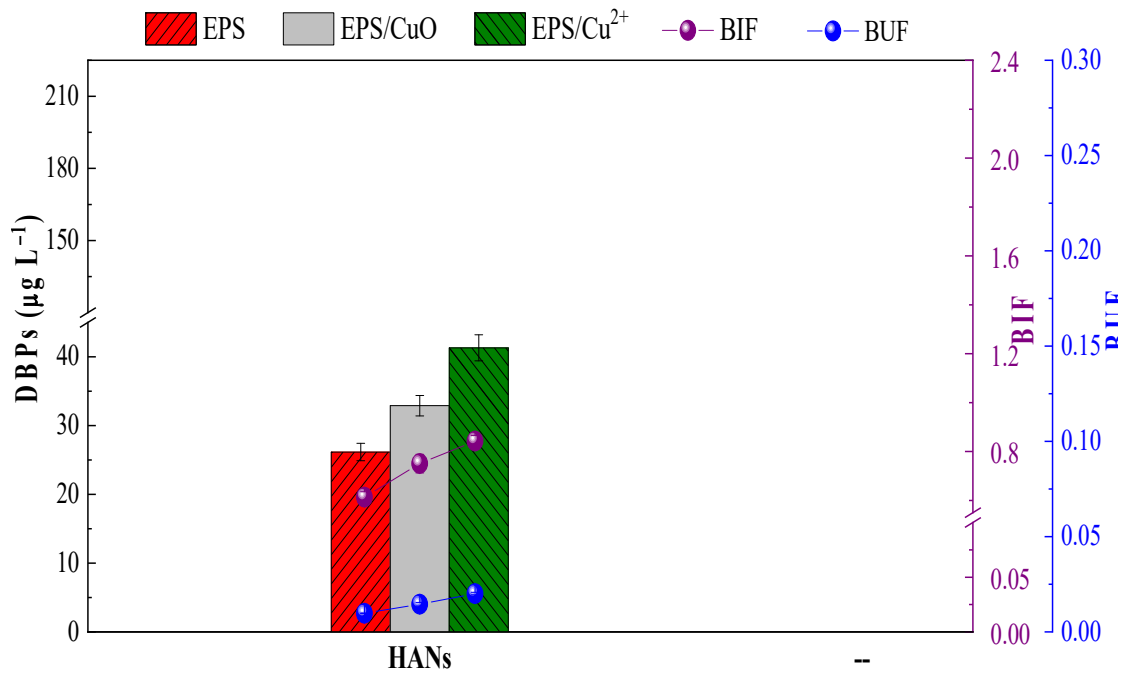
Fig 3.15 Effect of Br⁻ on the catalytic formation of HANs from EPS
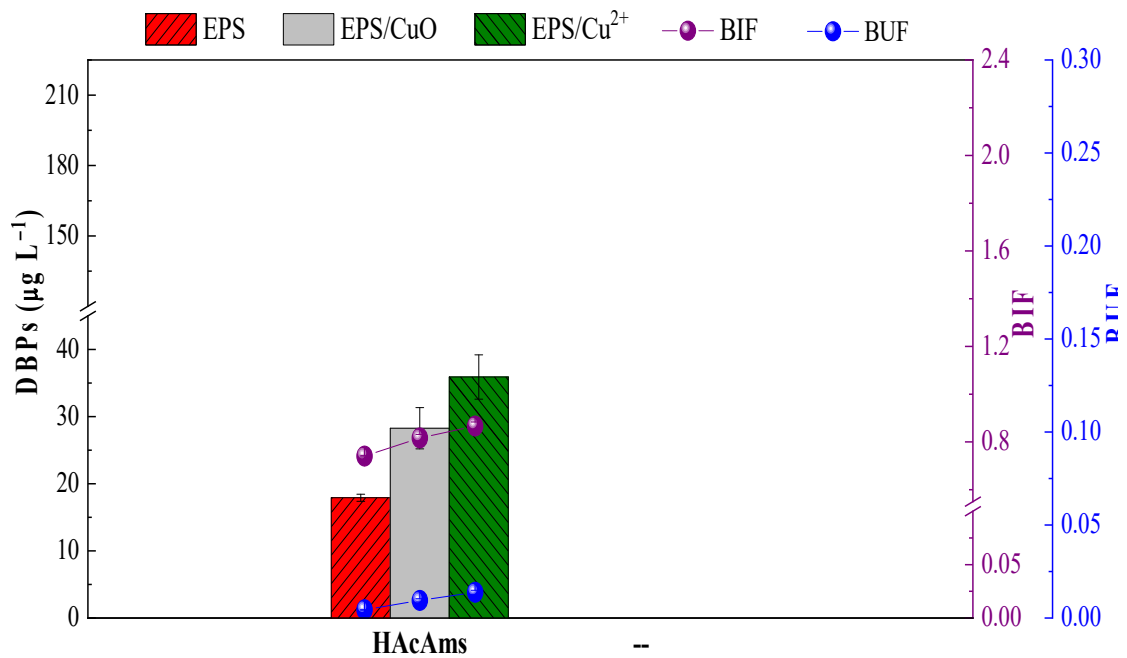
Fig 3.16 Effect of Br⁻ on the catalytic formation of HAcAms from EPS

3.2.4 Catalytic effect of CCPs on EPS protein and polysaccharide

According to literature reports [26], protein and polysaccharide are the main components in EPS (accounting for about 80%), so we extracted these two substances as precursors (3.0 mg C L^{-1}) for further study to evaluate the catalytic effect of CCPs. As shown in Figure 3.17−3.24, when CCPs are absent, polysaccharides cannot produce large amounts of DBPs because of their highly saturated carbon ring structure. Wang et al. [6] speculated that most of the precursors of DBPs were substances with phenolic structure or unsaturated/conjugated carbon bond structure. The polysaccharide monomers in EPS are mainly glucosamine, glucuronic acid, glucose, galactose, rhamnose and mannose. Only glucosamine contains organic nitrogen, which leads to the low N−DBPs production (& LT; 2.0 μg L^{-1}) [5]. The catalytic promotion effect of CCPs on polysaccharide was weaker than that of protein. For example, Cu^{2+} promoted the THMs production of protein and polysaccharide by 97.3% and 20.8%, respectively. The phenolic structure and unsaturated/conjugated groups in proteins have stronger electron absorption capacity than the carbon ring structure with higher saturation in polysaccharides. This results in a higher electron cloud density, which promotes complexation of the protein with Cu^{2+} and positively charged CuO surfaces. However, Liu and Croue[4] found that CuO promoted the less reactive NOMs isolates (which had a fulic acid structure and bound to a rich polysaccharide portion) much more than the more reactive isolates (which had more aromatic/phenolic structures and carboxyl groups) during chlorine bromide. This difference may be attributed to the generation of $HOBr/OBr^-$, which reacts with NOMs at a rate about 10 times $HOCl/OCl^-$ [22]. The presence of Br^- greatly reduces the promotional effect of CCPs because $HOBr/OBr^-$ responds faster than less reactive components such as polysaccharides.

Fig 3.17 Catalytic formation of THMs from EPS proteins

Fig 3.18 Catalytic formation of HAAs from EPS proteins
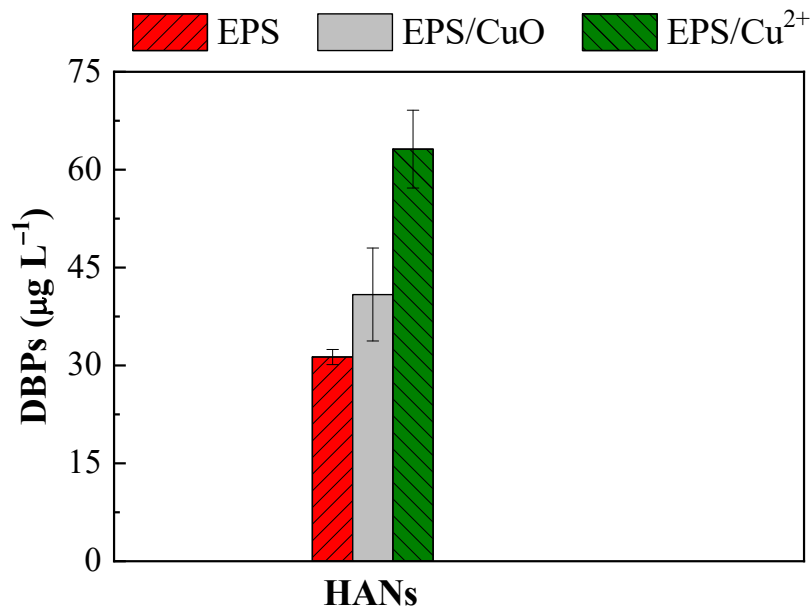
Fig 3.19 Catalytic formation of HANs from EPS proteins
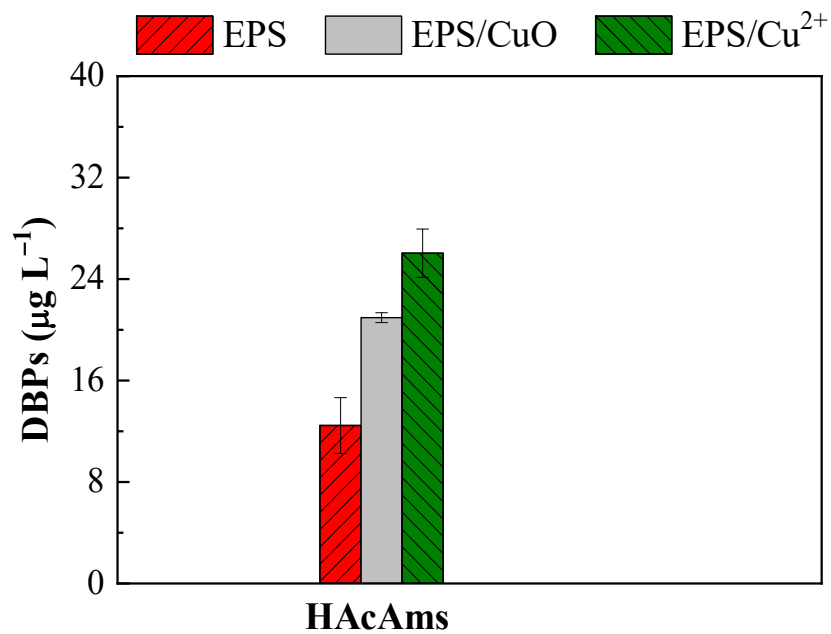
Fig 3.20 Catalytic formation of HAcAms from EPS proteins
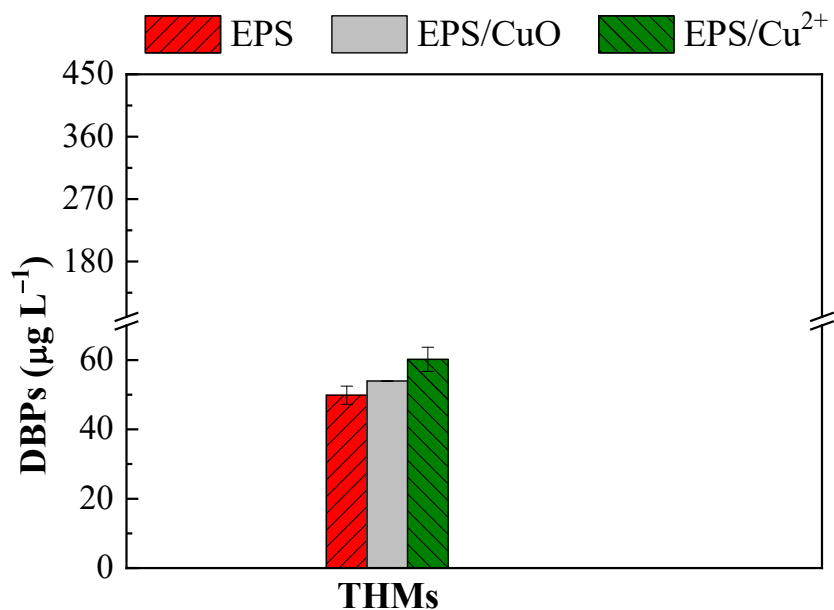
Fig 3.21 Catalytic formation of HAAs from EPS polysaccharides
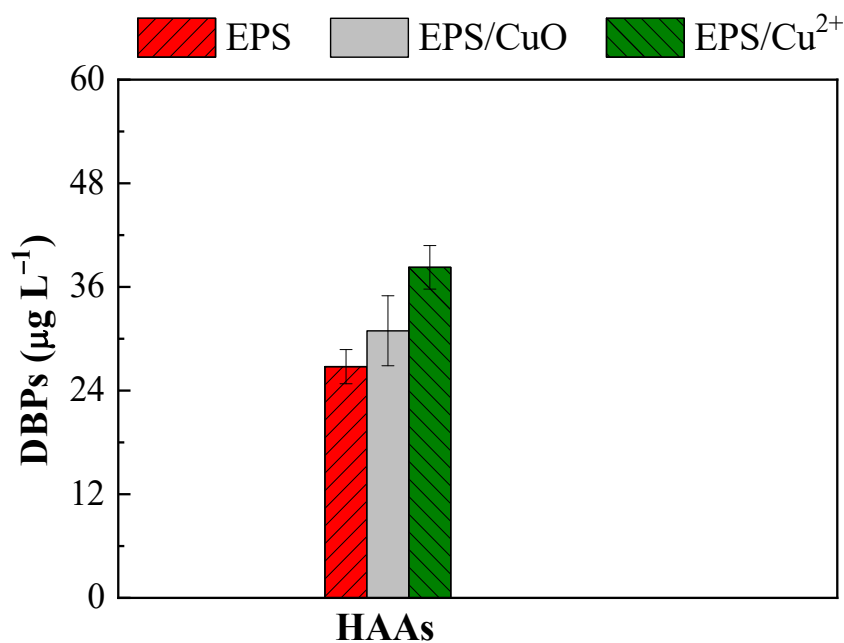
Fig 3.22 Catalytic formation of HAAs from EPS polysaccharides
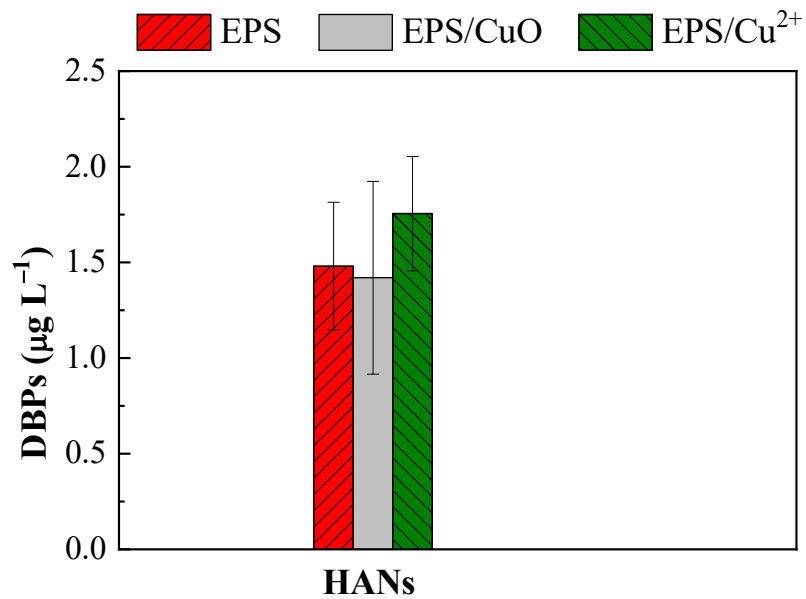
Fig 3.23 Catalytic formation of HANs from EPS polysaccharides
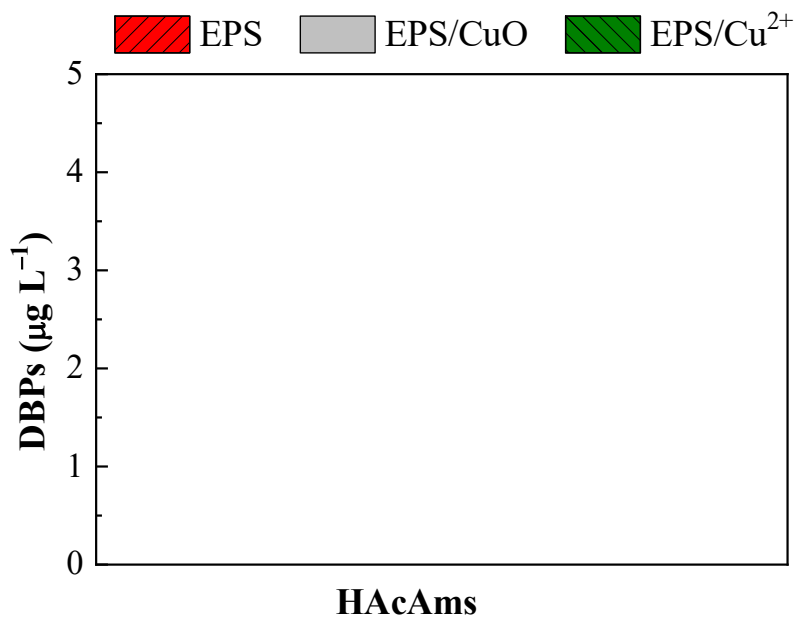
Fig 3.24 Catalytic formation of HAcAms from EPS polysaccharides

(no formation)

3.2.5 Catalytic effect of CCPs on amino acids

As mentioned in the previous section, CCPs mainly catalyzes the generation of DBPs from protein components in EPS. Therefore, we analyzed and identified the extracted proteins to obtain the types and contents of amino acids. As shown in Table 3.1, a total of 20 amino acids were identified, accounting for 99% of the total composition.

Table 3.1 Types and contents of amino acids in EPS protein components

Amino acid	The proportion	Molecular formula	Structure of molecules
Alanine (Ala)	12.0%	$C_3H_7NO_2$	
Glycine (Gly)	9.5%	$C_2H_5NO_2$	
Leucine (Leu)	8.1%	$C_6H_{13}NO_2$	
Valine (Val)	7.7%	$C_5H_{11}NO_2$	
Glutamic acid (Glu)	6.0%	$C_5H_9NO_4$	
Threonine (Thr)	5.6%	$C_4H_9NO_3$	
Serine (Ser)	5.6%	$C_3H_7NO_3$	
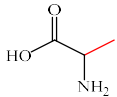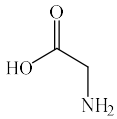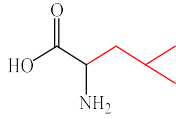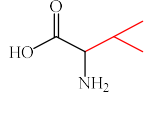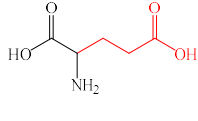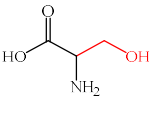
Aspartic acid (Asp)	5.5%	$C_4H_7NO_4$	
Isoleucine (Ile)	5.5%	$C_6H_{13}NO_2$	
Arginine (Arg)	5.0%	$C_6H_{14}N_4O_2$	
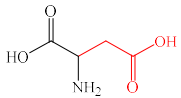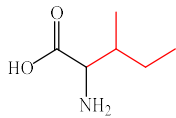
Table 3.1 Types and contents of amino acids in EPS protein components (continued)

Amino acid	The proportion	Molecular formula	Structure of molecules
Lysine (Lys)	4.4%	$C_6H_{14}N_2O_2$	
Proline (Pro)	4.3%	$C_5H_9NO_2$	
Asparagine (Asn)	3.9%	$C_4H_8N_2O_3$	
Phenylalanine (Phe)	3.7%	$C_9H_{11}NO_2$	
Glutamine (Gln)	3.1%	$C_5H_{10}N_2O_3$	
Tyrosine (Tyr)	2.5%	$C_9H_{11}NO_3$	
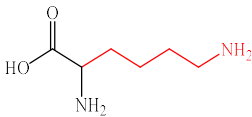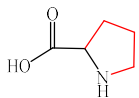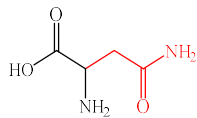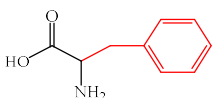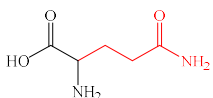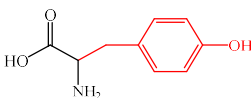
Methionine (Met)	2.5%	$C_5H_{11}NO_2S$	
Histidine (His)	1.9%	$C_6H_9N_3O_2$	
Cysteine (Cys)	1.2%	$C_3H_7NO_2S$	
Tryptophan (Trp)	1.0%	$C_{11}H_{12}N_2O_2$	
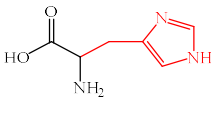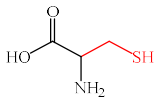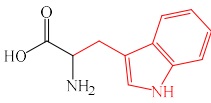
The effect of chemical structure of amino acids on CCPs catalysis was illustrated by using amino acids as precursors alone (3.0 mg C L^{-1}). As shown in Figure 3−6, in the absence of CCPs, Trp and Tyr have high potential for THMs generation, generating 314.8 and 150.6 μg L^{-1} THMs, respectively. Asn, Asp, His, Trp and Tyr can generate more HAAs. 80.2, 187.1, 102.2, 261.9 and 254.2 μg L^{-1}, respectively. Considering the contents of different amino acids in EPS protein, Tyr and Asp are considered to be the main contributors to the production of THMs and HAAs, respectively. Meanwhile, Ala, Asn, Asp, His, Trp and Tyr are the main precursors for the generation of HAcAms and HANs. In the absence of CCPs, Ala has better n-DBPs generation potential, second only to Asn, and Ala is the highest content of amino acid in EPS protein (12.0%), so it is the most important precursor of N−DBPs in EPS protein. These results are consistent with previous studies on DBPs generation using amino acids as precursors [27-30]. As shown in Figure 3.25-3.28, Asn, Asp, His, Trp and Tyr are the main contributors to DBPs generation among the 20 amino acids. Therefore, the influence of chemical structure on catalysis is mainly studied for these five amino acids.
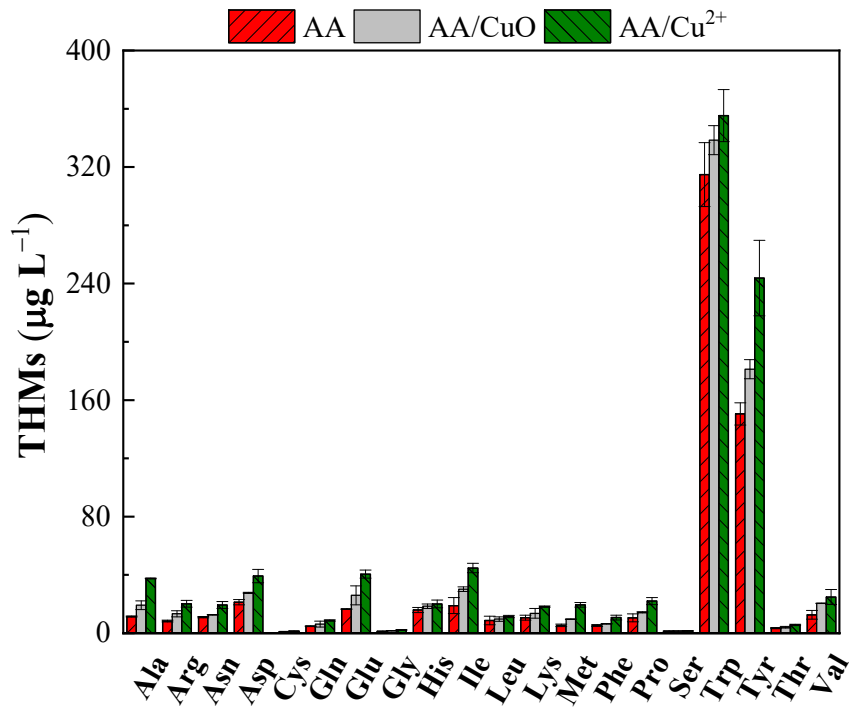
Fig 3.25 Catalytic formation of THMs from twenty amino acids (AAs)
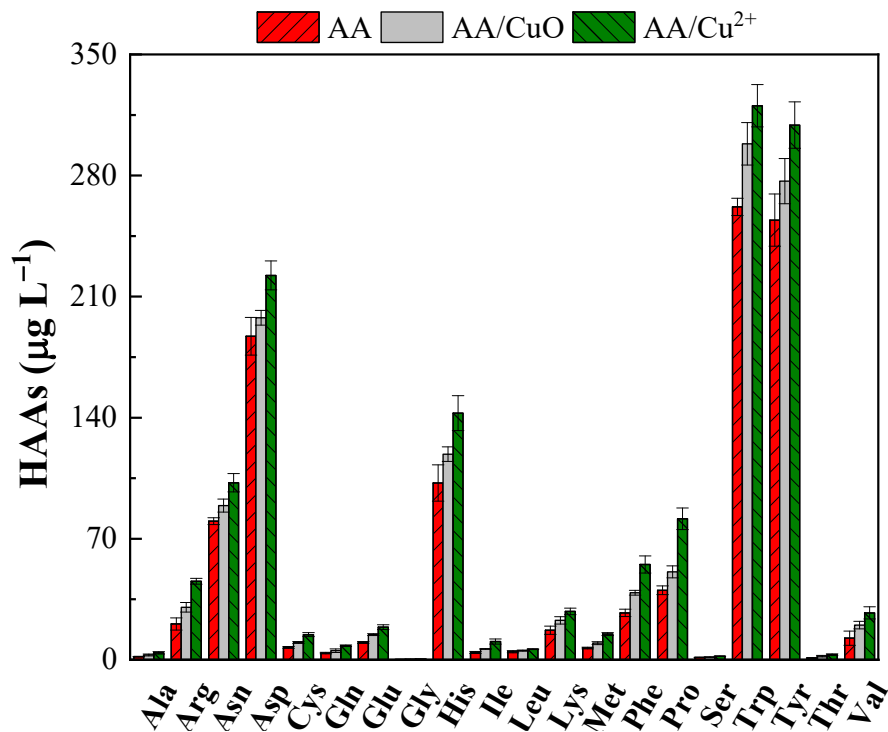
Fig 3.26 Catalytic formation of HAAs from twenty amino acids (AAs)
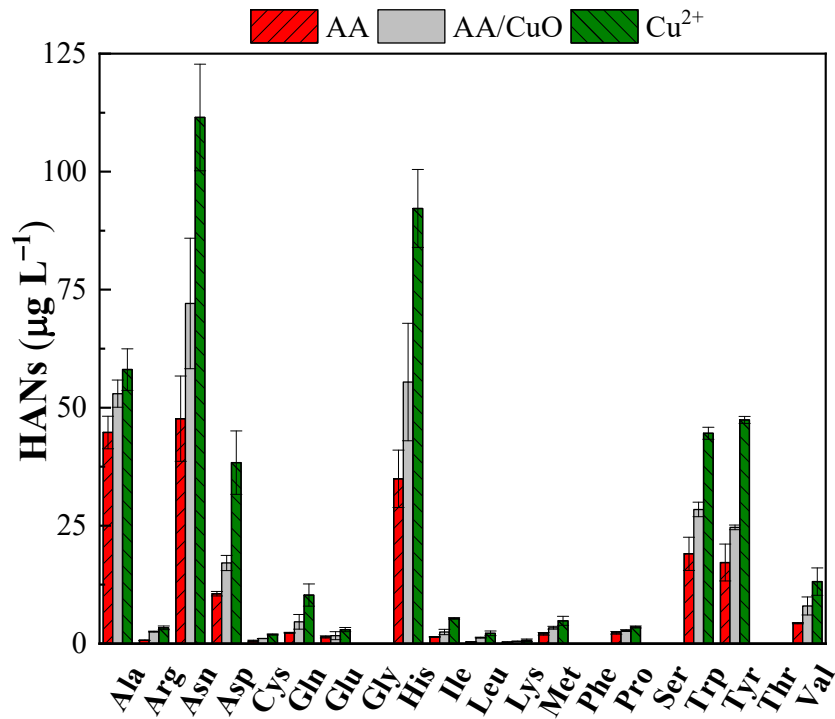
Fig 3.27 Catalytic formation of HANs from twenty amino acids (AAs)
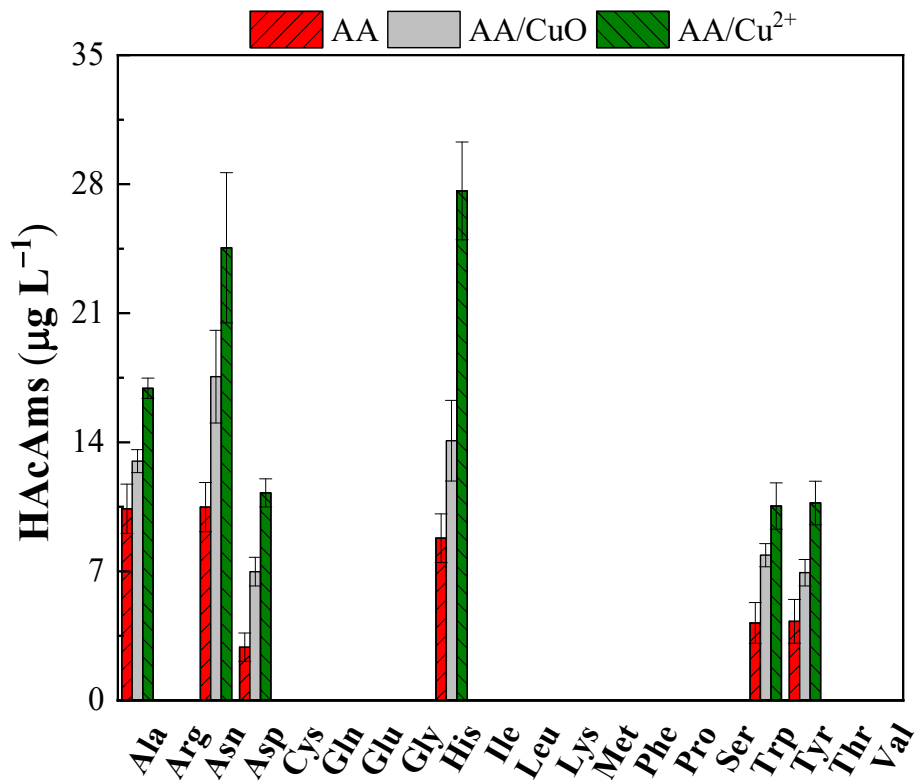
Fig 3.28 Catalytic formation of HAcAms from twenty amino acids (AAs)

The catalytic mechanism of CCPs is shown in Figure 3.29.

In terms of THMs generation, CCPs had a stronger promotion effect on Tyr than Trp. For example, Cu^{2+} promoted THMs formation of Tyr and Trp by 61.9% and 12.9%, respectively. Studies have shown that decarboxylation and chlorine substitution of Tyr can generate 4−hydroxyl−benzyl cyanide (4−HBC) and 2,4,6−trichlorophenol (2,4,6−TCP), among which the opening of benzene ring in 2,4,6−TCP is one of the main pathways of THMs generation [24].At present, the mechanism of the formation of THMs caused by Trp in the chlorination process has not been fully elucidated, but based on the atomic potential diagram of Trp (Figure 3.30), the breaking of C2−C3 and C4−C7 bonds (decarboxylation and chlorine substitution) is relatively easy to occur, resulting in the formation of 2−(indole-3-yl) cyanide (2−IAN) and 2−indole-3-yl (2−IC). The rupture of C7=C8 bond in pentacyclic ring is a key step in the generation of THMs [31]. CCPs have different catalytic capacities for benzene ring cleavage of 2,4,6−TCP and pentacyclic cleavage of 2−IC, which leads to different promoting effects on THMs generation of Tyr and Trp. First, N atoms in 2−IC have fewer lone pairs of electrons than O atoms in 2,4,6−TCP [32,33]. Second, the N atom in the pentacyclic ring can contribute its lone pair electrons to form p−π conjugation with π electrons in the C7=C8 bond other than the adjacent benzene ring [34]. The decrease of electron cloud density around N atom is not conducive to the complexation with CCPs, so the promoting effect of CCPs is weakened.

For HAAs generation, His showed the highest potential in the five amino acids under the catalytic action of CCPs. For example, Cu^{2+} promoted His, Asn, Asp, Trp and Tyr by 39.5%, 27.7%, 18.8%, 22.3% and 21.6%, respectively. According to literature reports, HAAs generation mechanisms mainly include decarboxylation, chlorine substitution and elimination of variable (R ') groups [28,35,36]. Similar to the principle of THMs generation, CCPs has different promotion effects on the elimination of different R 'groups, which plays an important role in promoting HAAs generation. Electrons in R 'groups are transferred by CCPs due to complexation,

which promotes the rupture of C−R' bonds.

For N−DBPs generation, CCPs has the best catalytic promotion effect on His among the five amino acids. For example, Cu^{2+} promoted His, Asn, Asp, Trp and Tyr by 214.2%, 134.1%, 116.7%, 151.0% and 149.5%, respectively. CCPs catalyzed the formation of HAAs, HANs and HAcAms in the five amino acids with consistent results, due to their associated production pathways. Elimination of R 'groups of amino acids after chlorine substitution and decarboxylation leads to the formation of HANs, whose further hydrolysis leads to the formation of HAcAms and HAAs[28,37,38]. Therefore, CCPs promotes the elimination of His imidazole pentacyclic ring, thus enhancing the generation of N−DBPs.
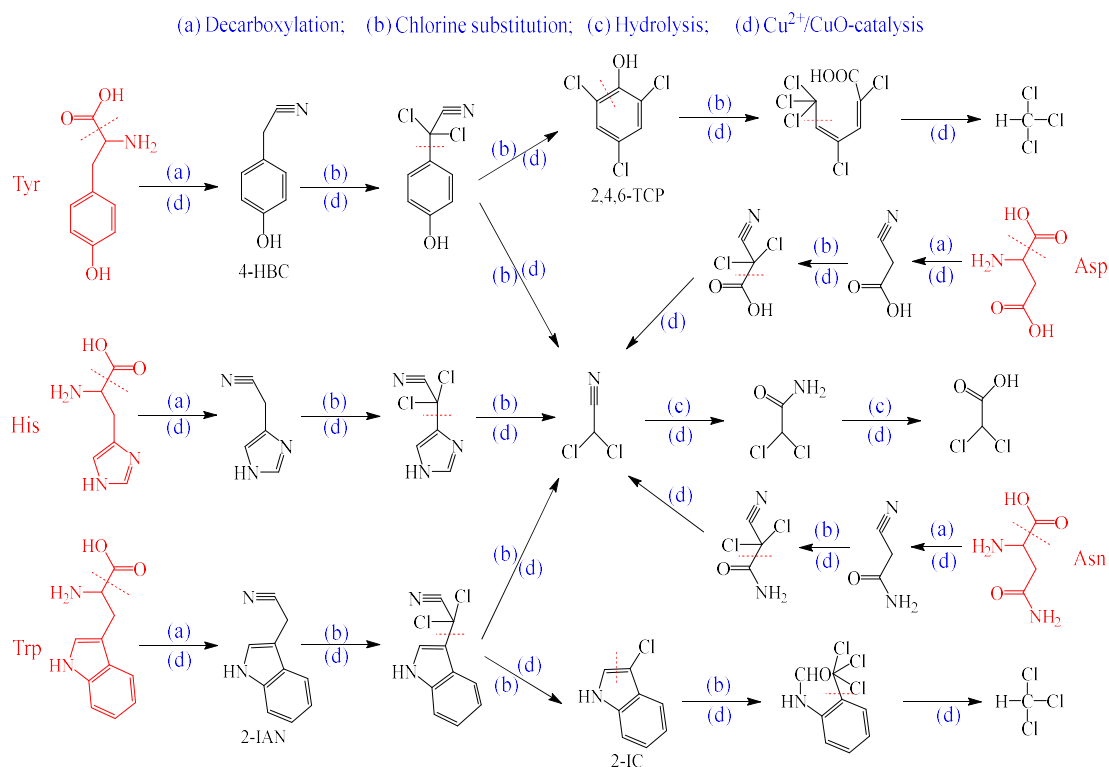
Fig 3.29 Proposed catalytic mechanism of the DBPs formation from amino acids
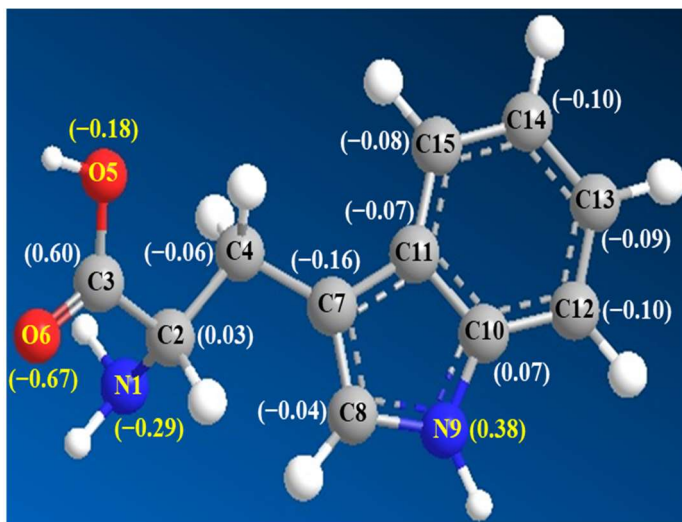
Fig 3.30 Atomic potentials in Trp

3.3 Conclusions

In this chapter, the catalytic effect of CCPs (CuO and Cu^{2+}) on the formation of C−DBPs and N−DBPs was studied using EPS and its components (protein and polysaccharide) as precursors. Based on the experimental results, the following conclusions are drawn:

（1）CCPs significantly promoted DBPs generation, especially N−DBPs. At the same time, the catalytic promotion effect of Cu^{2+} is better than that of CuO.

（2）pH has an important influence on the catalytic promotion effect of CCPs on C−DBPs and N−DBPs, and CCPs has better promotion effect under alkaline condition.

（3）CCPs can enhance BUF and BIF of Br^- and thus enhance Br−DBPs formation, but Br^- can weaken the catalytic effect of CCPs.

（4）The protein component of EPS catalyzed more DBPs than polysaccharide component. CCPs has similar catalytic effects on twenty common amino acids. CCPs had the best effect on Tyr catalytically generating THMs, while His showed the highest amount of catalytic production in HAAs, HANs and HAcAms.

Reference

[1]   Lin Y-P, Washburn M P, Valentine R L. Reduction of Lead Oxide (PbO2) by Iodide and Formation of Iodoform in the PbO2/I−/NOM System [J]. Environmental Science & Technology, 2008, 42(8): 2919-24.

[2]   Mckernan S, Carter C B, Ricoult D, et al. High-Resolution Electron Microscopy of Olivine-Magnetite Interfaces [J]. MRS Proceedings, 2011, 159(407.

[3]   Gallard H, Allard S, Nicolau R, et al. Formation of Iodinated Organic Compounds by Oxidation of Iodide-Containing Waters with Manganese Dioxide [J]. Environmental Science & Technology, 2009, 43(18): 7003-9.

[4]   Wingender J, Neu T R, Flemming H C. Microbial Extracellular Polymeric Substances [J]. 1999.

[5]   Wang Z.K., Li. L., Arissd R.W., et al. The role of biofilms on the formation and decay of disinfection by-products in chlor(am)inated water distribution systems [J]. Science of the Total Environment, 2021, 753: 141606.

[6]   Wang Z.K., Choi O.K., Seo Y.W. Relative contribution of biomolecules in bacterial extracellular polymeric substances to disinfection byproduct formation [J]. Environmental Science & Technology, 2013, 47: 9764–9773.

[7]   Richardson S.D., Plewa M.J., Wagner E.D., et al. Occurrence, genotoxicity, and carcinogenicity of regulated and emerging disinfection by-products in drinking water: A review and roadmap for research [J]. Mutation Research-Reviews in Mutation Research, 2007, 636: 178–242.

[8]   Richardson S D, Plewa M J, Wagner E D, et al. Occurrence, genotoxicity, and carcinogenicity of regulated and emerging disinfection by-products in drinking water: A review and roadmap for research [J]. Mutation Research/Reviews in Mutation Research, 2007, 636(1): 178-242.

[9]   Fang J, Ma J, Yang X, et al. Formation of carbonaceous and nitrogenous disinfection by-products from the chlorination of Microcystis aeruginosa [J]. Water Research, 2010, 44(6): 1934-40.

[10] Hu J, Qiang Z, Dong H, et al. Enhanced formation of bromate and brominated disinfection byproducts during chlorination of bromide-containing waters under catalysis of copper corrosion products [J]. Water Research, 2016, 98(302-8.

[11] Bougeard C M M, Goslan E H, Jeffersin B, et al. Comparison of the disinfection by-product formation potential of treated waters exposed to chlorine and monochloramine [J]. Water Research, 2010, 44(3): 729-40.

[12] Li B, Qu J, Liu H, et al. Effects of copper(II) and copper oxides on THMs formation in copper pipe [J]. Chemosphere, 2007, 68(11): 2153-60.

[13] Liu L, Hu Q, Le Y, et al. Chlorination-mediated EPS excretion shapes early-stage biofilm formation in drinking water systems [J]. Process Biochemistry, 2017, 55(41-8.

[14] Murray J.W. The surface chemistry of hydrous manganese dioxide [J]. Journal of Colloid and Interface Science, 1974, 46 (3) : 357−371.

[15] Zhang H, Andrews S A. Factors affecting catalysis of copper corrosion products in NDMA formation from DMA in simulated premise plumbing [J]. Chemosphere, 2013, 93(11): 2683-9.

[16] Blatchley E R, Margetas D, Duggirala R. Copper catalysis in chloroform formation during water chlorination [J]. Water Research, 2003, 37(18): 4385-94.

[17] Plewa M.J., Muellner M.G., Richardson S.D., et al. Occurrence, synthesis, and mammalian cell cytotoxicity and genotoxicity of haloacetamides: An emerging class of nitrogenous drinking water disinfection byproducts [J]. Environmental Science & Technology, 2008, 42 (3) : 955–961.

[18] Muellner M G, Wagner E D, Mccalla K, et al. Haloacetonitriles vs. Regulated Haloacetic Acids: Are Nitrogen-Containing DBPs More Toxic? [J]. Environmental Science & Technology, 2007, 41(2): 645-51.

[19] Zhang H, Andrews S A. Catalysis of copper corrosion products on chlorine decay and HAA formation in simulated distribution systems [J]. Water Research, 2012, 46(8): 2665-73.

[20] Gallard H, Von Gunten U. Chlorination of natural organic matter: kinetics of chlorination and of THM formation [J]. Water Research, 2002, 36(1): 65-74.

[21]   Westerhoff P, Chao P, Mash H. Reactivity of natural organic matter with aqueous chlorine and bromine [J]. Water Research, 2004, 38(6): 1502-13.

[22]   Deborde M, Von G U. Reactions of chlorine with inorganic and organic compounds during water treatment—Kinetics and mechanisms: A critical review [J]. Water Research, 2008, 42(1): 13-51.

[23]   Chu W, Gao N, Krasner S W, et al. Formation of halogenated C-, N-DBPs from chlor(am)ination and UV irradiation of tyrosine in drinking water [J]. Environmental Pollution, 2012, 161(8-14.

[24]   Chu W, Gao N, Yin D, et al. Formation and speciation of nine haloacetamides, an emerging class of nitrogenous DBPs, during chlorination or chloramination [J]. Journal of Hazardous Materials, 2013, 260(806-12.

[25]   Comte S, Guibaud G, Baudu M. Biosorption properties of extracellular polymeric substances (EPS) resulting from activated sludge according to their type: Soluble or bound [J]. Process Biochemistry, 2006, 41(4): 815-23.

[26]   Ueno H, Moto T, Sayato Y, et al. Disinfection by-products in the chlorination of organic nitrogen compounds: By-products from kynurenine [J]. Chemosphere, 1996, 33(8): 1425-33.

[27]   Hong H C, Wong M H, Liang Y. Amino Acids as Precursors of Trihalomethane and Haloacetic Acid Formation During Chlorination [J]. Archives of Environmental Contamination and Toxicology, 2009, 56(4): 638-45.

[28]   Chu W-H, Gao N-Y, Deng Y. Formation of haloacetamides during chlorination of dissolved organic nitrogen aspartic acid [J]. Journal of Hazardous Materials, 2010, 173(1): 82-6.

[29]   Yang X, Shen Q, Guo W, et al. Precursors and nitrogen origins of trichloronitromethane and dichloroacetonitrile during chlorination/chloramination [J]. Chemosphere, 2012, 88(1): 25-32.

[30]   Li C, Lin Q, Dong F, et al. Formation of iodinated trihalomethanes during chlorination of amino acid in waters [J]. Chemosphere, 2019, 217(355-63.

[31]   Gomathi D L, Krishnaiah G M. Photocatalytic degradation of p-amino-azo-benzene and

p-hydroxy-azo-benzene using various heat treated TiO2 as the photocatalyst [J]. Journal of Photochemistry and Photobiology A: Chemistry, 1999, 121(2): 141-5.

[32] M. A. WENDT J. MEILER F. WEINHOLD T. C F. Solvent and concentration dependence of the hydroxyl chemical shift of methanol [J]. Molecular Physics, 1998, 93(1): 145-52.

[33] Shaji S, Eappen S M, Rasheed T M A, et al. NIR vibrational overtone spectra of N-methylaniline, N,N-dimethylaniline and N,N-diethylaniline—a conformational structural analysis using local mode model [J]. Spectrochimica Acta Part A: Molecular and Biomolecular Spectroscopy, 2004, 60(1): 351-5.

[34] Hureiki L, Croué J P, Legube B. Chlorination studies of free and combined amino acids [J]. Water Research, 1994, 28(12): 2521-31.

[35] Li C, Gao N, Chu W, et al. Comparison of THMs and HANs formation potential from the chlorination of free and combined histidine and glycine [J]. Chemical Engineering Journal, 2017, 307(487-95.

[36] Chu W-H, Gao N-Y, Deng Y, et al. Precursors of Dichloroacetamide, an Emerging Nitrogenous DBP Formed during Chlorination or Chloramination [J]. Environmental Science & Technology, 2010, 44(10): 3908-12.

[37] Shah A D, Mitch W A. Halonitroalkanes, Halonitriles, Haloamides, and N-Nitrosamines: A Critical Review of Nitrogenous Disinfection Byproduct Formation Pathways [J]. Environmental Science & Technology, 2012, 46(1): 119-31.

[38] Li G.W., Bae Y., Mishrra A., et al. Effect of aluminum on lead release to drinking water from scales of corrosion products [J]. Environmental Science & Technology, 2020, 54 (10) : 6142–6151.

STUDY ON THE EXTRACELLULAR POLYMERIZATION AND TRANSFORMATION OF MICROORGANISMS UNDER THE OXIDATION OF LEAD DIOXIDE AND MANGANESE DIOXIDE TO GENERATE IODINATED DISINFECTION BY-PRODUCTS

Lead (Pb) is commonly released into drinking water from cast iron pipes, solder in pipe networks, and brass fittings [1]. During chlorination disinfection, the dissolved lead ions and the metallic lead on the surface can be oxidized to insoluble lead dioxide (PbO_2), which can be stably present in drinking water distribution systems [2]. As free chlorine is converted to chloramines, PbO_2 and chloramines react and the stability decreases, suggesting that PbO_2 is a weaker oxidant than free chlorine and stronger than chloramines. Therefore, iodide ions (I^-) in water can be oxidized by PbO_2 to form free iodine, iodine (I_2), and hypoiodous acid (HOI). In a previous study by Lin et al. [3], I^- was chosen as the reducing agent to study the oxidative properties of PbO_2, and the formation kinetics of triiodide (I_3^-) was described under this condition. However, in the study by Lin et al., I-concentrations greater than 63.5 mg L^{-1} did not correspond to actual I^- concentration levels in drinking water [4]. At low I^- concentrations, I_2/HOI is not further converted to I_3^-, so the kinetics of PbO_2 oxidation of I^- to I_2/HOI should be further revised.

In the presence of organic matter, I_2/HOI reacts rapidly with the active moiety of organic matter to form iodinated disinfection by-products (I-DBPs), which are more efficient than their chlorinated and brominated disinfection byproducts (Cl- and Br-DBPs). High cytotoxicity and genotoxicity [5]. I_2/HOI can also be converted to nontoxic iodate (IO_3^-) [6] through metal oxidation reactions [7] or disproportionation reactions [8]. To date, no studies have focused on the generation of I-DBPs and IO_3^- when I^-containing water bodies in the pipeline network come into contact with PbO_2. Although the generation of iodoform has been mentioned in previous studies, the generation of I-DBPs is still not fully understood [3].

The precursors of I-DBPs are mainly concentrated in natural organic matter (NOM), while biofilm extracellular polymers (EPS) are often seriously neglected. Biofilms are ubiquitous in drinking water networks and are composed of various biomolecules such as proteins and polysaccharides. Its biological composition is

usually rich in nitrogen and has a small molecular weight, thus changing the
generation rate and species of I-DBPs [9]. It has been reported that EPS presents
significant health risks due to the higher toxicity of nitrogen-containing disinfection
by-products (N-DBPs) than carbon-containing disinfection by-products (C-DBPs).

The presence of natural organic matter (NOM) usually leads to the formation of
biofilms in drinking water pipes,80% of which are extracellular polymers (EPS)
secreted by microorganisms [10]. The biomolecules in EPS (e.g., proteins and
nucleic acids) are usually rich in nitrogen and produce highly toxic
nitrogen-containing disinfection byproducts during chlorination. Therefore, EPS as a
non-negligible precursor, presents significant health risks and should be seriously
considered for elimination.

Manganese (Mn) is a rich transition metal, accounting for about 0.1% of the
earth's crust [11,12]. Manganese ions (Mn^{2+}) are chemically oxidized to form
insoluble manganese oxides (such as MnO_2), thus leading to the accumulation of
manganese deposits in drinking water pipes [1]. I^- has been reported to be
continuously oxidized by δ-MnO_2 to free iodine (I_2/HOI) and Iodate root (IO_3^-) in
the pH range of 4−8 (equations 1 and 2) [6]. In the presence of NOM, I_2/HOI can
react quickly with its active part to produce organic iodine [13]. The genotoxicity
and cytotoxicity of iodized disinfection by-products (I-DBPs) generated are much
higher than those of bromine and chlorination disinfection by-products [5].

$$MnO_2 + 2I^- + 4H^+ \rightarrow Mn^{2+} + I_2 + 2H_2O \tag{1}$$

$$5MnO_2 + I_2 + 8H^+ \rightarrow 5Mn^{2+} + 2IO_3^- + 4H_2O \tag{2}$$
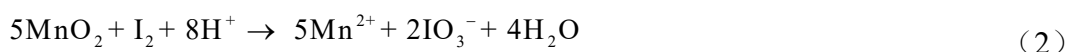
In this chapter, the kinetics of I^- oxidation to I_2/HOI in PbO_2 excess is investigated;
the generation and cytotoxicity of carbon- and nitrogen-containing I-DBPs (C- and
N-IDBPs) of two precursors EPS and NOM are compared; systematically
investigated the effects of water pH and PbO_2 dose and I-concentration on EPS

production of C and N-IDBPs; revealed that two main components (proteins and polysaccharides) and protein monomers (20 amino acid monomers) had significant effects on I- Contributions generated by DBPs. The aim of this study was to investigate the oxidation of I^- by MnO_2 in biofilms and the production of iodide disinfection by-products (I-DBPs) (Iodomethane, I-THMs, Iodoacetic acid, I-HAAs, Iodoacetonitrile, I-HANs, Iodoacetamide, I-HAcAms). The objectives of this study are as follows:(1) to compare the production of C-IDBPs and N-IDBPs containing carbon and nitrogen when NOM and EPS are used as precursors; (2) Determine the influencing factors (pH, I^-concentration and MnO_2 dose) of I-DBPs production; (3) Reveal the relative contribution of the two main components of EPS (protein and polysaccharide); (4) The I-DBPs generation of protein monomer (20 amino acids) was explained. Combined with the research results of this paper, it is helpful to find the corresponding control strategy of biofilm explosion in pipe network and put forward the solution.

4.1 Experimental condition

The experimental conditions are as follows: dark environment, continuous stirring with a magnetic stirrer, and temperature control at 25 °C to simulate the environment in the pipe network. The pH was kept constant before and after the reaction with phosphate buffer solution (50 mM). The pH_{PZC} and specific surface area of the as-prepared PbO_2 were 6.9 and 11.9 $m^2\,g^{-1}$, respectively.

In order to clearly observe the generation of I-DBPs, the doses of PbO_2, I^-, EPS and HA were increased synchronously, and the reaction conditions were set as follows: the initial dose of PbO_2 was set to 0.2 $g\,L^{-1}$, and the initial concentration of I^- was set to 1.0 $mg\,L^{-1}$. EPS and HA concentrations were set to 2.0 $mg\,C\,L^{-1}$.

After 72 h of reaction, the water sample was taken out and quickly filtered through a 0.45 μm aqueous membrane, and then an excess of ascorbic acid was rapidly added

to quench I_2/HOI for subsequent analysis of IO_3^- and I-DBPs. In the CHO chronic cytotoxicity experiment, the filtered water samples were passed through XAD resin to adsorb organics, eluted with ethyl acetate, and finally concentrated by a rotary evaporator, and then diluted to the corresponding times for chronic cell experiments [14]. The kinetics of I^- oxidation was carried out in the presence of benzene containing, aqueous and organic phases, respectively, by filtration through a 0.22 μm organic phase membrane to extract ionic iodine (i.e., I^- and IO_3^-) and reactive iodine (i.e., I_2) do a quick analysis.

All experiments were carried out under dark environment, magnetic agitation and temperature (25 ± 2 °C). Phosphate buffer solution (50 mM) was used to control the pH constant before and after the reaction. The pH_{PZC} and specific surface area of δ-MnO_2 are 4.2 and 369.4 m^2g^{-1}, respectively.

In order to observe the formation of I-DBPs, the dose of δ-MnO_2, I^-, EPS and HA increased synchronically. The reaction conditions were set as follows: the initial dose of δ-MnO_2 was set at 0.5 gL^{-1}, the initial concentration of I- was set at 1.0 mgL^{-1}, and the concentration of EPS and HA was set at 5.0 $mgCL^{-1}$.

After 72 h of reaction, the water sample was removed and rapidly filtered through a membrane of 0.45 μm, followed by rapid addition of excess ascorbic acid to quench I_2/HOI for subsequent IO_3^- and I-DBPs analysis.

4.2 Results discussion

4.2.1 Oxidation of I^- by PbO_2

Lin et al. [3] reported the oxidation of I^- to I_3^-, but the molar ratio of PbO_2 to I^- was very low ($R_{Pb/I}$, <0.1), and the reaction equations were (1)–(3):

$$PbO_2 + 2I^- + 4H^+ \rightarrow Pb^{2+} + I_2 + 2H_2O \qquad (1)$$

$$I_2 + H_2O \rightleftharpoons I^- + HOI + H^+ \tag{2}$$

$$I_2 + I^- \rightleftharpoons I_3^- \tag{3}$$

In this study, the oxidation of I^- by PbO_2 was investigated, and its $R_{Pb/I}$ value was greater than 100, which is a high molar ratio compared to the Lin study. At the same time, because of the low redox potential of PbO_2, I_2/HOI in water can be further oxidized to form IO_3^-, which is the final product of PbO_2 oxidation of I^- [6]. Theoretically, it is expected that 1 mol of I^- will be completely oxidized by 3 mol of PbO_2 (Equation 4). Under the conditions of this experiment, the dose of PbO_2 is far too much to generate I_3^-, so this experiment focuses on the oxidation of I^- to I_2/HOI.

$$3PbO_2 + I^- + 6H^+ \rightarrow 3Pb^{2+} + IO_3^- + 3H_2O \tag{4}$$
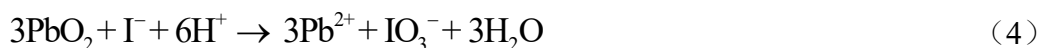
In this experiment, benzene was used as a fast extraction solvent for I_2, and I^- and I_2 were analyzed in aqueous and benzene phases, respectively. As shown in Figure 4.1 and 4.2, with the increase of pH, the consumption rate of I^- and the corresponding rate of I_2 generation decreased accordingly. As the pH increased from 6.0 to 9.0, $I^-([I^-]_w)$ and $I_2([I_2]_b)$ varied from 0.1 and 3.7 μM to 7.3 and 0.2 μM, respectively, after 15 min of reaction. After 15 min of reaction, the formation of IO_3^- in the aqueous phase $([IO_3^-]_w)$ of 0.07 μM was observed only at pH 6.0. Mass balance is always calculated in the range of 94.0%–99.1% (Equation 5).

$$[I^-]_0 = [I^-]_w + [IO_3^-]_w + 2[I_2]_b \tag{5}$$
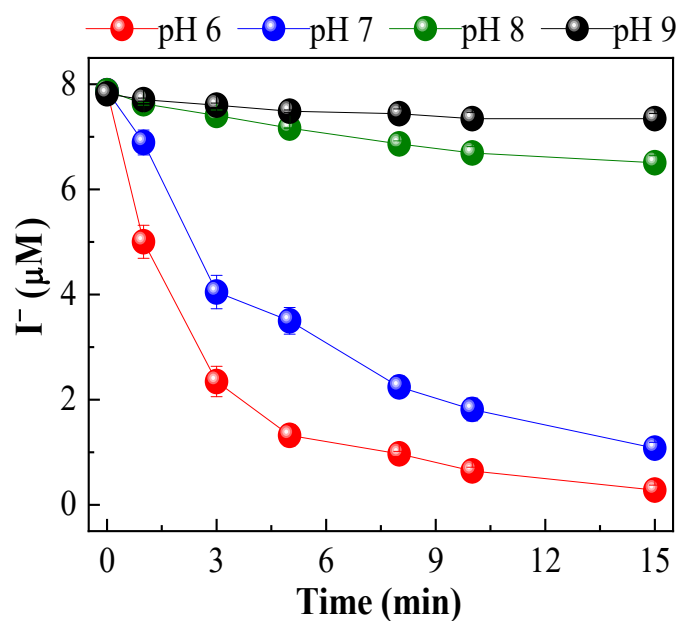
Figure 4.1 Plot of I⁻ concentration as a function of pH in the presence of benzene
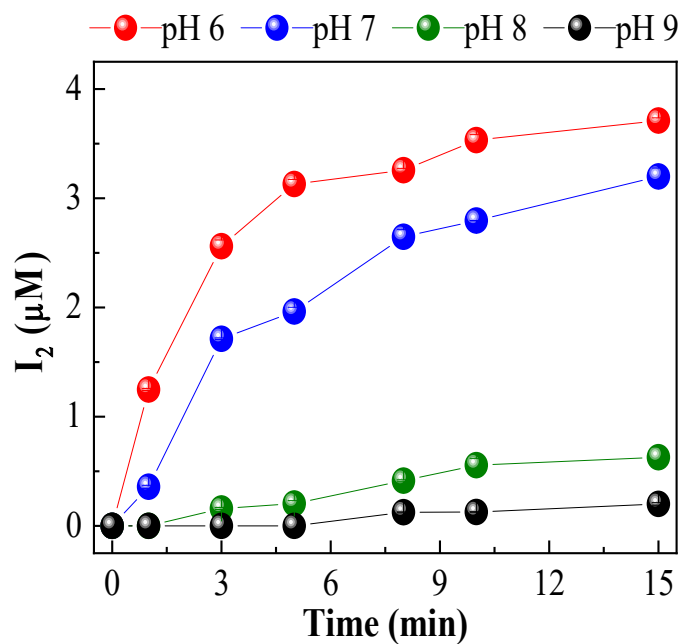
Figure 4.2 Plot of I₂ concentration as a function of pH in the presence of benzene

As shown in Figure 4.3 and 4.4, assuming that the oxidation of I⁻ follows a pseudo-second-order kinetic equation (Equation 6), by plotting $1/[I^-]^{-1}/[I^-]_0$ versus reaction time (t) The function performs a model fit with a slope equal to k'_{obs}. During

the experiment, it was found that even at pH 6.0, only 0.04% of Pb^{2+} was dissolved in water, so the dose of PbO_2 ($[PbO_2]$) was considered constant. Therefore, k'_{obs} divided by $[PbO_2]$ at pH 6.0, 7.0, 8.0 and 9.0 gave k_{obs} of 2.6×10^6, 8.0×10^5, 4.6×10^4 and 1.6×10^4 M^{-2} s^{-1}, respectively. The reaction order of H^+ is represented by the slope of the straight line, $\log(k_{obs}) = f(pH)$, which is equal to 0.79, and the calculated value of k is 1.6×10^{11} $M^{-2.79}$ s^{-1}.

$$-\frac{d[I^-]}{dt} = k'_{obs}[I^-]^2 = k_{obs}[PbO_2][I^-]^2 = k[PbO_2][I^-]^2[H^+]^n \qquad (6)$$
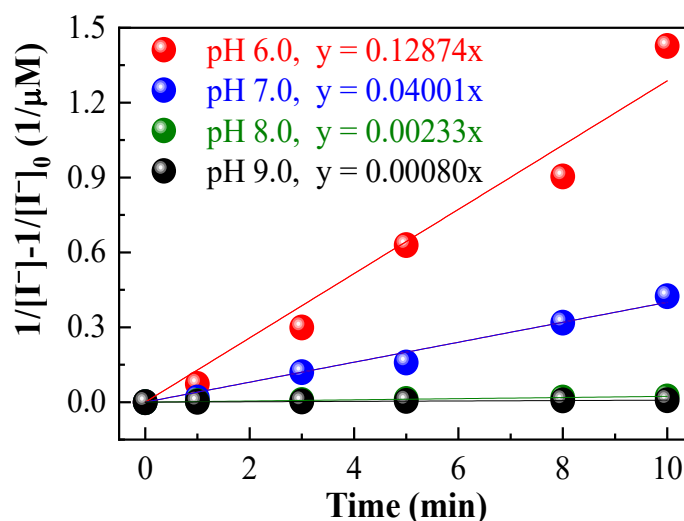
Figure 4.3 Kinetic fitting of I⁻ oxidation by PbO₂ in the presence of benzene
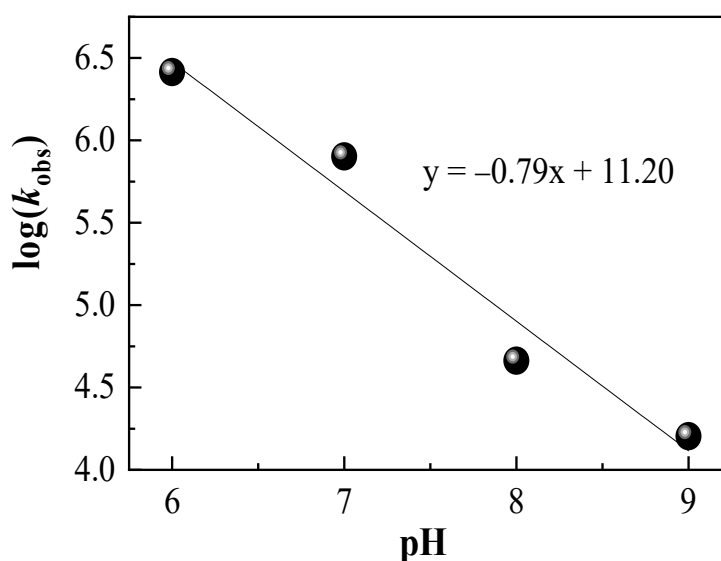
Figure 4.4 Kinetic fitting of I− oxidation by PbO2 in the presence of benzene

When EPS is used as the precursor, I_2/HOI will be further transformed into organic iodine through its reaction with organic matter, and into IO_3^- through metal oxide oxidation or disproportionation reaction. In order to better study the conversion of I^- of PbO_2 in EPS, this experiment simultaneously analyzes I^-, IO_3^- and I_2/HOI in water. However, due to the limited experimental conditions, the total organic iodine [TOI] content could not be detected using the instrument, so the TOI concentration was calculated by subtracting $[I^-]$, $[IO_3^-]$ and $[I_2/HOI]$ from $[I^-]$. As shown in Fig. 4.5, IO_3^- was slightly generated during the conversion of I^-, and most of I^- was converted to TOI in the presence of EPS, indicating that the reaction rate of I_2/HOI with EPS was higher than the disproportionation rate or oxidation by PbO_2 higher rate. For example, after 2 h of reaction, the values of $[IO_3^-]$, $[I_2/HOI]$ and [TOI] were 0.3, 0.1 and 7.3 μM, respectively.
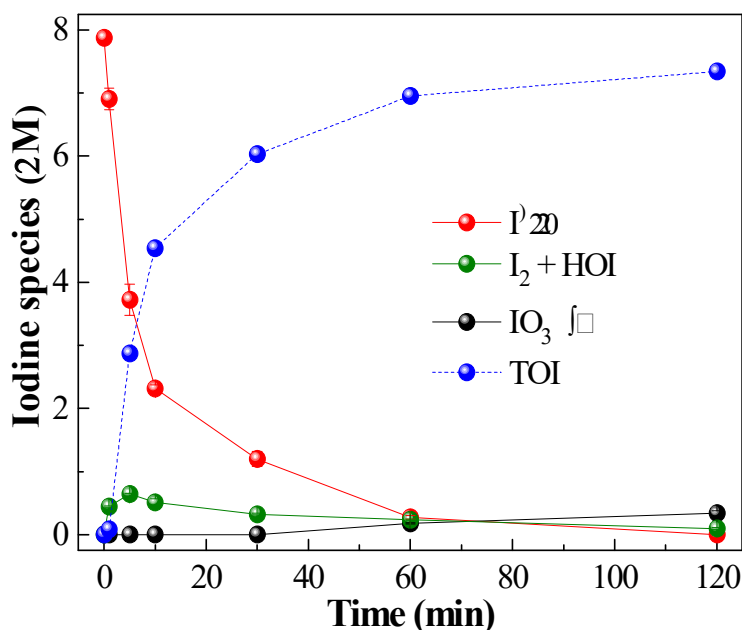
Figure 4.5 Mass balance of iodine element

4.2.2 Biofilm EPS generates I-DBPs

A large number of TOI transformations to generate I-DBPs have attracted attention. As shown in Fig. 4.6 and 4.7, I-DBPs were generated when EPS and HA were precursors, and only five species were identified, including triiodomethane

(TIM), iodoacetic acid (IAA), and diiodoacetic acid (DIAA), diiodoacetonitrile (DIAN) and diiodoacetamide (DIAcAm). It is obvious that when HA is the precursor, the total amount of carbon-containing iodine disinfection by-products (C-IDBP), namely TIM, IAA and DIAA, is higher than that when EPS is the precursor, which are 128.6 and 78.1 µg L^{-1}. However, the total amount of nitrogen-containing iodine disinfection by-products (N-IDBP), namely DIAN and DIAcAm, was higher when EPS was the precursor than the reaction when HA was the precursor, 16.4 and 7.2 µg L^{-1}, respectively.

The resulting water samples of I-DBPs were concentrated 100-fold and then diluted 10-70-fold to compare the chronic cytotoxicity of I-DBPs with EPS and HA as precursors. As shown in Fig. 4.8 and 4.9, at different dilution ratios, the CHO cell viability (ie, the average cell density as a percentage of the negative control) of EPS was lower than that of HA. For example, when EPS and HA were precursors with a dilution ratio of 10, the survival rates were 23.8% and 28.1%, respectively. HANs and HAcAms were reported to be nearly 100-fold more cytotoxic than HAAs in CHO cell assays [15]. Therefore, even though the content of biofilm EPS in water is relatively low relative to NOM, the health risks posed by biofilm EPS as a precursor cannot be ignored.
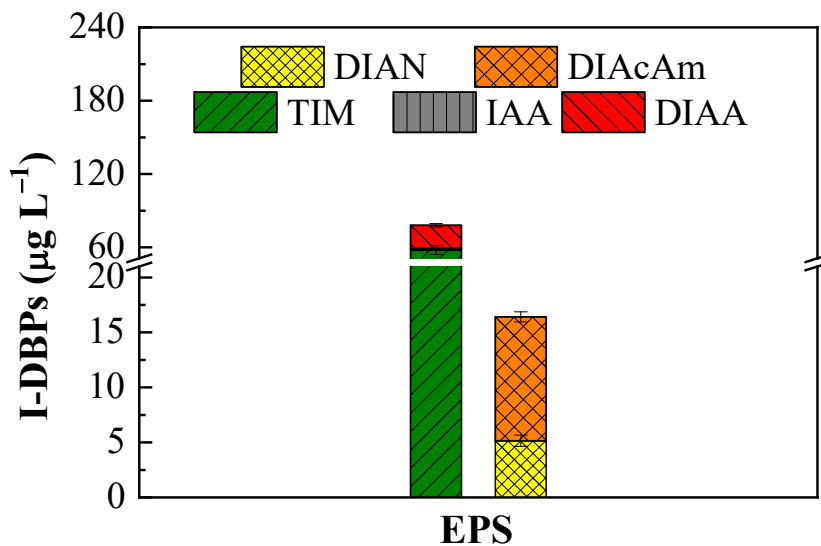
Figure 4.6 Generation of iodinated disinfection by-products (I-DBPs) from biofilm extracellular polymers (EPS)
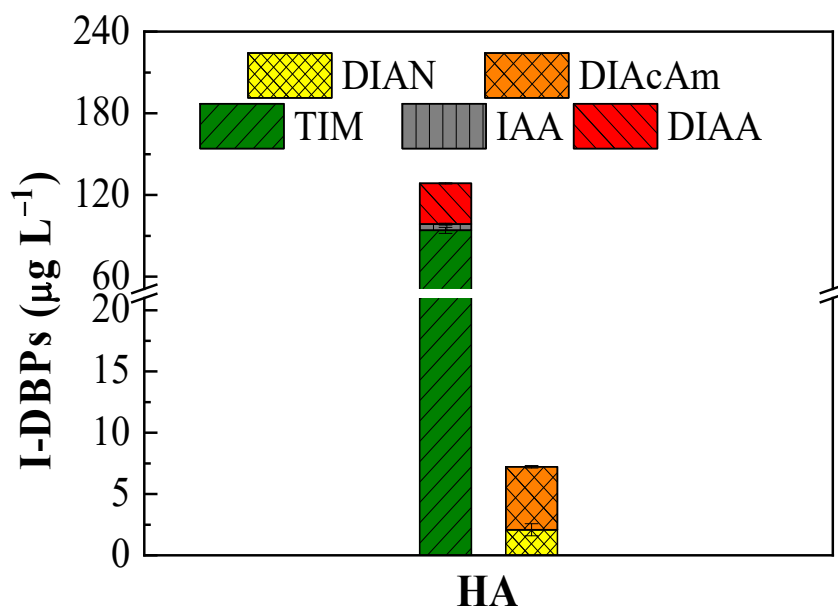
Figure 4.7 Generation of iodinated disinfection by-products (I-DBPs) from humic acid (HA)
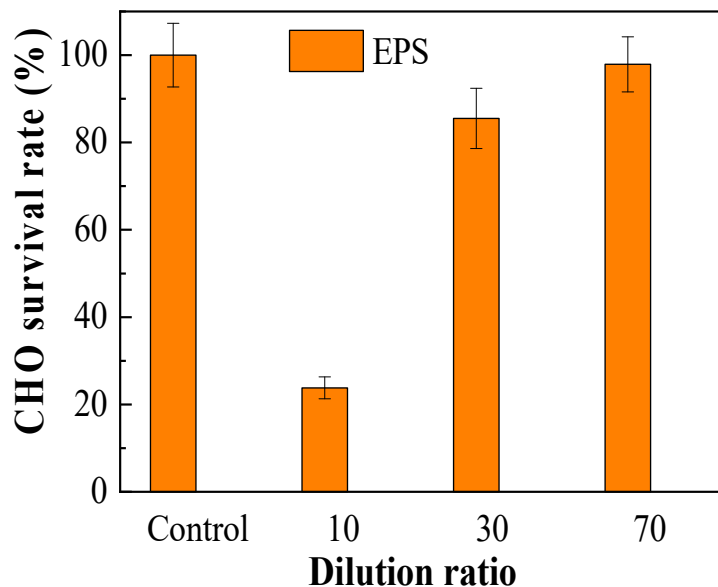
Figure 4.8 Chronic Cytotoxicity of Biofilm Extracellular Polymers (EPS)
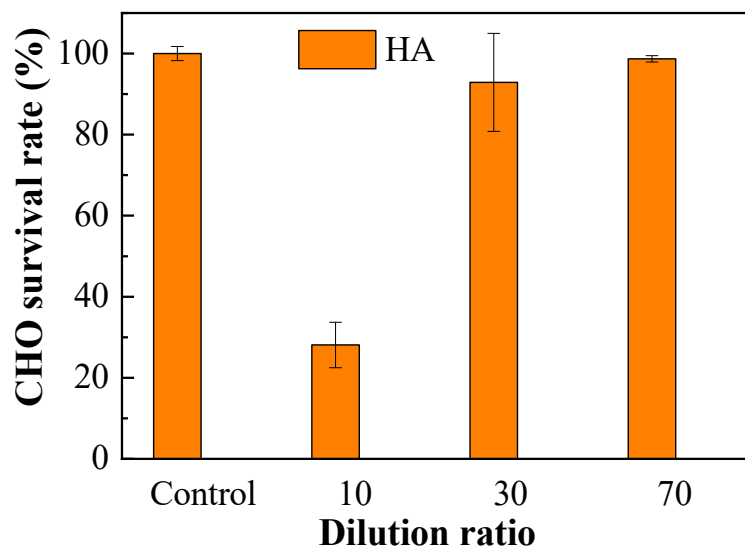
Figure 4.9 Chronic Cytotoxicity of humic acid (HA)

4.2.3 Effect of pH

In this experiment, the effect of pH 6.0−9.0 on the generation of I-DBPs was
investigated. The results are shown in Fig. 4.10-4.14, the generation of I-THMs,
I-HAAs and I-HANs decreased with the increase of pH. The formation potentials
(FPs) of TIMs were 81.5, 53.9, 34.9 and 13.3 μg L^{-1} at pH 6.0, 7.0, 8.0 and 9.0,
respectively. The pH effect of I-DBPs on the generation of disinfection byproducts
can be attributed to the following aspects. First, MnO_2, PbO_2 is considered a Lewis
acid because it accepts two electrons from I^- or I_2/HOI [16, 17]. And the
complexation of PbO_2 with I_2/HOI polarizes the iodine atom, thereby increasing the
electrophilicity and reactivity of PbO_2 with organic compounds [18]. At the same
time, higher pH also reduces the positive charge on the surface of PbO_2, thereby
weakening the electrostatic interaction and polarization of PbO_2 on I_2/HOI and I^-.
Second, according to the Nernst equation, alkaline pH reduces the electrochemical
driving force (ΔE_H) of PbO_2 for I^- oxidation, thereby hindering the generation of
I_2/HOI (Equation 1). Third, as shown in Figures 4.15 [19], at pH 6.0 and 7.0, I_2/HOI
exists in molecular form, and only a small fraction (< 5%) is converted to ionic form
as pH rises to 9.0 (OI^-). Therefore, it can be considered that HOI deprotonation
cannot significantly reduce the generation of I-DBPs. Furthermore, the FPs of
I-HAcAms were maximal at pH 7.0 with a concentration of 11.5 μg L^{-1}, which could
be attributed to two aspects. On the one hand, similar to the reasons for the other
three DBPs, the generation of I-HAcAms is promoted by the acidic conditions due to
the increase of the positive surface charge of PbO_2 and the increased ΔE_H of I^-
oxidation. On the other hand, HAcAms are in a metastable state, mainly generated
from the hydrolysis of HANs and further hydrolyzed to HAAs [20,21]. Previous
studies reported that the formation of dichloroacetamide reached a maximum at pH
8.0 during chlorination when Tyr was used as the precursor, because at pH 7–8,
dichloroacetonitrile and dichloroacetamide was the difference between the
hydrolysis rates is higher than other pH values [22]. With the transfer of halogen

from chlorine to iodine, both the hydrolysis rate of HANs and the decomposition rate of HAcAms with the same number of halogens in the substituents decrease [23]. Therefore, given the higher stability of DIAN and DIAcAm, the greatest difference is likely to be achieved at pH values above 8.0. Combining these two reasons, the generation of I-HAcAms in this study was maximal at pH 7.0 due to the two opposite effects of pH.
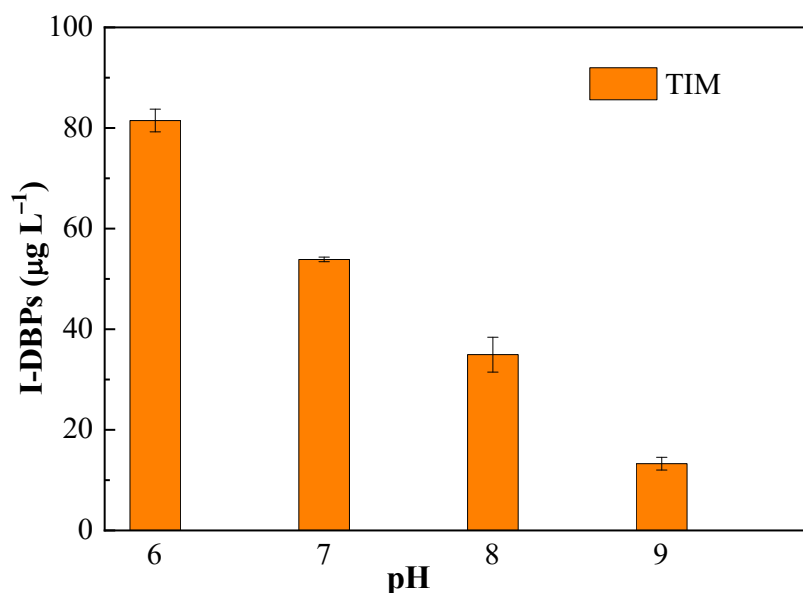
Figure 4.10 Effect of pH on the formation of TIM from EPS
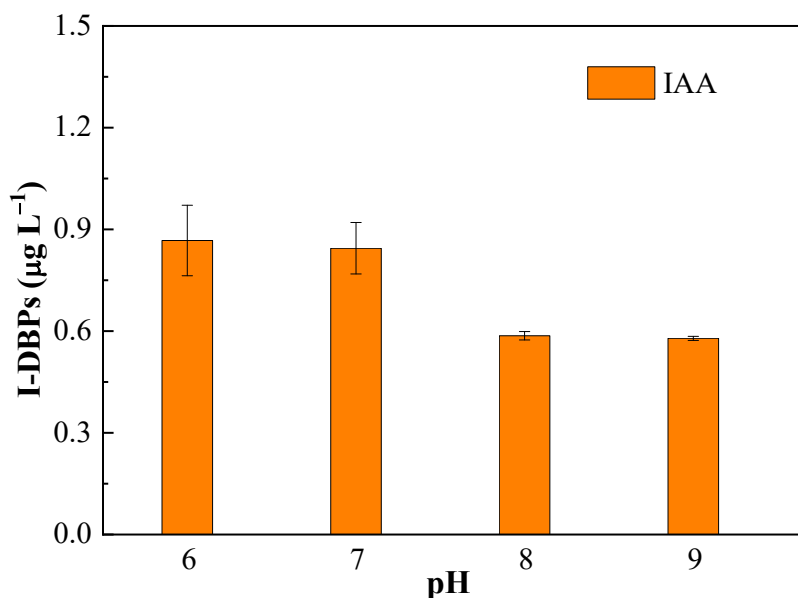
Figure 4.11 Effect of pH on the formation of IAA from EPS
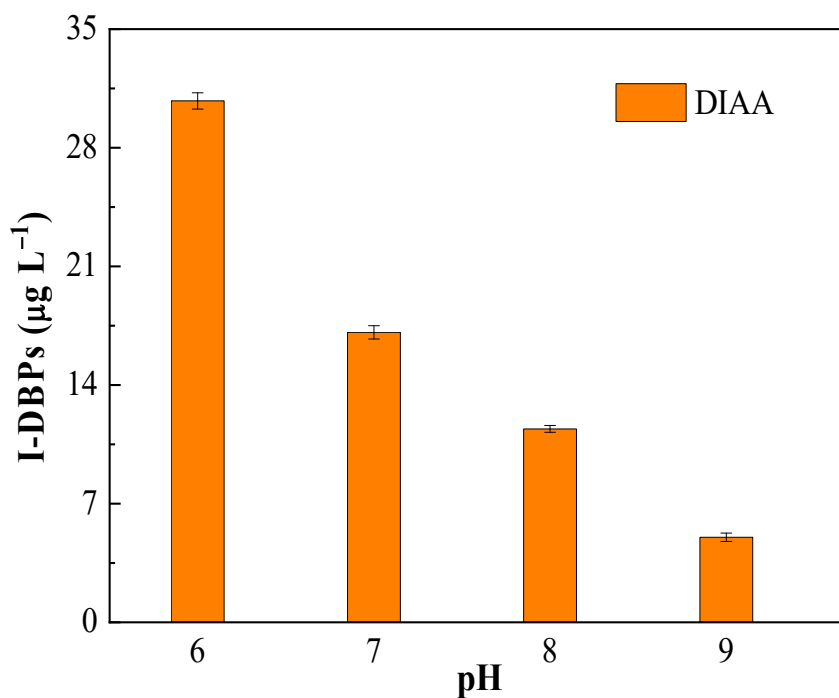
Figure 4.12 Effect of pH on the formation of DIAA from EPS
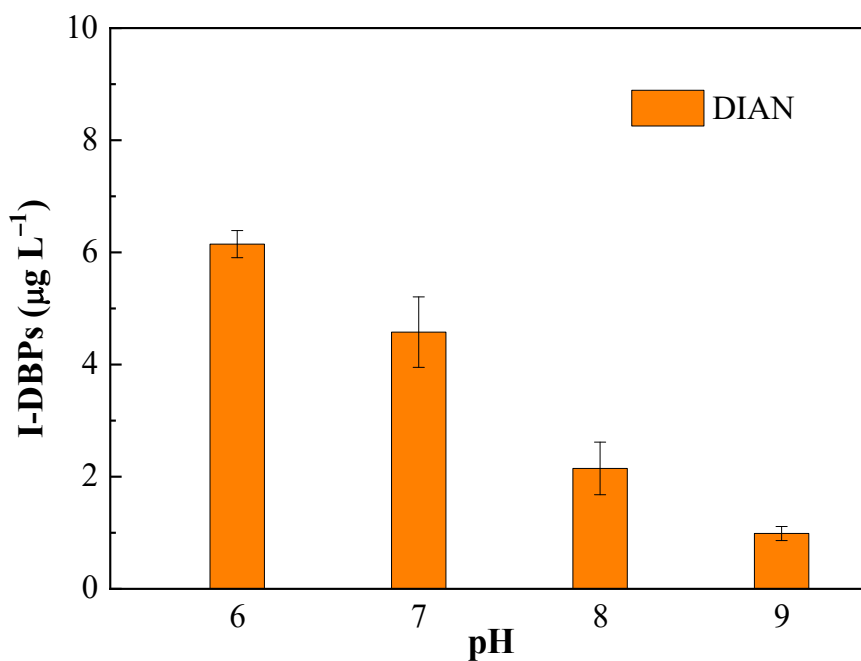
Figure 4.13 Effect of pH on the formation of DIAN from EPS
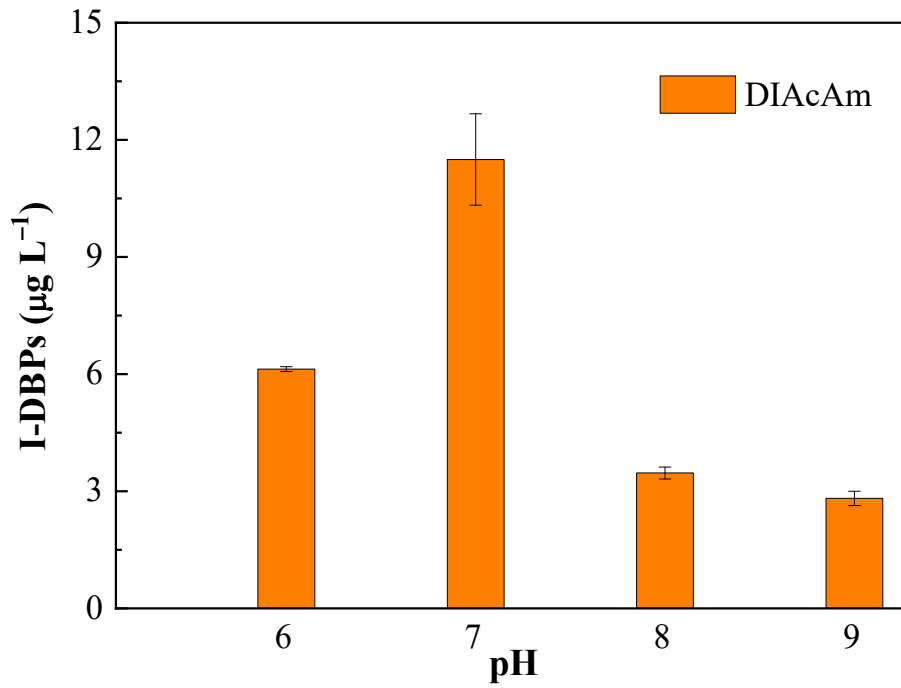
Figure 4.14 Effect of pH on the formation of DIAcAm from EPS
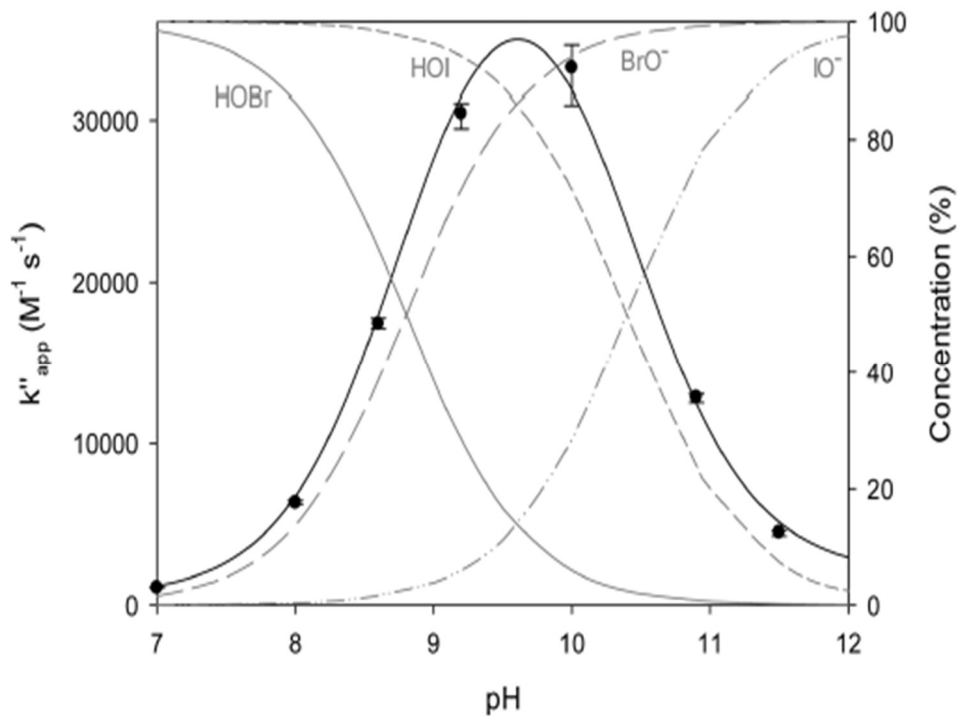
Figure 4.15 The influence of pH on the distribution of iodide

4.2.4 Effects of PbO$_2$ Dose and I$^-$ Concentration

As shown in Figure 4.16 and 4.17, the corresponding concentration ranges of PbO$_2$ dose and I$^-$ concentration were 0.05−1.0 g L^{-1} and 0.1−3.0 mg L^{-1}, respectively. As shown in Fig. 4.16 and 4.18, the generation potential of I-DBPs decreased with the increase of PbO$_2$ dose. The FPs of TIM were 76.1, 64.9, 56.5, 50.8 and 39.3 μg L^{-1}, and the corresponding PbO$_2$ doses were 0.05, respectively, 0.1, 0.2, 0.5 and 1.0 g L–1. The effect of PbO$_2$ dose on the generation of I-DBPs was mainly attributed to three aspects. First, increasing the dose of PbO$_2$ enhanced the electrochemical driving force (ΔE_H) of I$^-$ oxidation, thereby accelerating the generation of I$_2$/HOI. Second, the increasing dose of PbO$_2$ enhanced the polarization effect of PbO$_2$ on the iodine atoms in I$_2$/HOI, thereby promoting the PbO$_2$ response to EPS. Third, the increased dose of PbO$_2$ favors the oxidation of I$_2$/HOI to IO$_3^-$, thereby reducing the generation of I-DBPs. However, after 72 h of reaction, as the PbO$_2$ dose increased from 0.05 g L^{-1} to 1.0 g L^{-1}, the IO$_3^-$ concentration increased from 23.2 μg L^{-1} to 214.4 μg L^{-1}. This means that the negative effects on the generation of I-DBPs outweighed the positive effects at high PbO$_2$ doses. Gallard et al. [16] showed that the generation of TIMs decreased when the concentration of MnO$_2$ in the MnO$_2$/I$^-$/NOM system was higher than 0.5 g L^{-1}.
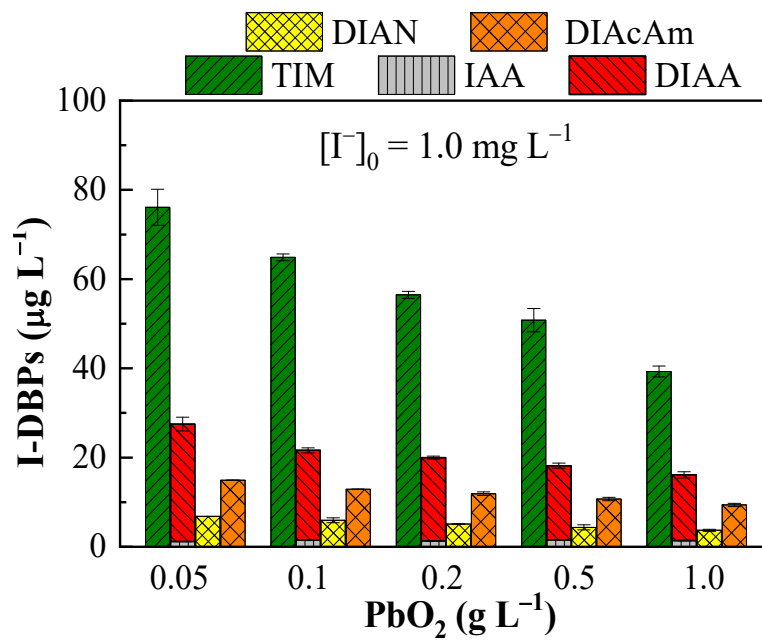
Figure 4.16 Effects of PbO₂ dosage on I-DBPs generation from EPS
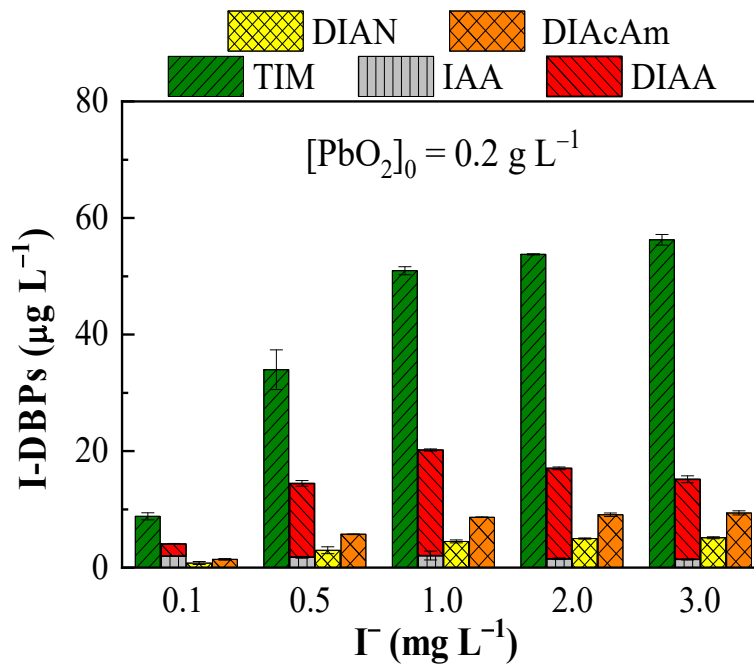
Figure 4.17 Effects of I⁻ concentration on I-DBPs generation from EPS
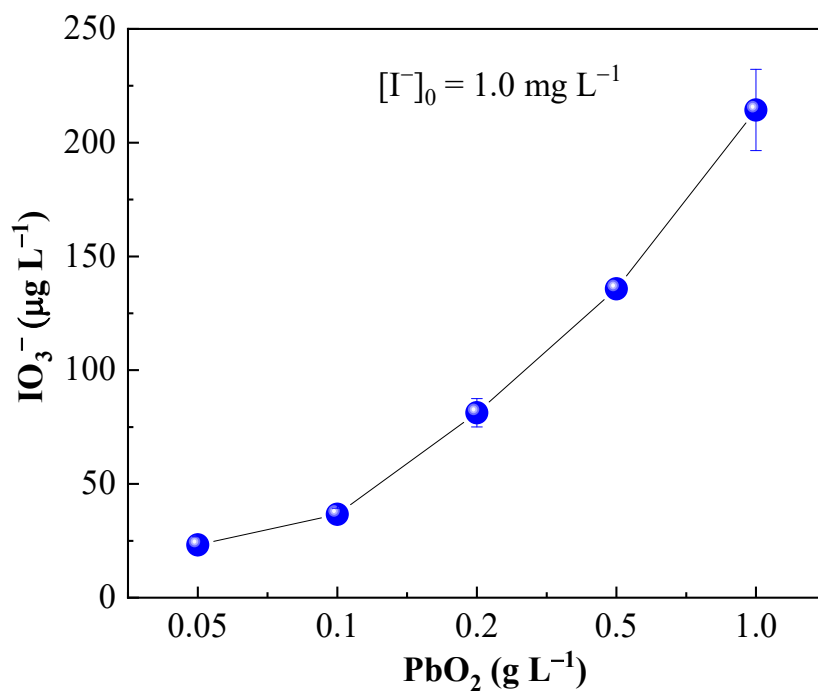
Figure 4.18 The effect of PbO$_2$ dosage on the generation of IO$_3^-$
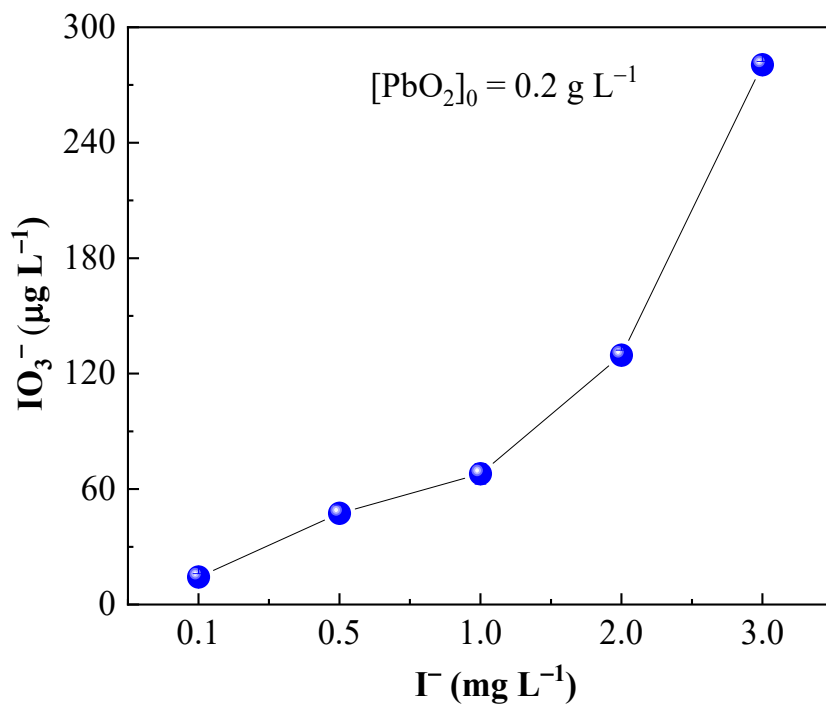
Figure 4.19 The effect of I$^-$ concentration on the generation of IO$_3^-$

As shown in Fig. 4.17 and 4.19, the generation of I-DBPs increased significantly with the increase of I^- concentration from 0.1 to 1.0 mg L^{-1}. And as the I^- concentration was further increased to 3.0 mg L^{-1}, the generation of I-DBPs remained almost unchanged. For example, when the FPs of DIAcAm were 1.4, 8.6 and 9.4 μg L^{-1}, the I^- concentrations were 0.1, 1.0 and 3.0 mg L^{-1}, respectively. The results showed that when the I_2/HOI reacted with EPS as the precursor was saturated, the excess I_2/HOI was further oxidized to IO_3^-. After 72 h of reaction, as the I^- concentration increased from 0.1 to 1.0 and 3.0 mg L^{-1}, the IO_3^- concentration increased from 14.3 to 67.9 and 280.5 μg L^{-1}.

4.2.5 EPS protein components and polysaccharides generate I-DBPs

It has been reported that proteins and polysaccharides are the main components (about 80%) of EPS [24]. According to the experimental procedure, proteins and polysaccharides were isolated from EPS, and the isolated proteins and polysaccharides were used as precursors to further elucidate the generation of I-DBPs. As shown in Figures 4.20-4.24, the C-IDBPs of proteins had higher potentials than polysaccharides, 201.8 and 52.7 μg L^{-1}, respectively. Hong et al. [25] showed that among the three biomolecules (ie, proteins, polysaccharides, and lipids), proteins are the most important precursors of THMs and HAAs. This can be explained as electron-withdrawing groups affect the electrophilic substitution reactivity of organic compounds. Proteins are mainly composed of amino acids containing unsaturated/conjugated bonds or phenolic structures, while polysaccharides are mainly composed of carbohydrates with saturated carbocyclic structures. Compared with saturated carbocyclic structures, unsaturated/conjugated bonds or phenolic structures are more likely to gain electrons from α-carbon, favoring electrophilic iodination. Besides, it has been reported that the uniform distribution of electron density is also not conducive to the occurrence of electrophilic substitution [16,26]. The N-IDBP production potential of the protein

was also higher compared to the polysaccharide, 2.5 and 41.8 $\mu g\ L^{-1}$, respectively. A previous study by Wang et al. [27] found that EPS extracted from Pseudomonas putida (mainly containing proteins) showed higher FPs of HANs than P. aeruginosa EPS (mainly containing polysaccharides) during the chlorination process. This result can be explained by the higher N content provided by proteins and more electrophilic iodination reaction sites than polysaccharides. Previous studies have also shown that galactose, glucosamine, glucose, mannose, glucuronic acid and rhamnose are the main monomers of EPS polysaccharides, however only one glucosamine contains nitrogen, and the other polysaccharide monomers do not contain nitrogen [28]. At the same time, as shown in Figure 4.25, when protein and polysaccharide are used as precursors, the cytotoxicity of protein as precursor is higher than that of polysaccharide as precursor. When the dilution ratio was 1:30, the cell viability was 30.8% and 36.9%, respectively. It also further proves that the toxicity of nitrogen-containing disinfection by-products is higher than that of carbon-containing disinfection by-products.
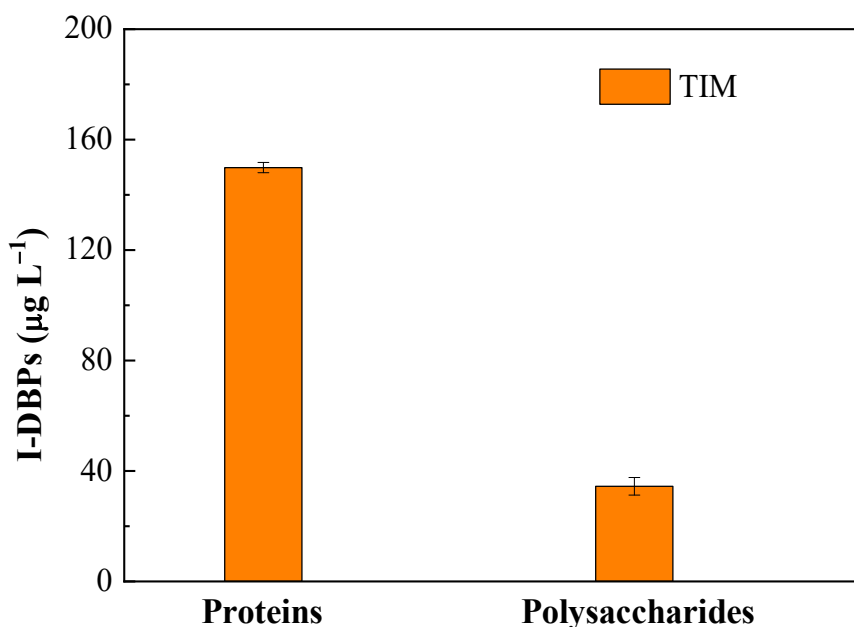
Figure 4.20 TIM formation from proteins and polysaccharides
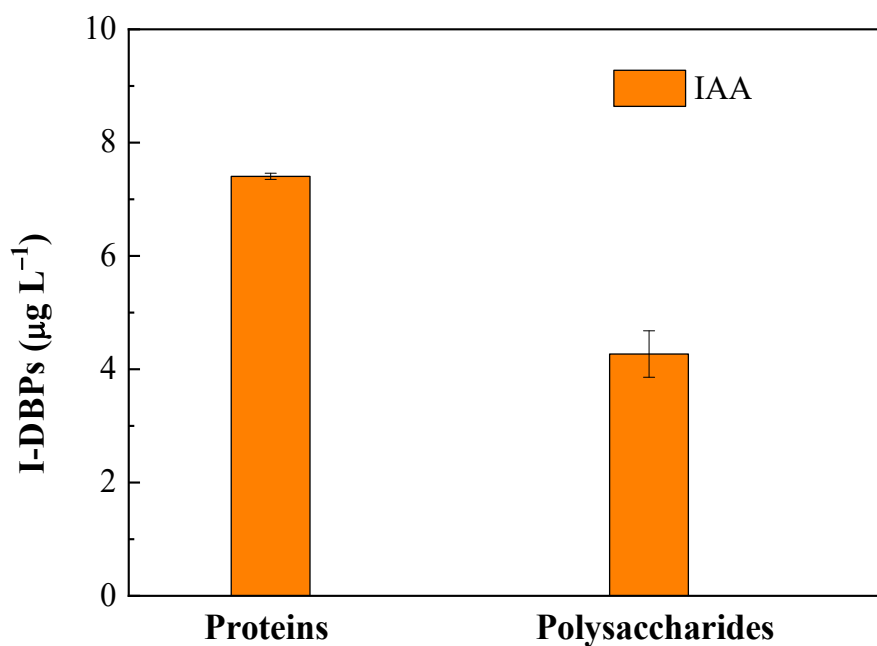
Figure 4.21 IAA formation from proteins and polysaccharides
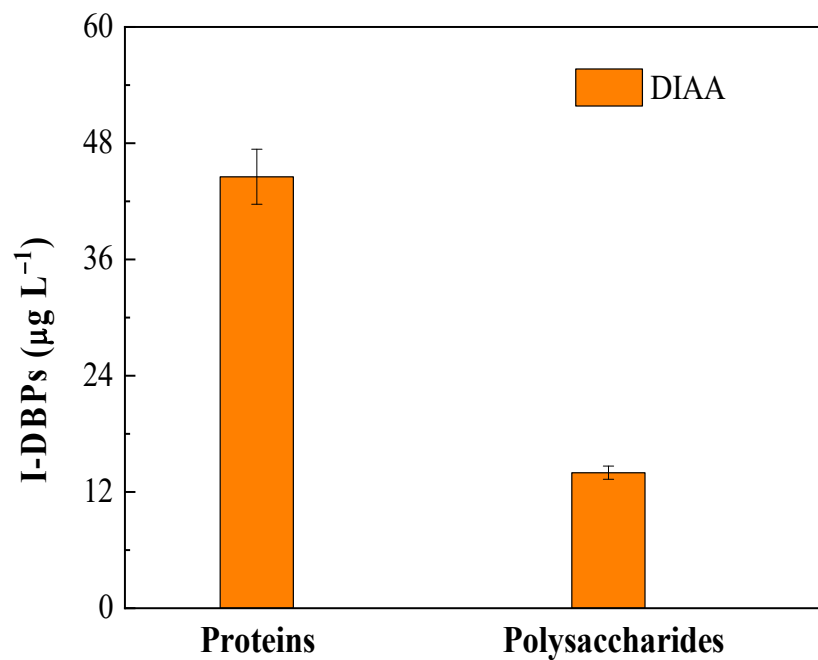
Figure 4.22 DIAA formation from proteins and polysaccharides
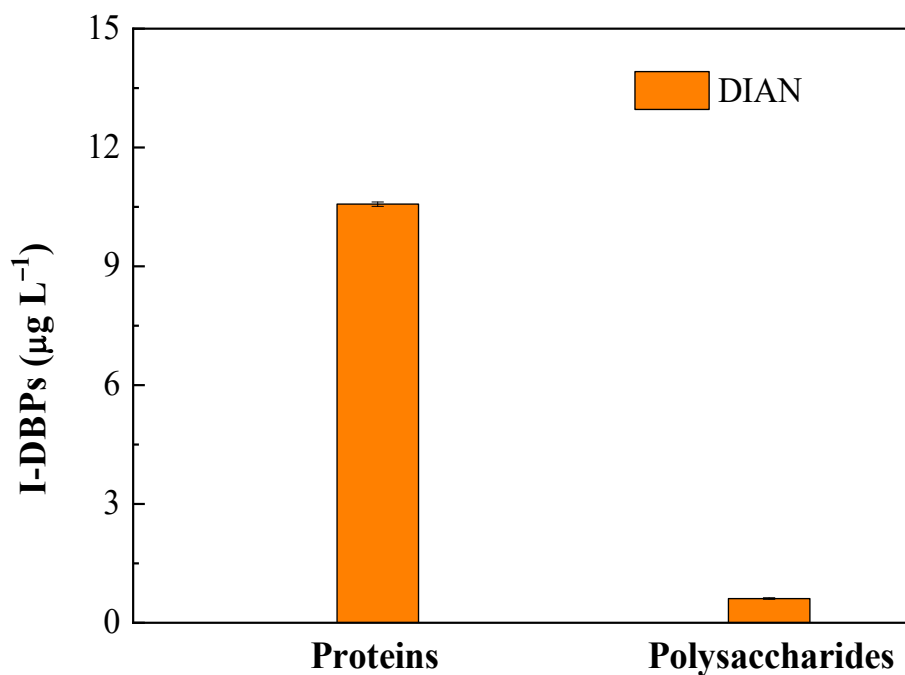
Figure 4.23 DIAN formation from proteins and polysaccharides
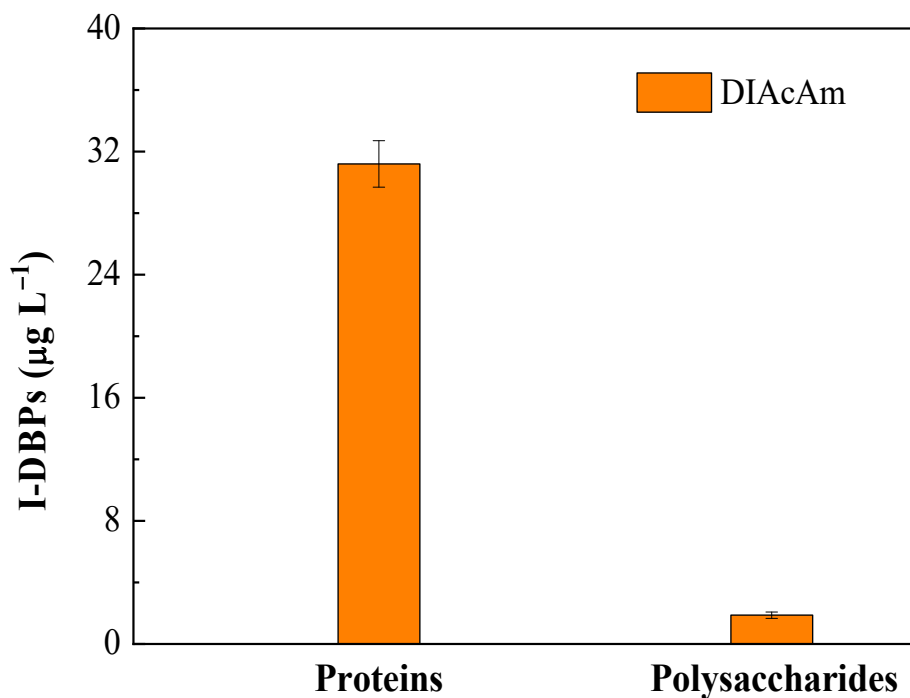
Figure 4.24 DIAcAm formation from proteins and polysaccharides
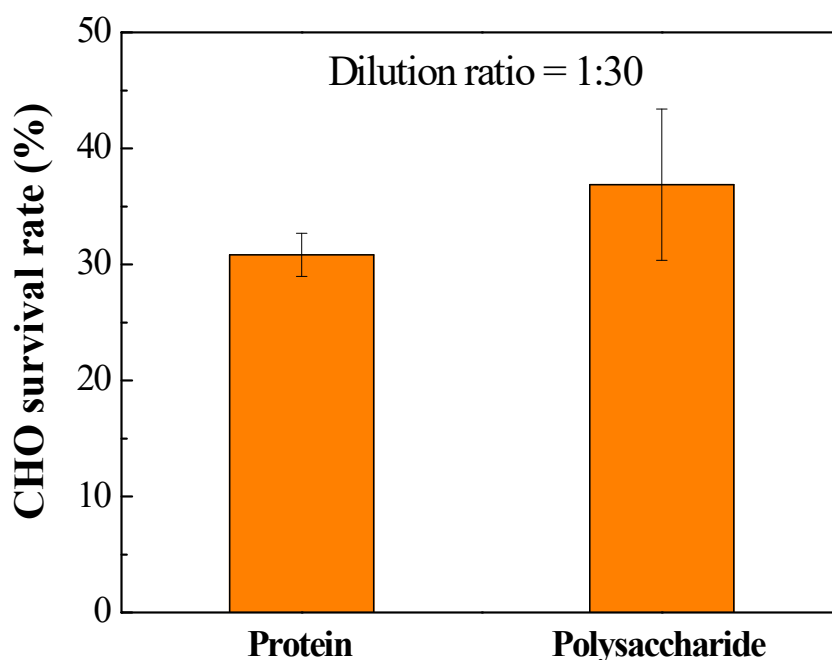
Figure 4.25 CHO cell chronic cytotoxicity of I-DBPs from the protein and polysaccharide components of EPS

4.2.6 Generation of I-DBPs from amino acids

As described in 2.5, EPS protein components were considered to be the main precursors for the generation of I-DBPs, and then, chemical composition analysis of EPS protein components was performed, and 20 amino acid monomers were detected. The structure and composition are shown in Table 4.1. In order to better study the effects of proteins on I-BDPs, 20 amino acids were used as precursors to conduct experiments at a concentration of 2.0 mg C L^{-1}, and the effects of chemical structures on the generation of I-DBPs were discussed.

As shown in Table 4.2, among I-THMs, aspartic acid (Asp), tryptophan (Trp) and histidine (His) have higher TIM generation potentials, which are 436.0, 281.9 and 133.3 μg, respectively L^{-1}. According to previous studies, the THM of Trp had the highest FPs during the chlorination process. The mechanism of Trp generating THMs includes decarboxylation and substitution to successively generate tryptamine and 3-chloroindole intermediates, and then cleave the five-membered heterocycle

[29]. Therefore, as shown in Figure 4.26, the generation pathway of I-THMs can be deduced in a similar way. However, in this study, Asp represented the highest generation potential of I-THMs. Liu et al. [26] previously reported that the formation potential of I-THMs of Asp was higher than that of alanine (Ala), glycine (Gly), His, and phenylalanine (Phe) during the chlorination of iodine-containing water. Proline (Pro) and Tyrosine (Tyr), but Asp and Trp could not be compared. Chen et al. [30] proposed that the generation of THMs from Asp may be achieved through the formation of chloroacetaldehyde, which is easy to eliminate acetaldehyde. Therefore, as shown in Figure 4.27(a), the TIM generation pathway of Asp can be deduced. Unfortunately, the formation of chloroacetaldehyde is low and structurally unstable, since chloroacetaldehyde, an intermediate product, cannot be detected. Therefore, it is unclear why Asp has a higher potential to generate I-THMs than Trp, which requires further investigation. Another difference from the previous literature is that the formation potential of I-THMs of His is relatively high, which can be explained by decarboxylation and substitution to generate 3-iodoimidazole followed by cleavage of the imidazole ring, as shown in Figure 4.28 for the generation of Trp pathway [31].

For I-HAAs, only Asp, Asn and Trp were observed to produce DIAA. Wang et al. [28] demonstrated the importance of the amine group for the generation of HAAs during chlorination by comparing the chemical compositions of Asp and succinic acid that lack amino groups on the α-carbon atoms. However, in this study, the two carboxyl groups in Asp were another reason for the high FPs of I-HAAs. The reason is as follows: The resulting nitrile ($R-CH_2-CN$) is a key intermediate in the initial reaction of amino acids. The hydrogen atom on the α-carbon is replaced by an iodine atom to form a diiodonitrile ($R-CI_2-CN$). Elimination of the side chain (-R) occurs to yield diiodoacetonitrile (CHI_2-CN). Subsequently, HOI induced the formation of N-iodoamides ($CHI_2-CO-NHI$) on the nitrile groups, and these nitrogen-containing iodoamides were rapidly hydrolyzed to DIAA [26]. In addition, the R group in Asp is

a carboxyl group with electron-withdrawing effect, which contributes to the elimination of the carboxyl group to generate I-HAAs. The DIAA formation potential of Asp is much higher than that of Asn and Trp, which are 50.5, 10.3 and 6.7 μg L^{-1}, respectively. The possible reason is that the R groups of acyl and indolyl groups have weaker electron withdrawing ability than carboxyl groups. I-HAAs generated by Leu, Ser and Phe were not observed, leucine (Leu), serine (Ser) and Phe contain alkyl, hydroxyl and phenyl R groups, respectively, which have electron donating ability, thus, further confirming that the carboxyl group in Asp promotes the generation of I-HAAs.

For I-HANs and I-HAcAms, the FPs of DIAN and DIAcAm of Asp, Asn and Tyr were all relatively high, 8.8 and 11.8, 8.2 and 9.2, and 7.6 and 9.4 μg L^{-1}, respectively. I-HAcAms were mainly obtained by the hydrolysis of I-HANs, which could explain the consistency of FPs generation between I-HANs and I-HAcAms. Therefore, as shown in Figures 4.27(b) and 4.29, both Asp and Asn are mainly produced by eliminating the R groups (carboxyl and acyl groups of Asp and Asn, respectively) in dichloronitrile (R-CCl$_2$-CN) Promote the generation of HANs [28]. The formation pathway of Tyr is shown in Figure 4.30. In addition to the 4-hydroxy-benzyl cyanide (HOC$_6$H$_5$-CH$_2$-CN) intermediate (except cyano), benzyl cyanide (C$_6$H$_5$-CH$_2$-CN) is also the substitution of the I atom on the α-carbon generates DIAN [22]. As shown in Figures 4.31, Asp exhibited the highest chronic cytotoxicity, which could partly explain its high FPs of C- and N-IDBPs. Meanwhile, considering the ratio of amino acids and FPs of I-DBPs, Asp was the main contributor to the generation of I-THMs and I-HAAs, while Asp, Asn and Tyr were important precursors of I-HANs and I-HANs.

Table 4.1 The structure of twenty amino acids

Amino acid	Molecular formula	Structure of molecules	Amino acid	Molecular formula	Structure of molecules	Amino acid	Molecular formula	Structure of molecules
Alanine acid	$C_3H_7NO_2$		Glycine acid	$C_2H_5NO_2$		Proline line	$C_5H_9NO_2$	
Amino acid arginine	$C_6H_{14}N_4O_2$		Histidine	$C_6H_9N_3O_2$		Serine	$C_3H_7NO_3$	
Asparagine acid	$C_4H_8N_2O_3$		Isoleucine acid	$C_6H_{13}NO_2$		Threonine acid	$C_4H_9NO_3$	
Aspartic acid	$C_4H_7NO_4$		Leucine acid	$C_6H_{13}NO_2$		Tryptophan	$C_{11}H_{12}N_2O_2$	
Cysteine	$C_3H_7NO_2S$		Lysine	$C_6H_{14}N_2O_2$		Tyrosine	$C_9H_{11}NO_3$	
Glutamine	$C_5H_{10}N_2O_3$		Methionine	$C_5H_{11}NO_2S$		Valine	$C_5H_{11}NO_2$	
Glutamic acid	$C_5H_9NO_4$		Phenylalanine	$C_9H_{11}NO_2$				
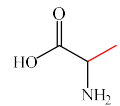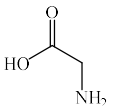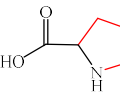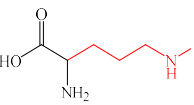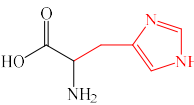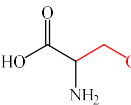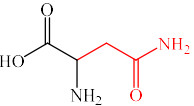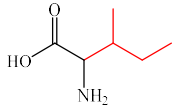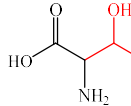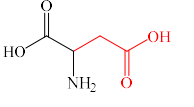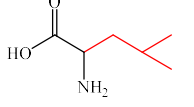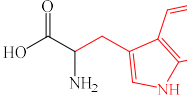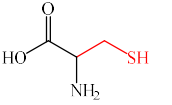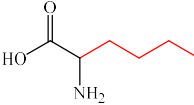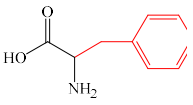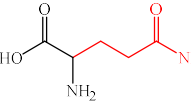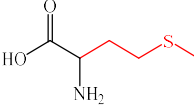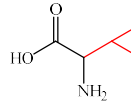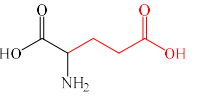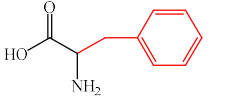
Table 4.2 Formation of iodinated disinfection byproducts (I-DBPs) from twenty amino acids

Amino acid	The proportion (%) [a]	I-THMs (µg L^{-1})	I-HAAs (µg L^{-1})		I-HANs (µg L^{-1})	I-HAcAms (µg L^{-1})
		TIM	MIAA	DIAA	DIAN	DIAcAm
Alanine acid	12.0	12.3 ± 5.2	/ [b]	/	/	2.11 ± 0.12
Amino acid arginine	5.0	7.6 ± 0.9	/	/	/	/
Asparagine acid	3.9	7.9 ± 1.8	/	10.3 ± 2.2	8.2 ± 0.5	9.2 ± 0.1
Aspartic acid	5.5	436.0 ± 13.0	2.3 ± 0.6	50.5 ± 6.4	8.8 ± 1.5	11.8 ± 1.2
Cysteine	1.2	23.2 ± 2.4	/	/	/	/
Glutamine	3.1	9.2 ± 1.3	/	/	/	/
Glutamic acid	6.0	9.1 ± 0.2	/	/	/	/
Glycine acid	9.5	4.3 ± 0.8	/	/	/	/
Histidine	1.9	133.3 ± 4.0	/	/	/	/
Isoleucine acid	5.5	0.8 ± 0.2	/	/	/	/
Leucine acid	8.1	4.9 ± 0.2	/	/	/	/
Lysine	4.4	2.0 ± 1.0	/	/	/	/
Methionine	2.5	25.2 ± 4.8	/	/	/	/
Phenylalanine	3.7	4.1 ± 1.9	/	/	/	/
Proline line	4.3	2.1 ± 0.9	/	/	/	/
Serine	5.6	1.7 ± 0.4	/	/	/	/
Threonine acid	5.6	32.9 ± 4.0	/ [b]	/	/	/
Tryptophan	1.0	281.9 ± 7.5	/	6.7 ± 1.6	/	3.6 ± 0.9
Tyrosine	2.5	23.1 ± 3.1	/	/	7.6 ± 1.1	9.4 ± 0.3
Valine	7.7	9.8 ± 1.6	/	/	/	/

a：a small fraction of proteins are not accurately identified b：not detected
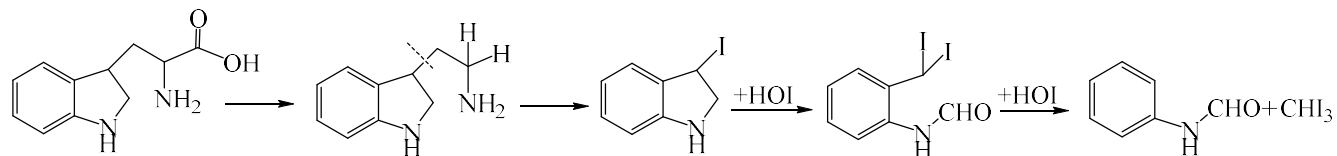
Figure 4.26 TIM formation pathway of Trp as a precursor
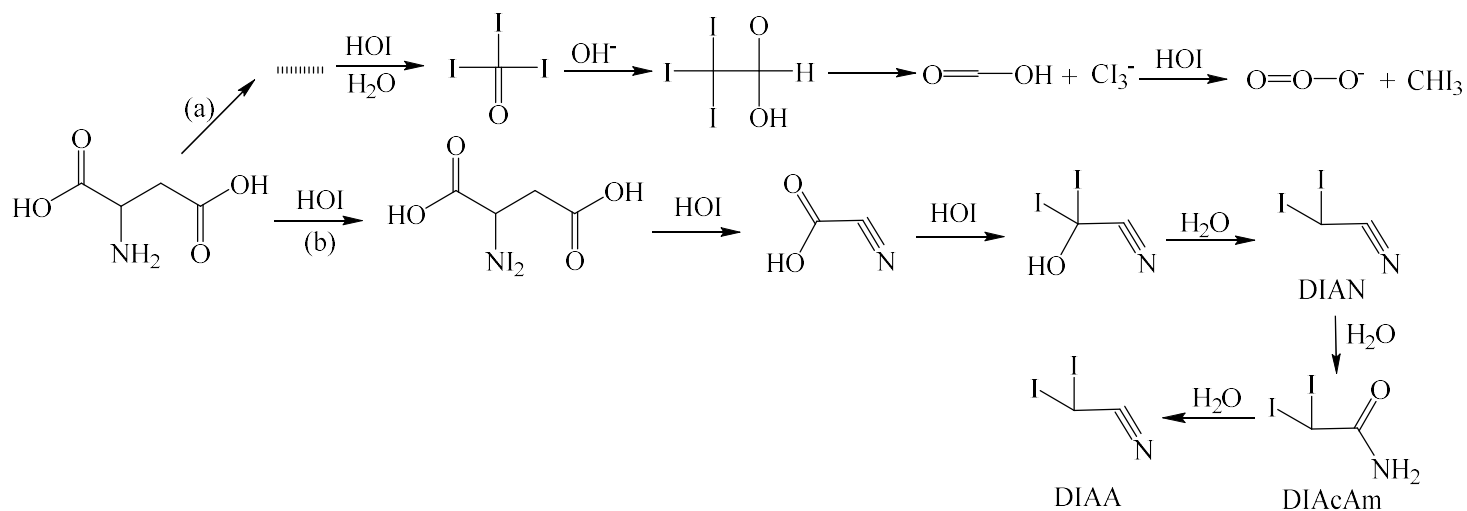
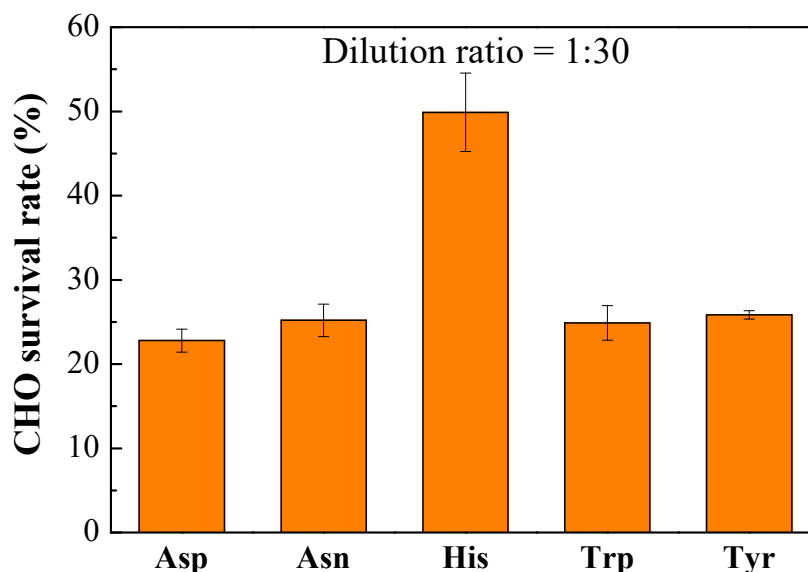**Figure 4.27 TIM、DIAA、DIAND and IAcAm formations pathways of Asp as a precursor**
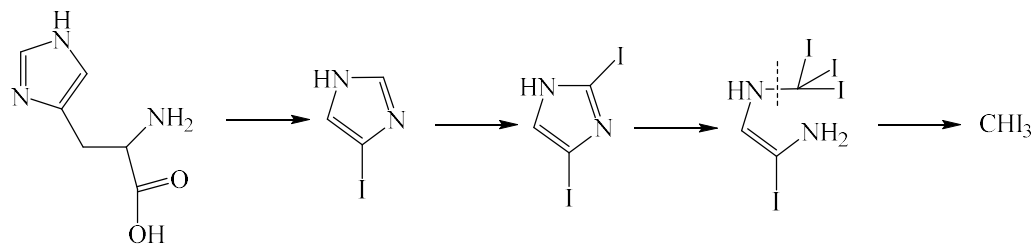
Figure 4.28 TIM formation pathway of His as a precursor
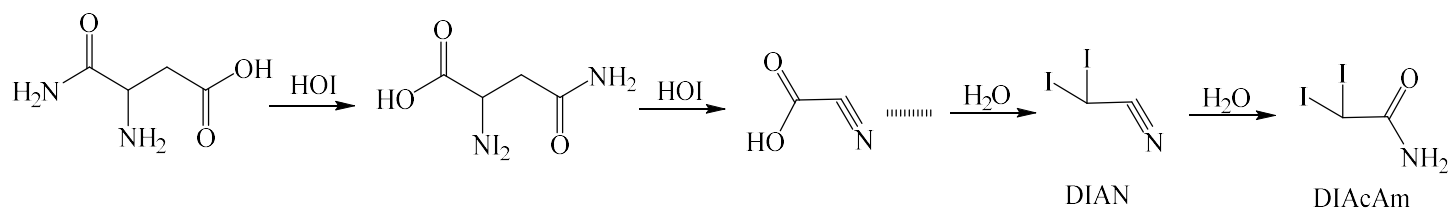
Figure 4.29 DIAN and DIAcAm formations pathways of Asn as a precursor
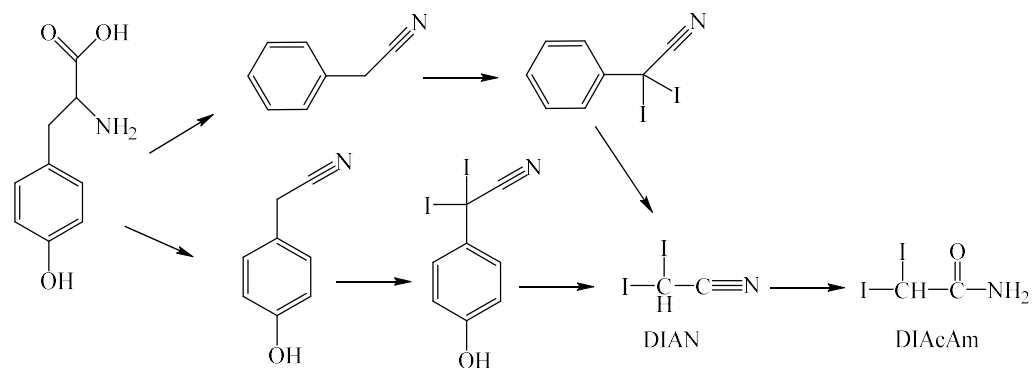
Figure 4.30 DIAN and DIAcAm formations pathways of Tyr as a precursor

Figure 4.31 CHO cell chronic cytotoxicity of I-DBPs from five amino acids

4.2.7 The oxidation of δ -MnO₂ yields I-DBPs

The I$^-$ in water is oxidized by MnO$_2$ to form I$_2$/HOI and IO$_3^-$. The resulting I$_2$/HOI is converted to organic iodine by reaction with the active group in water. This experiment analyzed the formation of IO$_3^-$, I$^-$ and I$_2$/HOI with reaction time, and studied the transformation trend of iodine in MnO$_2$/I$^-$/EPS system. From equation 1, the total organic iodine [TOI] is calculated by subtracting [IO$_3^-$], [I$^-$] and [I$_2$/HOI] from [I$^-$]$_0$. As shown in Figure 4.32-4.35, the measured values of [TOI], [IO$_3^-$], [I$^-$] and [I$_2$/HOI] are 5.4, 0.3, 2.1 and 0.1 μM, respectively. The experimental results show that more than 93% of I$^-$ is converted to TOI, but the oxidation rate of I$_2$/HOI by MnO$_2$ is much lower than the reaction rate between I$_2$/HOI and EPS, so the generation of I-DBPs is lower than that of PbO$_2$. However, in chapter 3 PbO$_2$/I$^-$/EPS research system, I$^-$ is almost completely transformed into IO$_3^-$ and TOI, accounting for 3.8% and 92.7%, respectively. The difference between the two systems can be explained as the low conversion rate of I$^-$ is caused by the weak electrochemical driving force (ΔE$_H$) of the oxidation of I$^-$ to I$_2$/HOI. The standard oxidation potential (E$_0$) of MnO$_2$ and PbO$_2$ is 1.29V and 1.45V, respectively [3,6]. According to the Nernst equation, ΔE$_H$ of MnO$_2$

(pH 6) and PbO_2 (pH 7) is 0.58 V and 0.71V, respectively.

$$[TOI] = [I^-]_0 - [I^-] - [IO_3^-] - 2[I_2] \text{ or } [HOI]$$ （3）
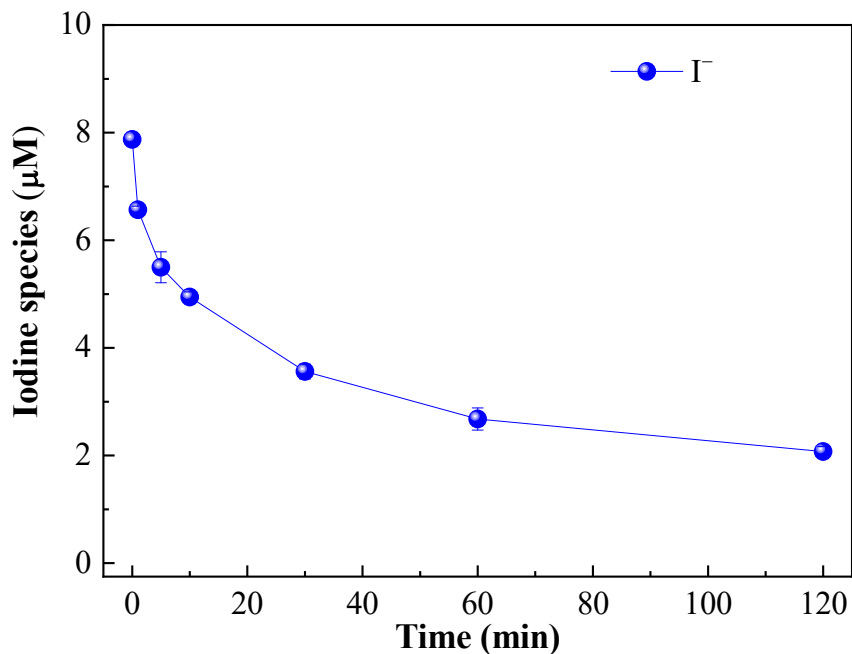

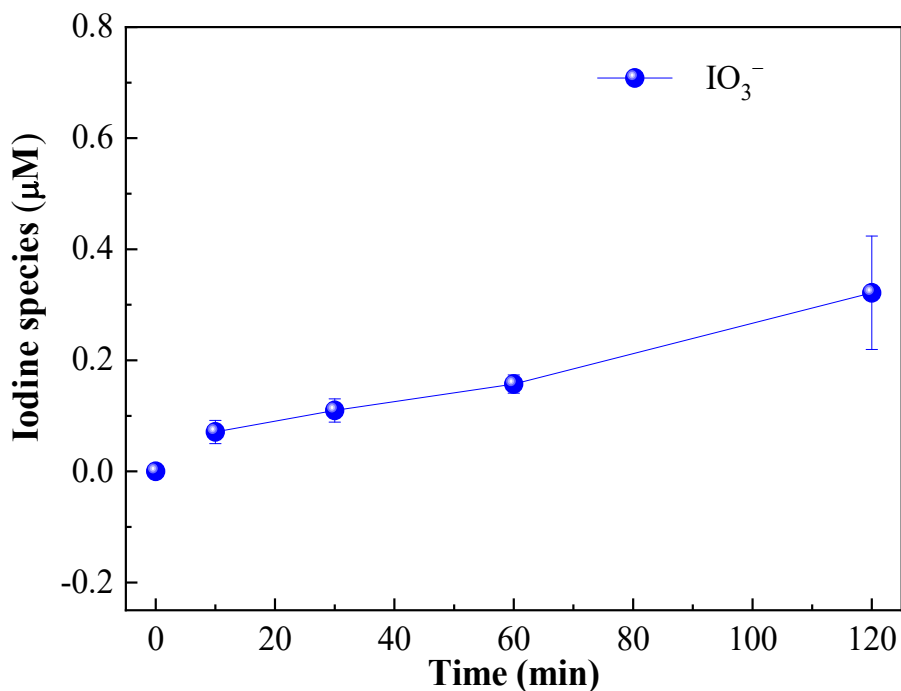**Figure 4.32 Mass balance of I⁻**
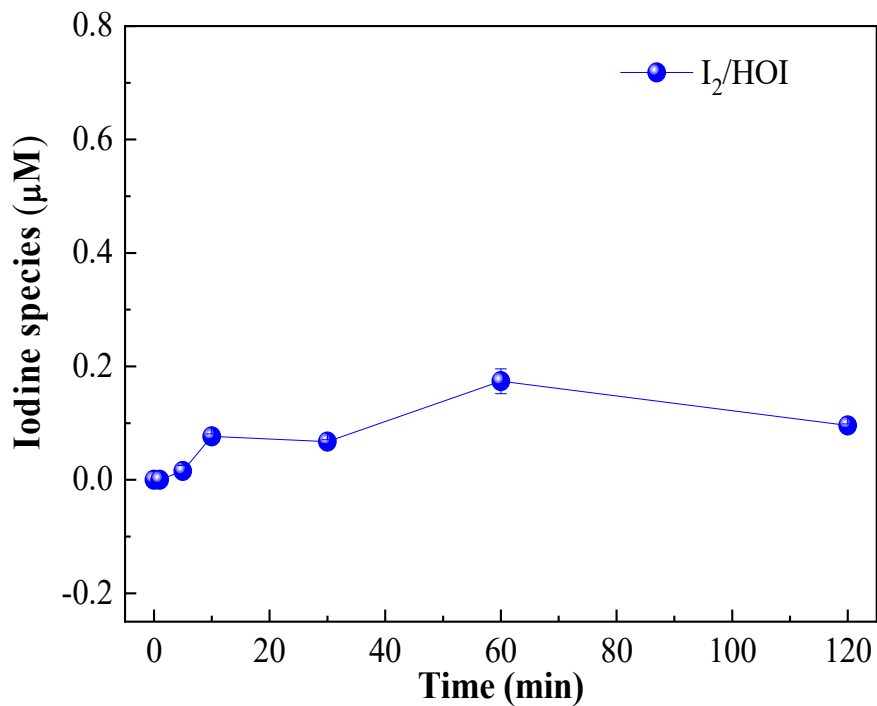

Figure 4.33 Mass balance of IO₃⁻
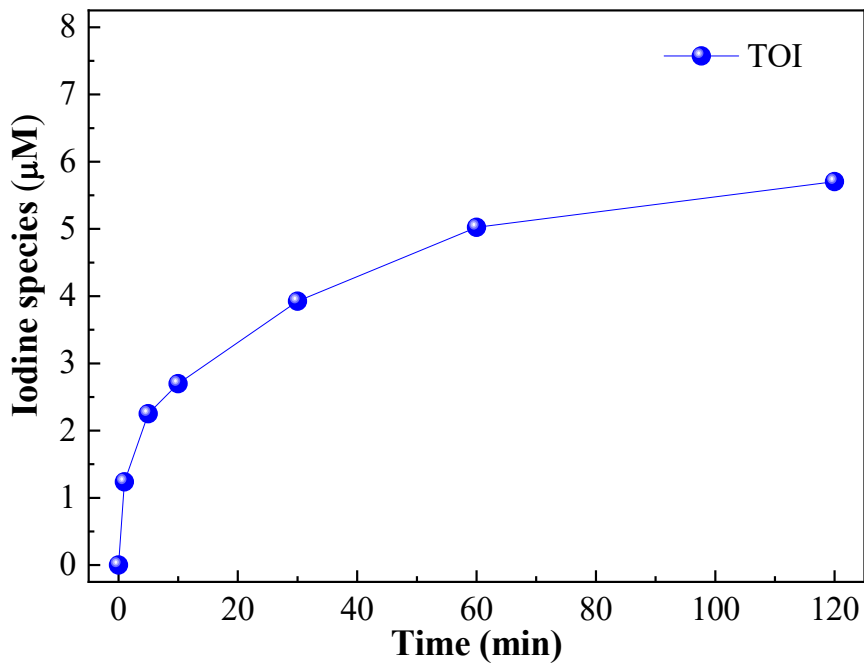
Figure 4.34 Mass balance of I₂/HOI

Figure 4.35 Mass balance of TOI

Due to the large TOI produced in this system, the generation of I-DBPs has attracted people's attention. As shown in Figure 4.36-4.40, the production of Triiodomethane (TIM), Diiodoacetic acid (DIAA), Iodoacetic acid (IAA), Diiodoacetamide (DIAcAm) and Diiodoacetonitrile (DIAN) in HA and EPS were compared. Obviously, the N-IDBP generation (the sum of DIAcAm and DIAN) of EPS was higher than that of HA, while the C-IDBPs generation (the sum of TIM, DIAA and IAA) was lower. The N-IDBPs and C-IDBPs generation potential (FPs) of HA and EPS were 5.8 and 88.9 µg L^{-1}, respectively. And 8.4 and 29.1 µg L^{-1}.
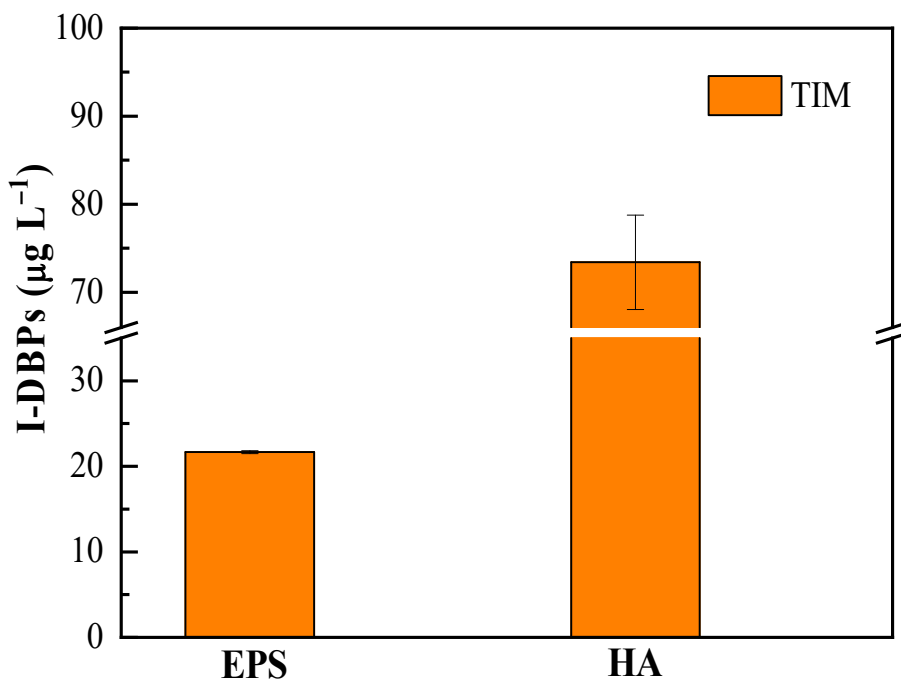
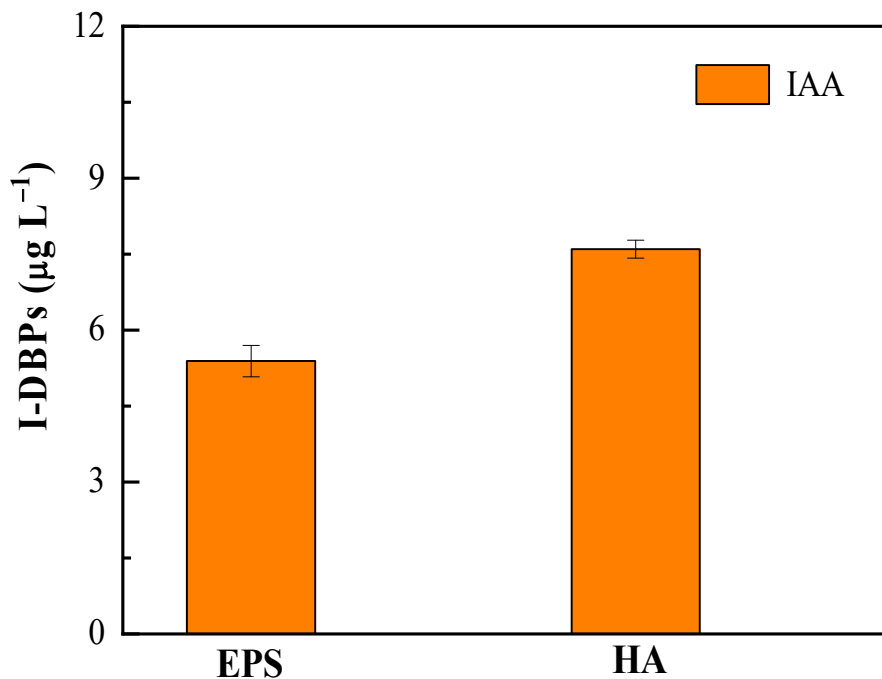**Figure 4.36 TIM yield from HA and EPS**

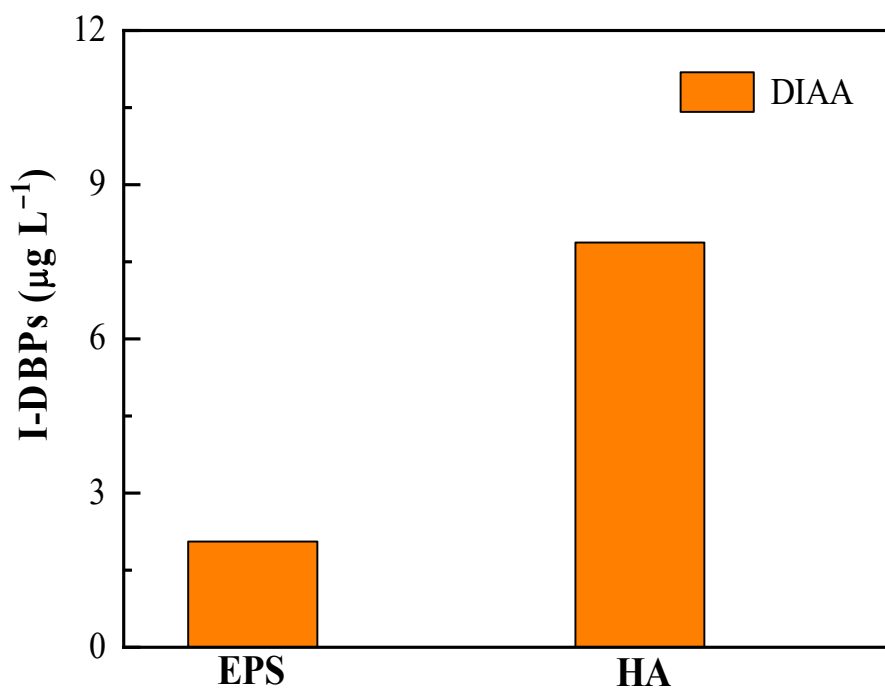**Figure 4.37 IAA yield from HA and EPS**

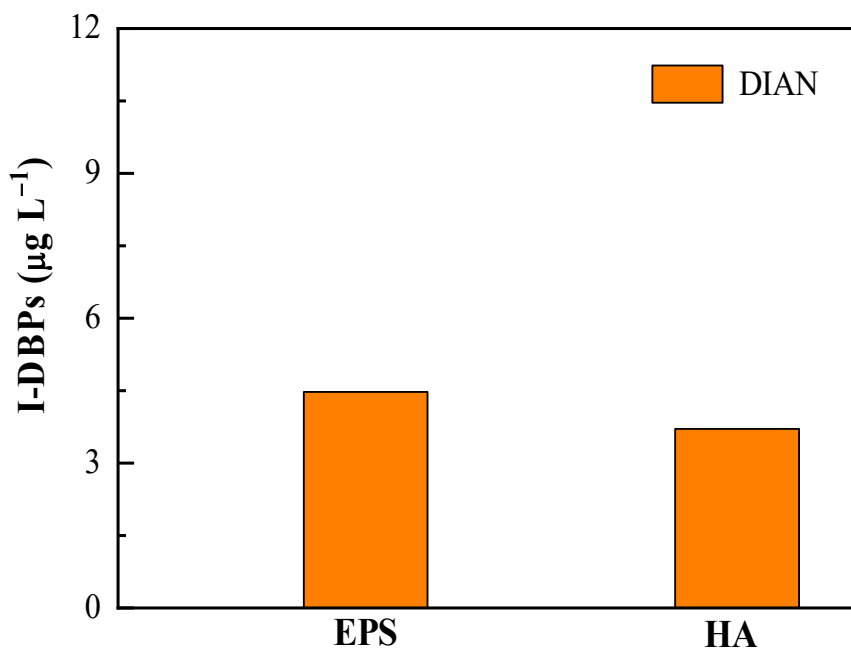**Figure 4.38 DIAA yield from HA and EPS**
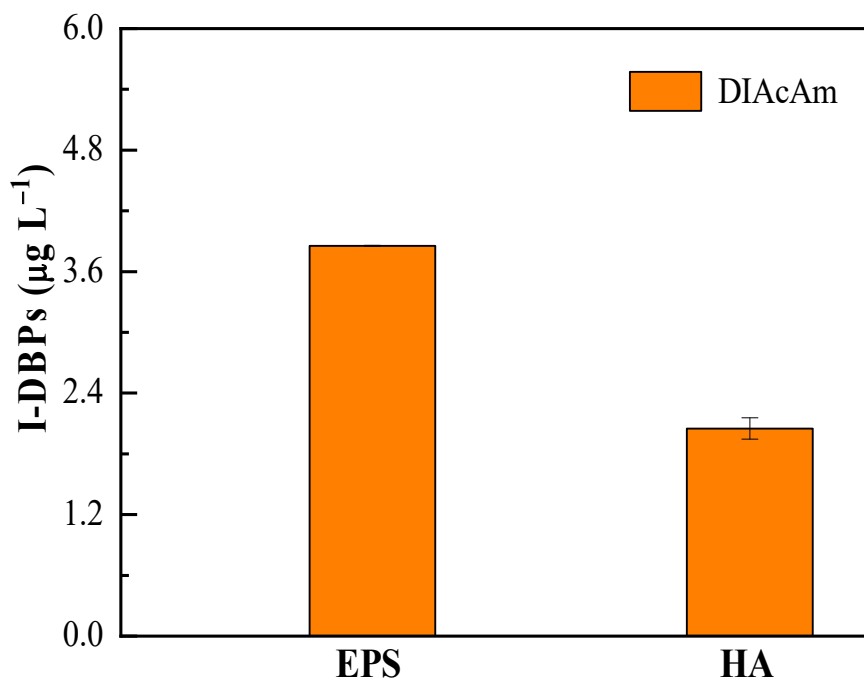
Figure 4.39 DIAN yield from HA and EPS

Figure 4.40 DIAcAm yield from HA and EPS

4.2.8 The influence of pH

The effect of pH on I-DBP$_S$ production was investigated in the range of 5.0 to 8.0. As shown in Figure 4.41-4.45, the production of I-ThMs, I-HAAs and I-HANs significantly decreases with increasing pH. For example, TIM's FPs at pH 5.0, 6.0, 7.0, and 8.0 were 81.3, 22.2, 9.3, and 5.2 μg L^{-1}, respectively. The relationship between I-DBPs generation and pH can be explained by two aspects: on the one hand, high pH results in a decrease in ΔE_H of MnO$_2$ oxidation of I$^-$ the formation of I$_2$/HOI (Equation 1). On the other hand, the iodine atom in I$_2$/HOI forms a complex that is polarized by MnO$_2$, thus enhancing the reactivity of I$_2$/HOI to organic matter [16,18]. The effect of MnO$_2$ on the polarization of I$_2$/HOI is weakened by the increase of MnO$_2$ surface negative charge from pH 5.0 to 8.0. In addition, as shown in Fig 4.46, different from these three species, the generation of I-HACams reaches its maximum value at pH 6.0. DIAcAm's FPs at 5.0, 6.0, 7.0, and 8.0 were 2.1, 3.9, 1.8, and 1.2 μg L^{-1}, respectively. This can be interpreted as that haloacetamide (HAcAms) is a metastable disinfection by-product, which is mainly generated from the hydrolysis of haloacetonitrile (HANs) [20] to haloacetic acid (HAAs), which is then generated by further hydrolysis [32]. Therefore, the generation of HAcAms depends largely on the difference between the hydrolysis rate of HANs and the decomposition rate of HAcAms. Since HANs is more stable under acidic conditions, the hydrolysis rate increases as pH increases to. In addition, previous studies have confirmed that the hydrolysis rate of HANs with the same number of halogen substituents decreases as halogens are transferred from chlorine to bromine [33]. Therefore, it can be inferred that at the same pH value, the hydrolysis rate of DIAN is relatively lower than that of dichloroacetonitrile (DCAN) and dibromoacetonitrile (DBAN). The decomposition rate of HAcAms consists of two parts: hydrolysis rate and halogenation rate. Both of them increase with the increase of pH value, and the hydrolysis rate of iodine is slower and more stable than chlorine and bromine disinfection by-products [23]. For example, dichloride, dibromo and diiodoacetamide (DCAcAm, The k_{HO}- (alkaline hydrolysis) and k_{ClO}- (chlorination of

hypochlorite) values of DBAcAm and DIAcAm were 2.4×10^3, 1.6×10^3 and 8.0×10^2 M^{-1} h^{-1} and 3.8×10^4, 1.2×10^5 and 8.2×10^4 M^{-1} h^{-1}, respectively. Both HANs and HAcAms become unstable with increasing PH, and their stability follows iodination>Bromide> Chloride sequence. Chu et al [22] showed that at pH 8.0, the generation of DCAcAm was maximized in the reaction between free chlorine and tyrosine, and the difference in hydrolysis rate between DCAcAm and DCAN was higher at Ph 7-8 than at other pH values.This is due to the greater stability of DIAcAm and DIAN, and therefore maximum differences can be achieved at pH values above 8.0. According to the reasons mentioned above, it was explained more systematically that inK this experiment, combined with the higher I_2/HOI production in acidic solution, the production of DIAcAm reached its maximum value at pH 6.0. However, in the process of oxidizing I^- in water with PbO_2, the DIAcAm production of EPS reached its maximum at pH 7.0. This difference can be explained as the oxidation potential of MnO_2 is lower than that of PbO_2, so less I_2/HOI is generated at the same pH value [3, 6].
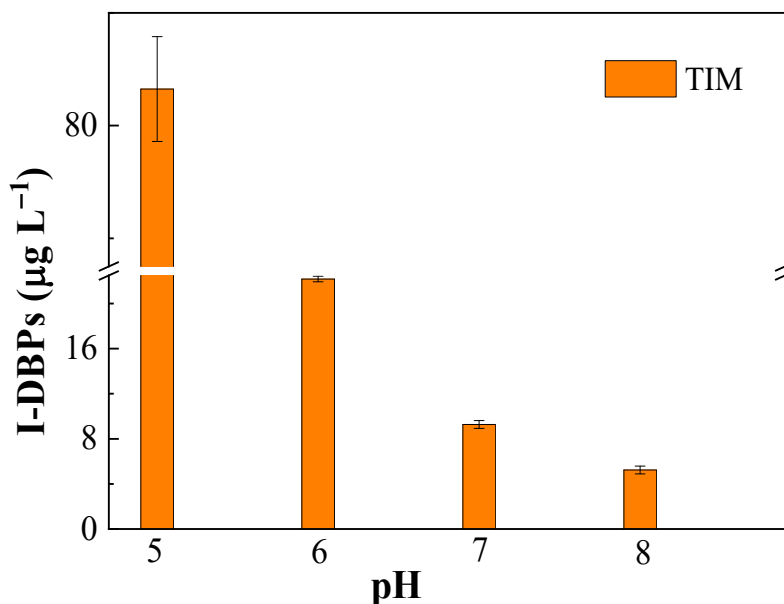

Figure 4.41 Effect of pH on the oxidation formation of TIM from EPS
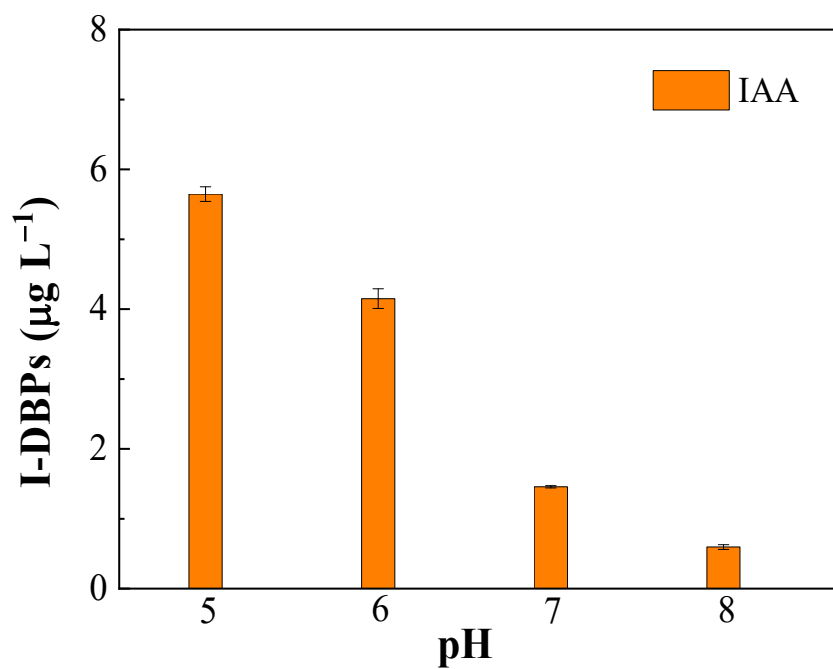
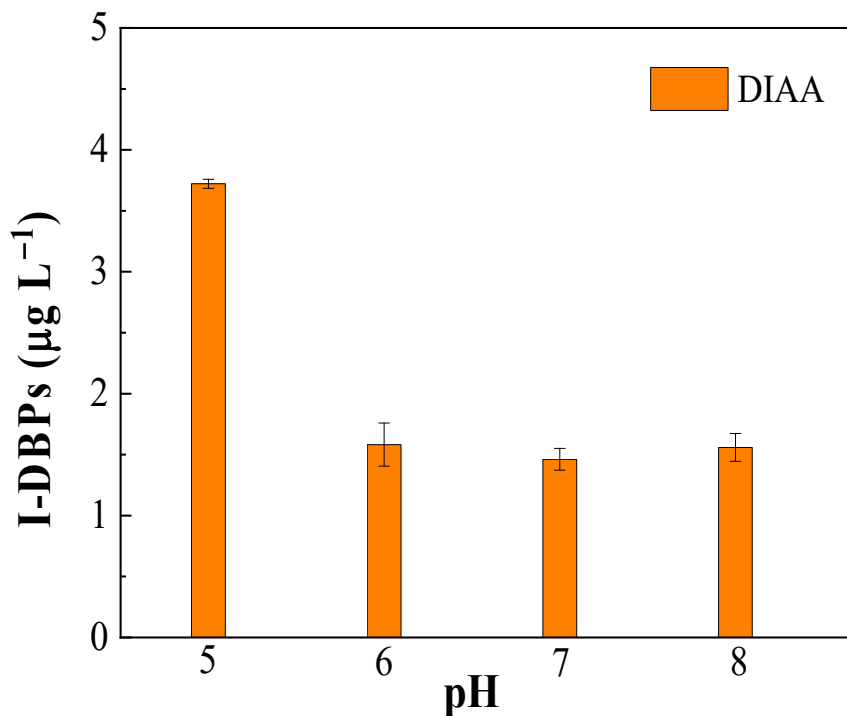**Figure 4.42 Effect of pH on the oxidation formation of IAA from EPS**

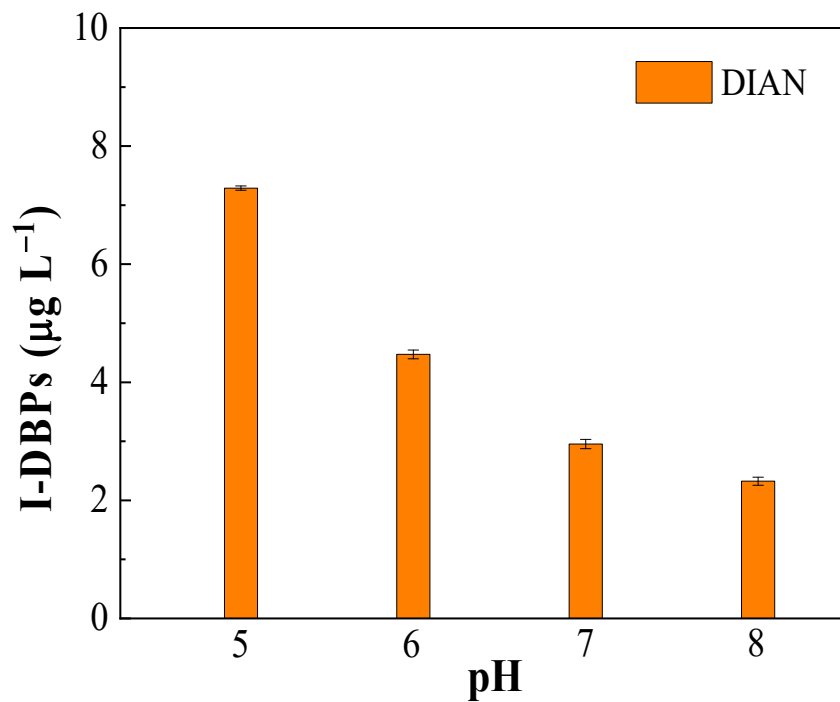Figure **4.43 Effect of pH on the oxidation formation of DIAA from EPS**

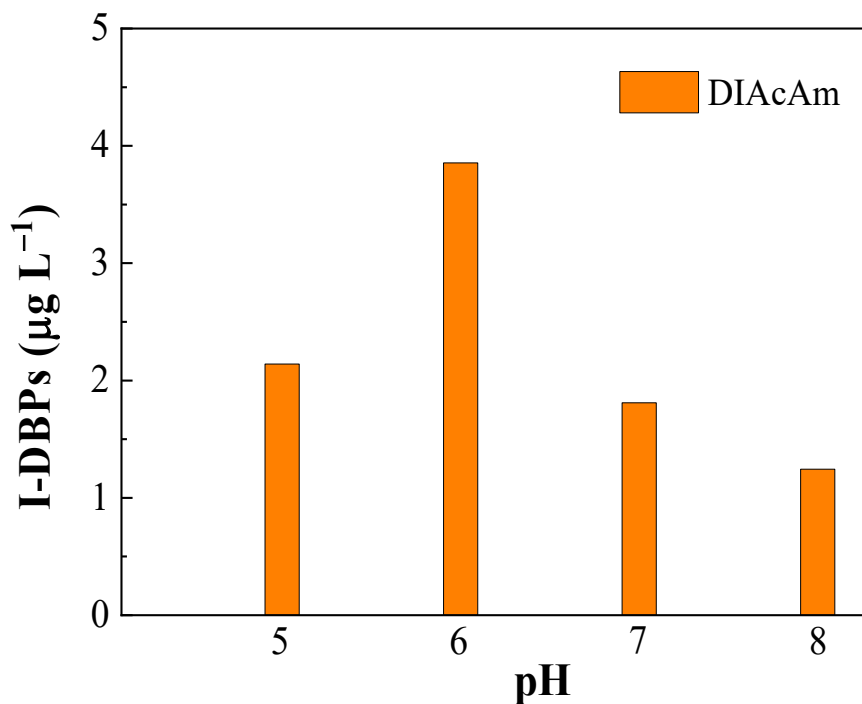**Figure 4.44 Effect of pH on the oxidation formation of DIAN from EPS**

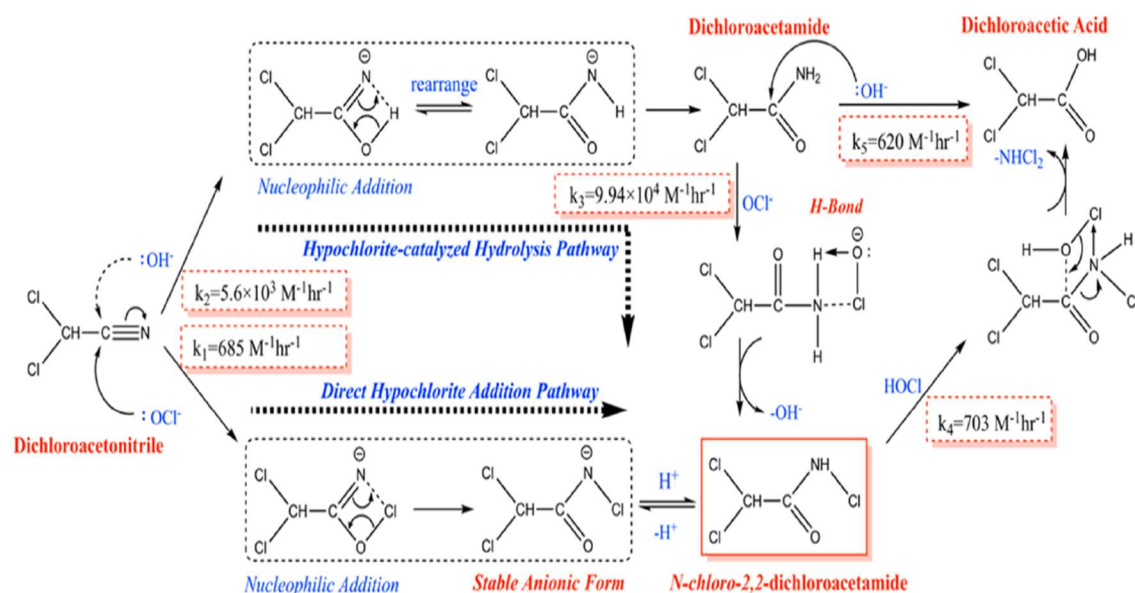**Figure 4.45 Effect of pH on the oxidation formation of DIAcAm from EPS**

Figure 4.46 Formation and decomposition of chloroacetamides[21]

4.2.9 Effects of MnO₂ dose and I⁻ concentration

Figure 4.47-4.56 shows the effect of I - concentration and MnO2 dose on I-DBPS generation, with I- and MnO2 dose being 0.1−3.0 mg L -1 and 0.1−2.0 g L -1, respectively. As shown in Figure 4.47-4.51,I-DBPs production increased significantly with the increase of I- concentration. For example, DIAN's FPs increased from 2.6 μg L^{-1} to 9.0 μg L^{-1} as the I⁻concentration increased from 0.1 mg L $^{-1}$ to 3.0 mg L $^{-1}$. The production of IO$_3^-$ also increased with the concentration of I⁻. As shown in Figure4.47-4.51, the concentrations of IO$_3^-$ were 26.4, 35.2, 86.6, 176.1 and 270.6 μg L $^{-1}$, and the concentrations of I⁻ were 0.1, 0.5, 1.0, 2.0 and 3.0 mg L $^{-1}$, respectively. These results indicate that the active sites on MnO$_2$ surface are not fully occupied by I⁻ or I$_2$/HOI, so the increase of I⁻ promotes the generation of IO$_3^-$ and I-DBPs.

As shown in Figure 4.52-4.56, the increase of MnO$_2$ dose accelerates the generation of IO$_3^-$, but decreases the production of I-DBPs. For example, as the concentration of MnO$_2$ increased from 0.1 g L to 2.0 gL^{-1}, the FPs of I-THMs, I-HAAs, I-HANs, and I-HAcAms decreased from 77.4 to 7.7, 8.8 to 4.1, 8.7 to 3.7, and 4.9 to 2.4 μg L $^{-1}$. At the same time, the concentration of IO$_3^-$ increased from 8.6 to 189.4 μg L $^{-1}$. This can be

interpreted as follows: although the increase of MnO_2 dose increases the ΔE_H value of I^- oxidation, thus promoting the formation of I_2/HOI. However, when MnO_2 is used as oxide, the reaction between I_2/HOI and EPS generates I-DBPs and IO_3^- has a competitive relationship. Experimental results show that high concentration of MnO_2 is more conducive to IO_3^- production, which is consistent with the results of the MnO_2/I^-/NOM system previously studied by Gallard et al. [16].

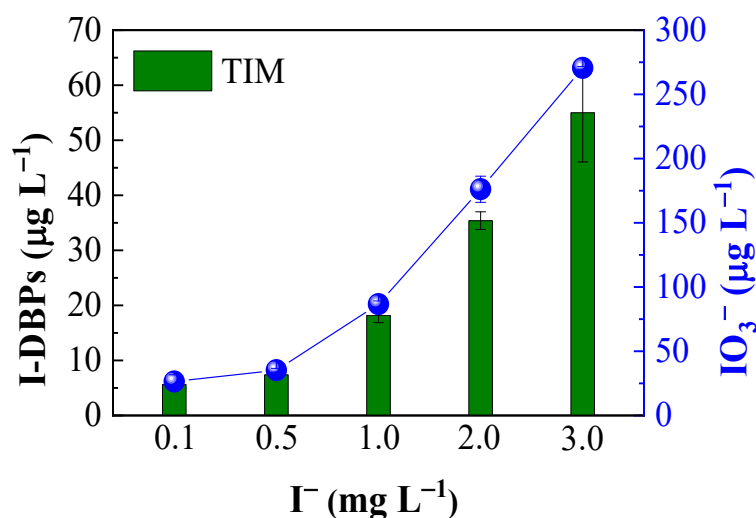**Figure 4.47 Effect of I^- initial concentration on the oxidation formation of TIM from EPS**

Figure 4.48 Effect of I^- initial concentration on the oxidation formation of IAA from EPS

Figure 4.49 Effect of I⁻ initial concentration on the oxidation formation of DIAA from EPS

Figure 4.50 Effect of I⁻ initial concentration on the oxidation formation of DIAN from EPS

Figure 4.51 Effect of I− initial concentration on the oxidation formation of DIAcAm from EPS

Figure 4.52 Effect of MnO2 initial concentration on the oxidation formation of TIM from EPS

Figure 4.53 Effect of MnO2 initial concentration on the oxidation formation of IAA from EPS

Figure 4.54 Effect of MnO2 initial concentration on the oxidation formation of DIAA from EPS

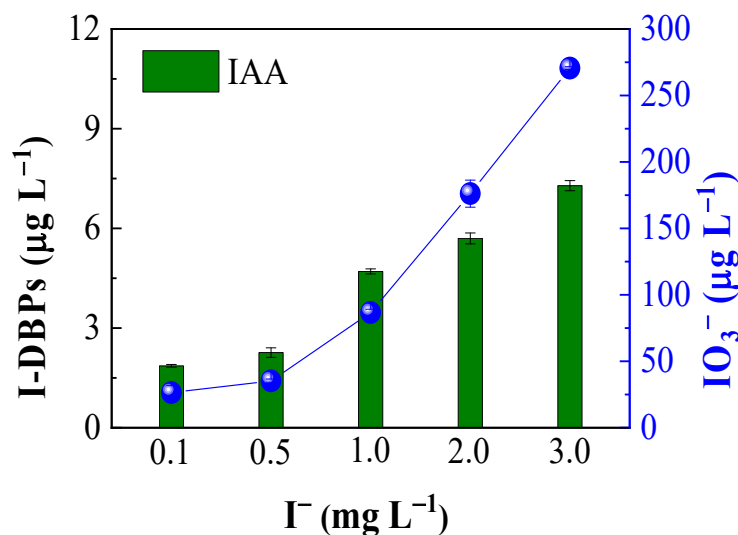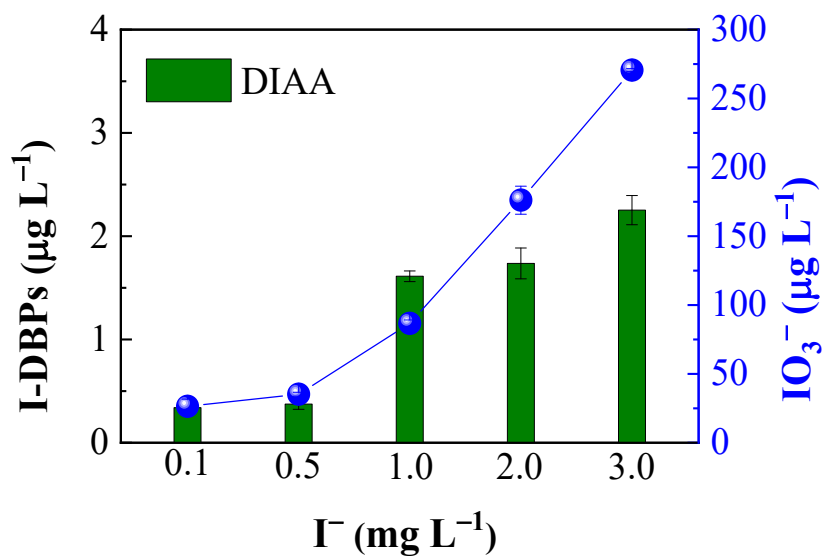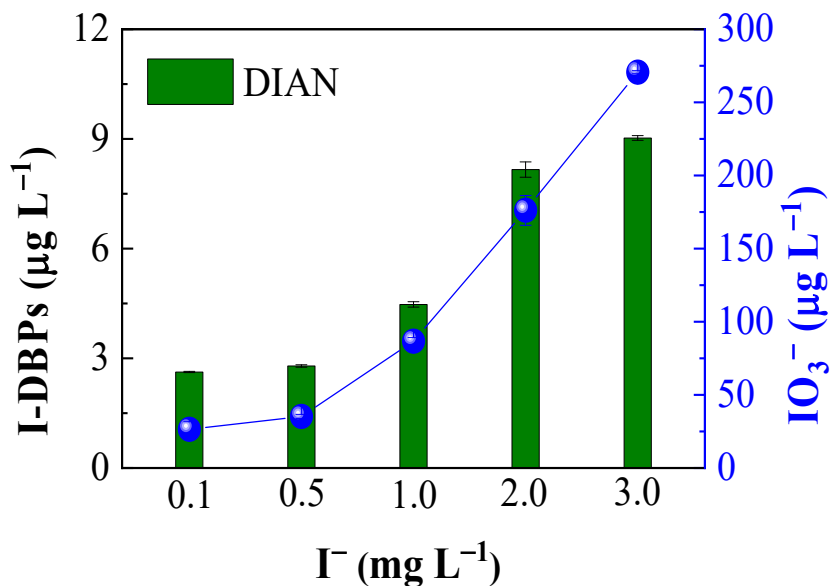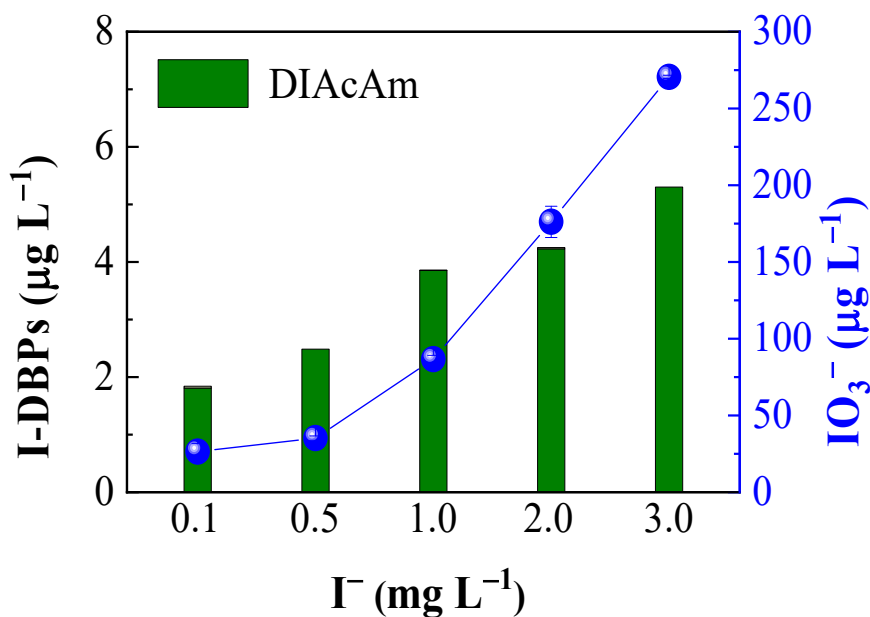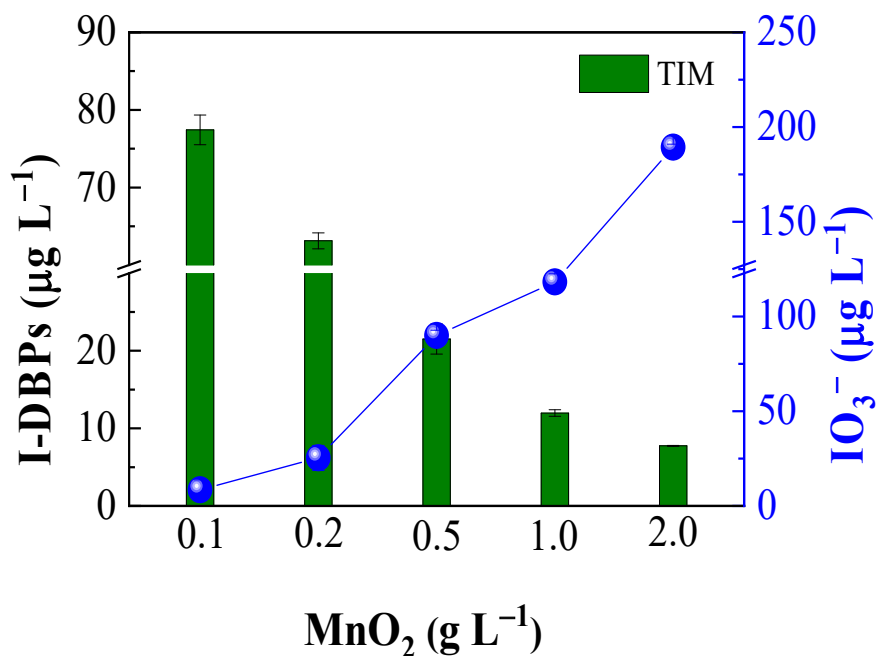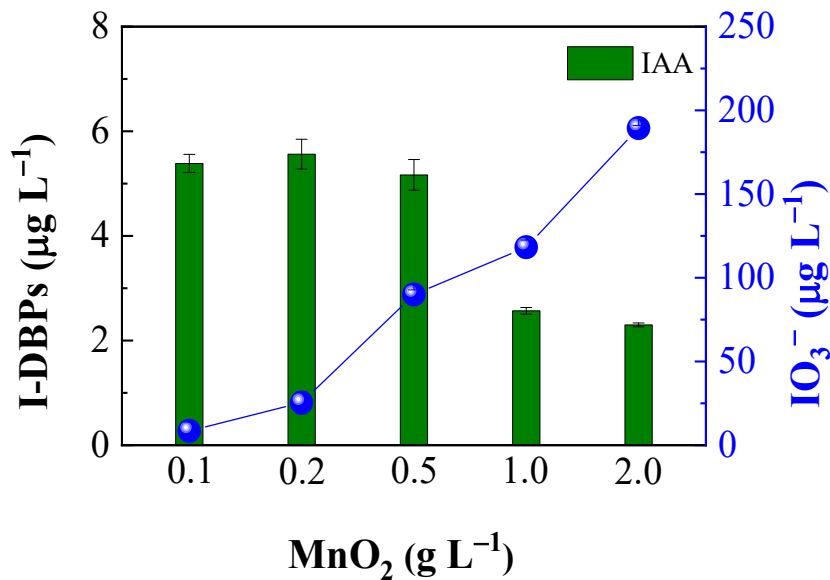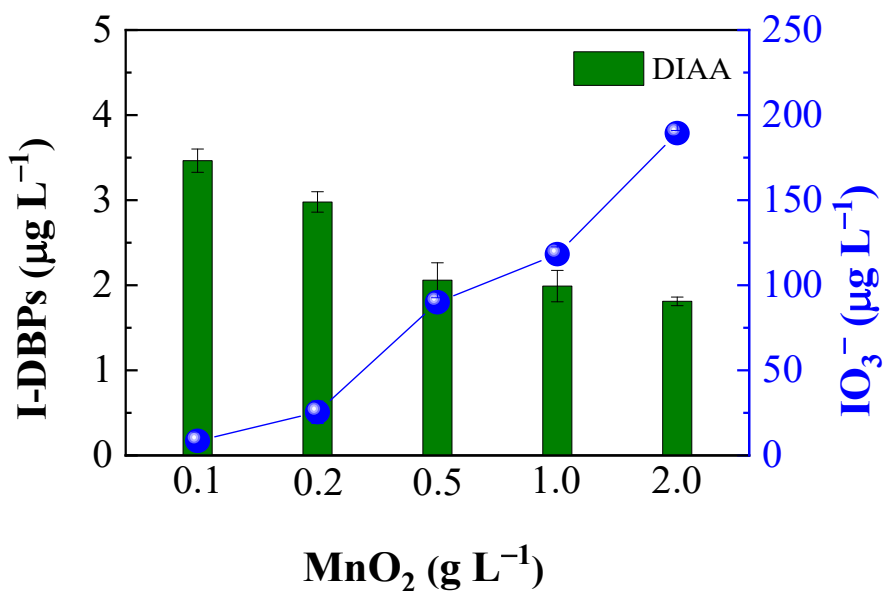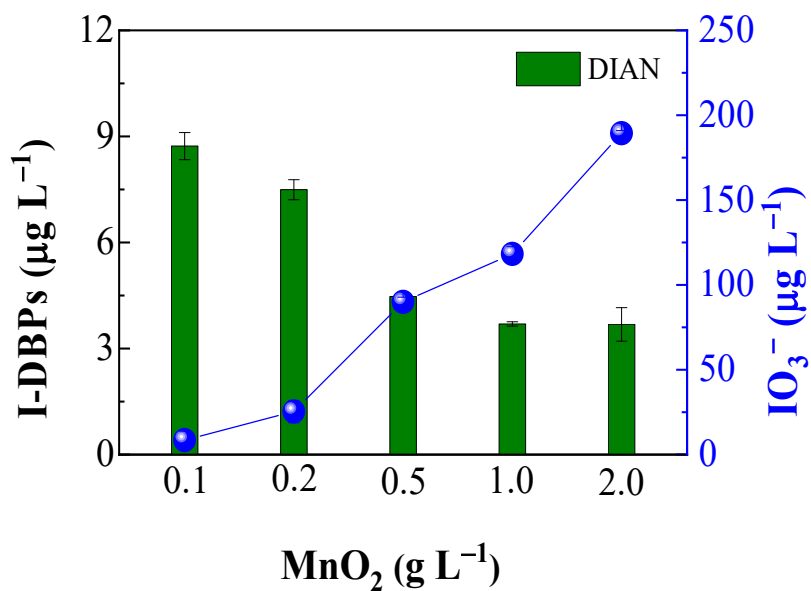**Figure 4.55 Effect of MnO₂ initial concentration on the oxidation formation of DIAN from EPS**
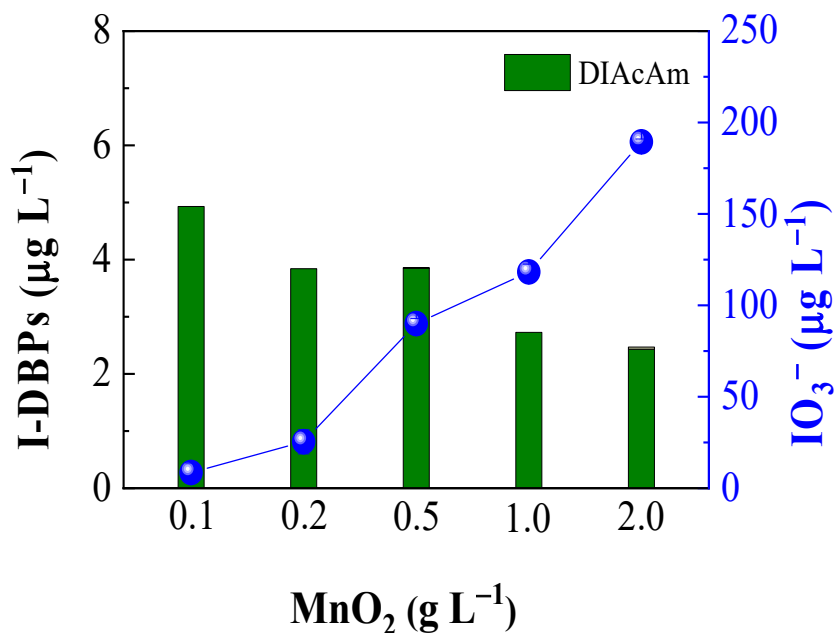
Figure 4.56 Effect of MnO2 initial concentration on the oxidation formation of DIAcAm from

EPS

4.2.10 EPS protein components and polysaccharides produce I-DBPs

About 80% of EPS is composed of protein and polysaccharide. The production of I-DBPs was studied using protein and polysaccharide as precursors. As shown in Figure 4.57-4.61, N-IDBPs and C-IDBPs production of polysaccharides was lower than that of proteins. FPs for I-THMs, I-HAAs, I-HANs and I-HAcAms from proteins and polysaccharides were 72.5, 19.5, 12.9 and 8.2 $\mu g\ L^{-1}$, and 15.8, 8.2, 1.0 and 0.4 $\mu g\ L^{-1}$, respectively. The results can be attributed to completely different chemical compositions between the two biomolecules. The explanation is as follows: proteins are composed of amino acids including unsaturated (conjugated) bonds, while polysaccharides are composed of carbohydrates with saturated ring structures [34]. The former has a stronger ability to acquire electrons from α-carbon than the latter, resulting in heterogeneous distribution of electron clouds and promoting electrophilic iodination reactions, thus generating I-DBPs. In addition, for the amount of N-IDBPs production, the nitrogen content in protein is higher than that in polysaccharide. It has been reported that polysaccharide monomers contain only glucosamine and a small amount of nitrogen. In previous studies by Hong et al. [25], proteins were considered to be the most important precursors of two C-IDBPs in biofilm biomolecules. Wang et al. [27] also proved that Pseudomonas putida EPS (protein type) had higher HANs production than EPS (polysaccharide type) of Pseudomonas aeruginosa.
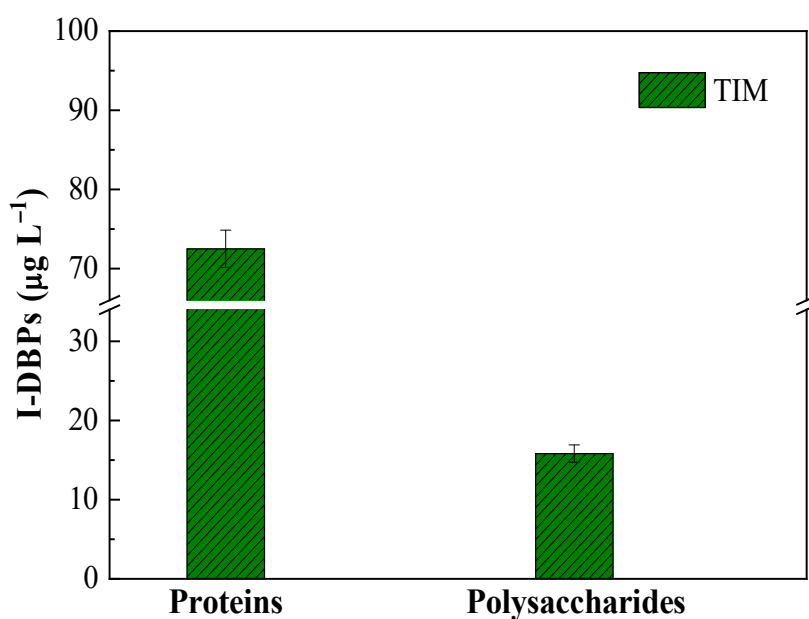
Figure 4.57 Oxidation formation of TIM from EPS proteins and polysaccharides

Figure 4.58 Oxidation formation of IAA from EPS proteins and polysaccharides

Figure 4.59 Oxidation formation of DIAA from EPS proteins and polysaccharides
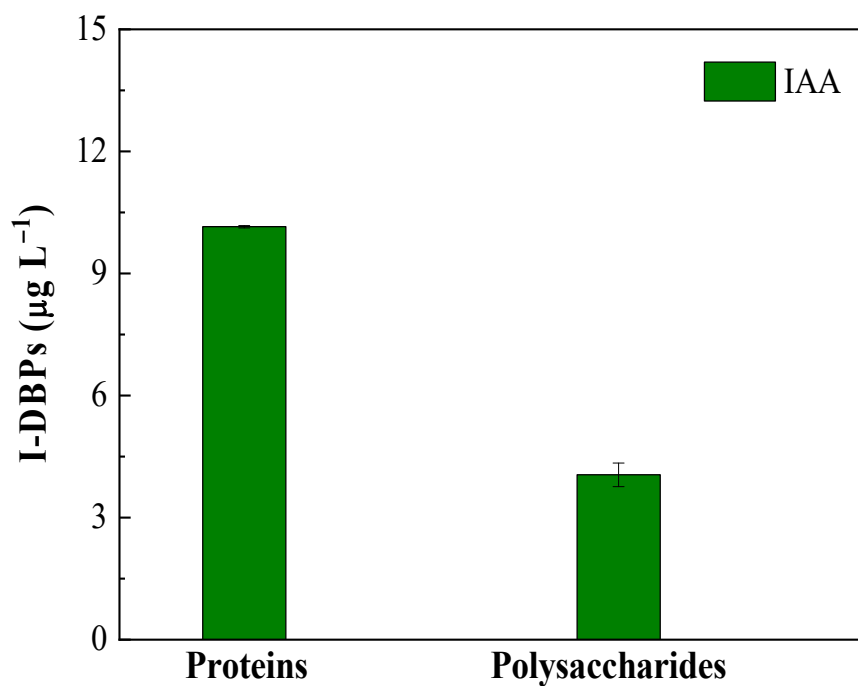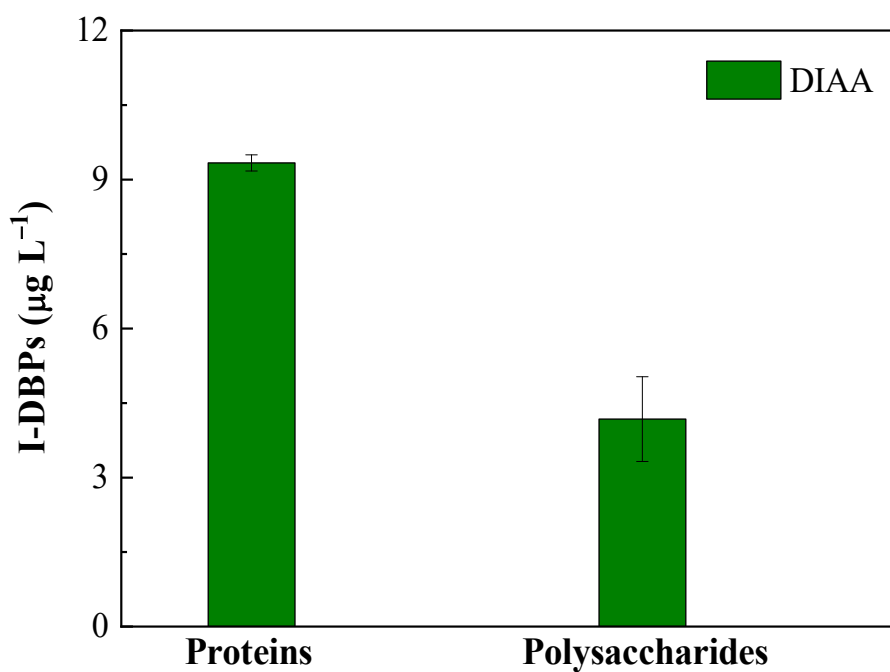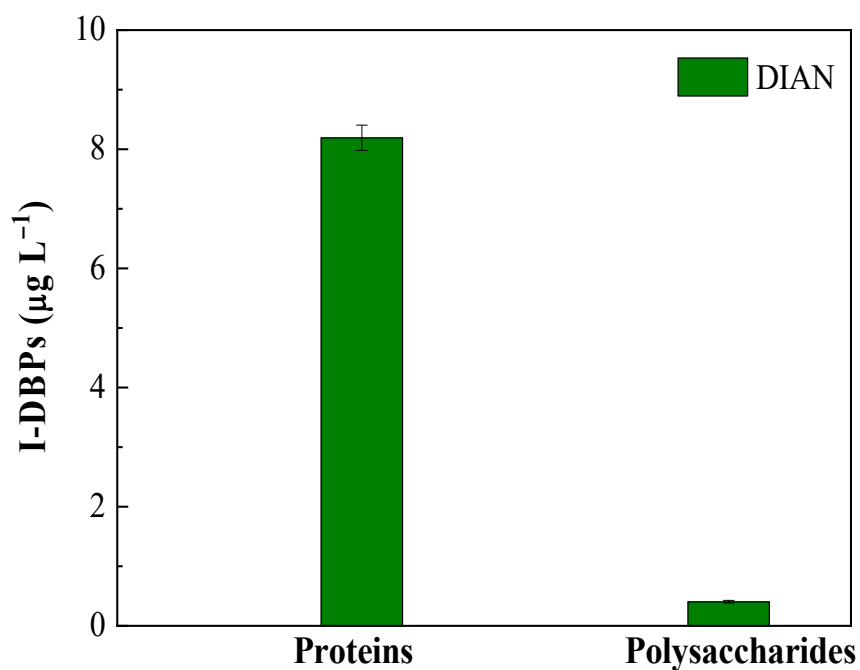
Figure 4.60 Oxidation formation of DIAN from EPS proteins and polysaccharides
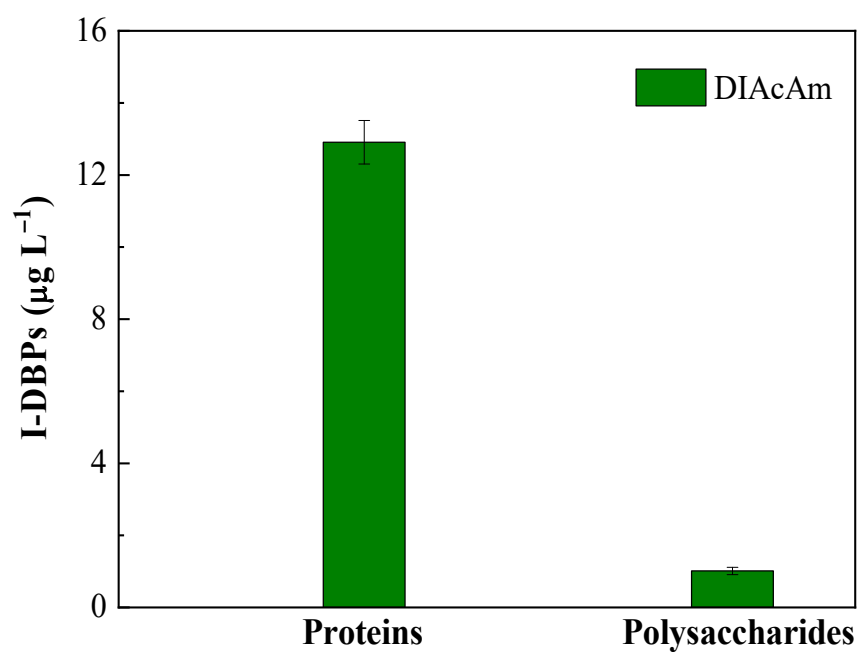

Figure 4.61 Oxidation formation of DIAcAm from EPS proteins and polysaccharides

4.2.11 I-DBPs are formed from amino acids

Through the identification of proteins, 20 amino acids were identified, and these 20 amino acids were used as precursors for experiments to study the effects of different chemical structures on I-DBPs production in MnO_2/I^- /EPS system. Figure 4.62 shows the effects of major amino acid precursors of C-IDBPs and N-IDBPs on I-DBPs yield.

For I-THMS, aspartic acid (Asp), tryptophan (Trp) and histidine (His) showed relatively high TIM production, with the values of 54.2, 98.5 and 52.3 μg L^{-1}, respectively. This result is consistent with the study on THMs generation by Hong et al. [25]. As shown in Fig. 4.27 (a), Li et al. [29] explained the formation mechanism of THMs, so the formation mechanism of I-THMS corresponds to it. The reaction involves a series of reactions, for example, continuous decarylation and substitution to generate tryptamine and 3-iodoindole, followed by five-member heterocyclic cleavage. As shown in Table 3.1, the content of Trp (1.0%) is much lower than Asp (5.5%). Therefore, although Trp has the highest FPs, Asp is still the most important amino acid precursor of I-THMS.

For I-HAAs, Asp showed the highest FPs of MIAA and DIAA at 136.8 and 34.6 μg L^{-1}, respectively. As shown in figure 4.27 (b), the generation of I-HAAs involves two key steps :(1) hydrogen atoms on α -carbon atoms in nitrile ($R-CH_2-CN$) are replaced by iodine to generate monoiodine and diiodinitrile ($R-CI-CN$ and $R-CI_2-CN$); (2) Elimination of monoiodoacetonitrile (CI-CN) and diiodoacetonitrile (CHI_2-CN) produced by the R group [26]. In addition, the FPs of Asp I-HAAs is much higher than that of Asn and Trp, which can be explained by the fact that carboxyl groups are more likely to gain electrons from α -carbon bonds, thus facilitating iodine substitution and the elimination of R groups. Compared with PbO_2/I^- /EPS system, the generation of MIAA but not DIAA was promoted in MnO_2/I^- /EPS system. This can be interpreted as that the difference in the generation of I-HAAs species may be due to the higher oxidation potential of PbO_2 than MnO_2, resulting in more I_2/HOI participating in iodine substitution reactions.

For I-HAcAms and I-HANs, as shown in Figure 4.27 (b), 3-13, 3-14, the DIAN and DIAcAm generation of aspartic acid (Asp), asparagine (Asn) and tyrosine (Tyr) are roughly the same. The main FPs of DIAcAm and DIAN came from Asp, Asn and Tyr, which were 9.0 and 8.8, 8.2 and 8.2, and 6.2

and 7.6 μg L^{-1}, respectively. The I-HANs pathway is produced by eliminating the carboxyl, acyl and phenyl groups in Asp, Asn and Tyr, respectively. The formation of I-HANs is followed by hydrolysis, which leads to the formation of I-HAcAms. Since Asp has the most extensive influence in C-IDBPs and N-IDBPs, Asp is also considered to be the most important amino acid precursor produced by I-HAAs, I-HAcAms and I-HANs.
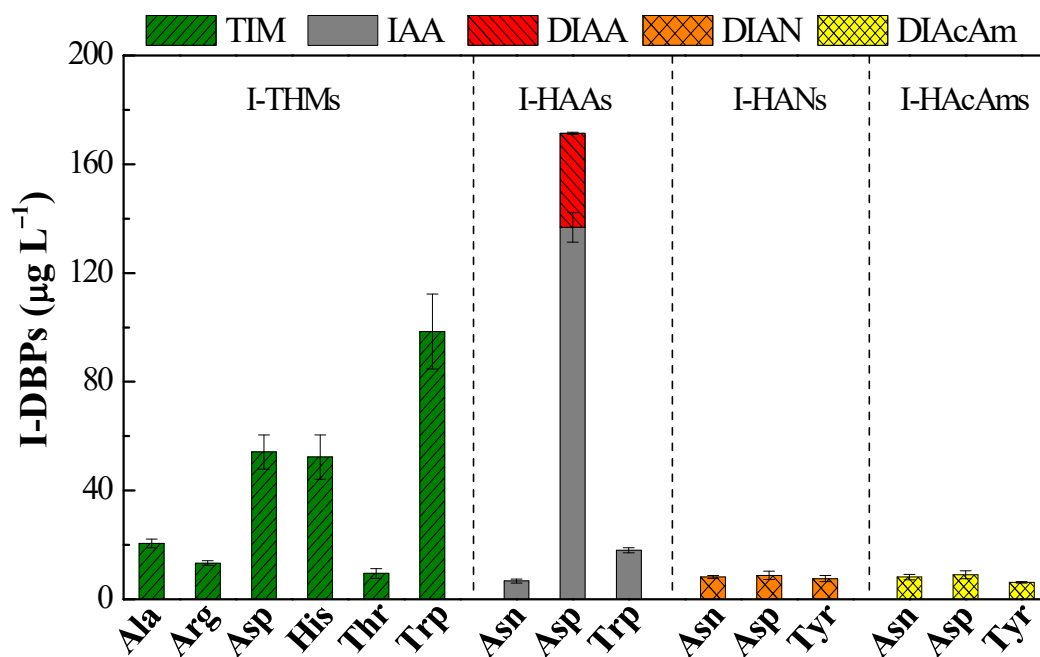
Figure 4.62 Oxidation formation of I-DBPs from EPS proteins and polysaccharides

4.2.12 The control strategy

Combined with the lead containing water pipe in Chapter 3 and manganese containing water pipe in this chapter, some countermeasures to control I-DBPs generation when biofilm erupts are discussed. Countermeasures are as follows:

(1) Increase the alkalinity and hardness of water. PH increases to some extent with increasing alkalinity, which reduces the electrochemical driving force (ΔE_H) of I-DBPs generation. In addition, the increase in alkalinity and hardness promotes the precipitation of calcium carbonate ($CaCO_3$), which covers the corroded surface and thus reduces the contact area between the corroded products and large amounts of water.

(2) Use free chlorine, persulfate and other disinfectants and keep high residue. When excess free chlorine is present, most I$^-$ is oxidized to IO$_3$$^-$, however, large amounts of free chlorine may lead to an increase in Cl-DBPs. Appropriate increase of free chlorine can also effectively control the growth of EPS in the pipe network. However, some studies have found that disinfectants cannot completely prevent the formation of biofilms, so attention should be paid to the selection and dosage of disinfectants [35].

(3) Biofilm removal by hydraulic scouring. It is well known that hydraulic scour is an effective method for biofilm shedding from pipe interface. There are two ways to choose hydraulic scour, one is air-water combined scour, the other is direct hydraulic scour. It has been pointed out that regular hydraulic scour is of great significance to improve water quality and reduce the growth of microorganisms. However, the disadvantage of hydraulic scour is that corrosion products can be released into large amounts of water when the biofilm is removed. Among them, water pressure and flow rate are key factors, which need to be carefully selected [35].

4.3 The summary of this chapter

In this chapter, the oxidation of C-DBPs and N-DBPs formation by PbO$_2$ and MnO$_2$ with EPS and its components (protein and polysaccharide) as precursors was studied. Based on the experimental results, the following conclusions are drawn:

（1）When the R$_{Pb}$/I value was high, the I$^-$ oxidation rate decreased with the increase of pH, the H$^+$ reaction order was 0.79, and the constant rate (k) was determined to be 1.6×10^{11} M$^{-2.79}$ s^{-1}. In the presence of EPS, most I$_2$/HOI (>92%) were further converted to TOI.

（2）Compared with HA, I-DBPs of EPS showed stronger chronic cytotoxicity due to the higher generation potential of N-IDBPs. PbO$_2$ dose and I$^-$ concentration also had important effects on the generation of I-DBPs.

（3）The proteins showed higher potentials for both C- and N-IDBPs than polysaccharides due to more electrophilic sites and higher N content.

（4）Among the 20 amino acids, Asp was the main precursor to generate I-THM and I-HAAs,

and Asp, Asn and Tyr were important precursors of I-HANs and I-HAcAms

(5) In MnO_2/I^- /EPS system, more than 93% of the generated I_2/HOI was further converted to TOI. Compared with HA, EPS had lower C-IDBPs production, but higher N-IDBPs production.

(6) The formation of I-HACAms is larger under acidic conditions, while the other three I-DBPs are more favorable under acidic conditions. There was a positive correlation between I-DBPS production and I^- concentration, and a negative correlation between I-DBPs production and MnO_2 dose.

(7) Due to higher nitrogen content and more unsaturated (conjugated) bonds, protein has higher N-IDBPs and C-IDBPs yields than polysaccharide.

(8) In view of the proportion of amino acids in proteins, Asp is the main amino acid precursor in the production of I-DBPs studied.

(9) When the biofilm erupts in the pipe network, methods such as increasing the alkalinity and hardness of water, disinfecting with free chlorine and maintaining high residual amount, and removing the biofilm by hydraulic flushing can be appropriately taken to remove it.

Reference

[1]   Lytle D.A., Schock M.R. Formation of Pb(IV) oxides a in chlorinated water [J]. Journal American Water Works Association, 2005, 97 (11) : 102–114.

[2]   Bichsel Y., von Gunten U. Oxidation of iodide and hypoiodous acid in the disinfection of natural waters [J]. Environmental Science & Technology, 1999, 33 (22) : 4040−4045.

[3]   Lin Y.P., Washburn M.P., Valentine R.L. Reduction of lead oxide (PbO2) by iodide and formation of iodoform in the PbO2/I−/NOM System [J]. Environmental Science & Technology, 2008, 42 (8) : 2919–2924.

[4]   Richardson S.D., Fasano F., Ellington J.J., et al. Occurrence and mammalian cell toxicity of iodinated disinfection byproducts in drinking water [J]. Environmental Science & Technology, 2008, 42 (22) : 8330–8338.

[5]   Dong H.Y., Qiang Z.M., Richardson S.D. Formation of iodinated disinfection byproducts (I-DBPs) in drinking water: Emerging concerns and current issues [J]. Accounts of

Chemical Research, 2019, 52 (4) : 896−905.

[6]   Allard S., von Gunten U., Sahli E., et al. Oxidation of iodide and iodine on birnessite (δ-MnO2) in the pH range 4–8 [J]. Water Research, 2009, 43 (14) : 3417−3426.

[7]   Allard S., Nottle C.E., Chan A., et al. Ozonation of iodide-containing waters: Selective oxidation of iodide to iodate with simultaneous minimization of bromate and I-THMs [J].

[8]   Wingender J., Neu T.R., Flemming H.C. Wingender, J., Neu, T. R., Flemming, H. C. [M]. Berlin: Springer, 1999.

[9]   Hu J, Wang C, Shao B.J, et al. Enhanced formation of carbonaceous and nitrogenous disinfection byproducts from biofilm extracellular polymeric substances undercatalysis of copper corrosion products [J]. Science of the Total Environment, 2020, 723: 138–160.

[10]   Gerke T.L., Little B.J., Maynard J.B. Manganese deposition in drinking water distribution

[11]   Cerrato J.M., Falkinham J.O., III, Dietrich A.M., et al. Manganese-oxidizing and -reducing microorganisms isolated from biofilms in chlorinated drinking water systems [J]. Water Research, 2010, 44 (13) : 3935–3945.

[12]   systems [J]. Science of the Total Environment, 2016, 541: 184–193.

[13]   Revetta R P, Gomez-Alvarez V, Gerke T L, et al. Establishment and early succession of bacterial communities in monochloramine-treated drinking water biofilms [J]. FEMS Microbiology Ecology, 2013, 86(3): 404-14.

[14]   Dong S.K., Lu J.F, Pewa M.J., et al. Comparative mammalian cell cytotoxicity of wastewaters for agricultural reuse after ozonation [J]. Environmental Science & Technology, 2016, 50 (21) : 11752−11759.

[15]   Muellner M G, Wagner E D, Mccalla K, et al. Haloacetonitriles vs. Regulated Haloacetic Acids: Are Nitrogen-Containing DBPs More Toxic? [J]. Environmental Science & Technology, 2007, 41(2): 645-51.

[16]   HEEB M B, CRIQUET J, ZIMMERMANN-STEFFENS S G, et al. Oxidative treatment of bromide-containing waters: Formation of bromine and its reactions with inorganic and organic compounds — A critical review [J]. Water Research, 2014, 48(15-42.

[17]   Fox P.M., Davis J.A., Luther G.W., III. The kinetics of iodide oxidation by the manganese

oxide mineral birnessite [J]. Geochimica Et Cosmochimica Acta, 2009, 73 (10) : 2850–2861.

[18]   Stavber S., Jereb M., Zupan M. Electrophilic iodination of organic compounds using elemental iodine or iodides [J]. Synthesis-Stuttgart, 2008, (10) : 1487–1513.

[19]   Criquet J., Allard S., Salhi E., et al. Iodate and iodo-trihalomethane formation during chlorination of iodide-containing waters: Role of bromide [J]. Environmental Science & Technology, 2012, 46 (13) : 7350–7357.

[20]   Shah A D, Mitch W A. Halonitroalkanes, Halonitriles, Haloamides, and N-Nitrosamines: A Critical Review of Nitrogenous Disinfection Byproduct Formation Pathways [J]. Environmental Science & Technology, 2012, 46(1): 119-31.

[21]   Chu W.H., Gao N.Y., Deng Y., et al. Precursors of dichloroacetamide, an emerging nitrogenous DBP formed during chlorination or chloramination [J]. Environmental Science & Technology, 2010, 44 (10) : 3908−3912.

[22]   Chu W, Gao N, Yin D, et al. Formation and speciation of nine haloacetamides, an emerging class of nitrogenous DBPs, during chlorination or chloramination [J]. Journal of Hazardous Materials, 2013, 260(806-12.

[23]   Chu W., Gao N., Krasner S.W., et al. Formation of halogenated C-, N-DBPs from chlor(am)ination and UV irradiation of tyrosine in drinking water [J]. Environmental Pollution, 2012, 161: 8–14.

[24]   Comte S., Guibaud G., Baudu M. Biosorption properties of extracellular polymeric substances (EPS) resulting from activated sludge according to their type: Soluble or bound [J]. Process Biochemistry, 2006, 41: 815−823.

[25]   Fang J, Ma J, Yang X, et al. Formation of carbonaceous and nitrogenous disinfection by-products from the chlorination of Microcystis aeruginosa [J]. Water Research, 2010, 44(6): 1934-40.

[26]   Hong H.C., Mazumder A., Wong M.H., et al. Yield of trihalomethanes and haloacetic acids upon chlorinating algal cells, and its prediction via algal cellular biochemical composition[J]. Water Research, 2008, 42 (20) : 4941–4948.

[27] Wang Z.K., Kim J., Seo Y. Influence of bacterial extracellular polymeric substances on the formation of carbonaceous and nitrogenous disinfection byproducts. [J]. Environmental Science & Technology, 2012, 46: 11361–11369.

[28] Wang Z.K., Choi O.K., Seo Y.W. Relative contribution of biomolecules in bacterial extracellular polymeric substances to disinfection byproduct formation [J]. Environmental Science & Technology, 2013, 47: 9764–9773.

[29] Gomathi D L, Krishnaiah G M. Photocatalytic degradation of p-amino-azo-benzene and p-hydroxy-azo-benzene using various heat treated TiO2 as the photocatalyst [J]. Journal of Photochemistry and Photobiology A: Chemistry, 1999, 121(2): 141-5.

[30] Li C., Lin Q.F., Dong F.L., et al. Formation of iodinated trihalomethanes during chlorination of amino acid in waters [J]. Chemosphere, 2019, 217: 355–363.

[31] Li A. The Chlorination Disinfection by-products formation potential and pathway of amino acids [D]. Harbin Institute of Technology, 2011.

[32] Luo Z.F. Influence Factors and Control Methods of Biofilm Growth in Drinking Water Distribution Networks [D]. Zhejiang University, 2016.

[33] Yu Y., Reckhow D.A. Kinetic analysis of haloacetonitrile stability in drinking waters [J].Environmental Science & Technology, 2015, 49 (18) : 11028–11036.

[34] Wang Z.K., Li. L., Arissd R.W., et al. The role of biofilms on the formation and decay of disinfection by-products in chlor(am)inated water distribution systems [J]. Science of the Total Environment, 2021, 753: 141606.

[35] Wingender J., Neu T.R., Flemming H.C. Wingender, J., Neu, T. R., Flemming, H. C. [M]. Berlin: Springer, 1999.

CONCLUSION AND OUTLOOK

5.1 Conclusion

In order to prevent the problem of "secondary pollution" of drinking water and ensure the cleanliness and safety of drinking water in the process of distribution in the water supply network. In this paper, the catalytic effect of CCPs on the formation of DBPs was studied when EPS was used as a precursor under chlorine disinfection conditions. The effects of water pH and inorganic ion concentration on its catalytic effect were discussed in detail, and the protein and polysaccharide components in EPS were separated. To explore the effect of precursor structure and composition on the catalysis of CCPs, and finally select amino acids as model molecules to speculate on the catalysis mechanism of CCPs. The main conclusions are as follows:

(1) Compared with HA, when EPS was used as the precursor, the generation of DBPs was reduced, but it showed a higher potential for N−DBPs generation. Taking into account the relationship between DBPs concentration and toxicity (TIC−TOC), the health threat posed by EPS in pipe network biofilms cannot be ignored.

(2) The existence of CCPs can significantly catalyze the generation of DBPs, and the catalytic effect of N−DBPs is better than that of C−DBPs. The change of water pH significantly affected the catalytic effect of CCPs on DBPs, and the catalytic effect of CCPs was enhanced with the increase of pH. When Br^- exists in water, CCPs can also catalyze the formation of Br−DBPs, but the catalytic effect is weaker than that of Cl−DBPs. Catalytic effect of CCPs on EPS protein components Due to the polysaccharide component, the unsaturated structure in the protein component can promote the catalytic effect of CCPs. Under the condition of chlorination disinfection, the catalytic effect of CCPs on the formation of DBPs is mainly realized by the promotion of electrophilic substitution, oxidative decarboxylation, and ring-opening reactions.

(3) In the water containing I^-, PbO_2 can react with EPS through oxidation to generate I−DBPs. pH plays an important role in the oxidation capacity of PbO_2 and the

generation of I−DBPs. With the increase of pH, the oxidative ability of PbO_2 weakened and the generation of I−DBPs decreased. With the increase of I^- initial concentration, the I−DBPs generated by PbO_2 oxidation increased, and the proportion of triiodine DBPs increased. However, with the increase of PbO_2 concentration, the generation of I−DBPs gradually decreased. The composition and structure of precursors (proteins and polysaccharides) can significantly affect the effect of PbO_2 oxidation to generate I-DBPs. PbO_2 has better oxidation effect on precursors with more unsaturated structures such as phenolic or conjugated. In addition, PbO_2 can oxidize the precursor to a certain extent to generate smaller molecular weight species, thereby promoting the reaction of HOI/I_2 with the precursor to generate I−DBPs.

(4) In the $PbO2/I^-/EPS$ system, the I^- oxidation rate decreases with the increase of pH, the H^+ reaction order is 0.79, and the constant rate (k) is $1.6 \times 10\ 11\ M^{-2.79}s^{-1}$. Most I_2/HOI (>92%) were further converted to TOI. Compared with HA, EPS has higher N-IDBPs generating potential and stronger cytotoxicity.

(5) The formation potential of I-THMs, I-HANs and I-HAAs decreased under the oxidation of PbO_2 and MnO_2, which was due to the effect of polarization and redox potential by pH. The formation potential of I-HAcAms mainly depends on the difference between the hydrolysis rate of I-HANs and the decomposition rate of I-HAcAms. Therefore, in the $PbO_2/I^-/EPS$ system, it reaches the maximum at pH 7.0; in the $MnO_2/I^-/EPS$ system, the The maximum is reached at pH 6.0. The difference between PbO_2 and MnO_2 depends on the oxidizing ability of its oxide itself. With the increase of the initial concentration of I^-, the amount of I-DBPs produced by the oxidation of PbO_2 and MnO_2 increased, while with the increase of the PbO_2 dosage, the production of I-DBPs gradually decreased.

(6) The composition and structure of precursors (proteins and polysaccharides) can significantly affect the oxidation of PbO_2 and MnO_2 to generate I-DBPs. The proteins showed higher potentials for both C- and N-IDBPs than polysaccharides due to more electrophilic sites and higher N content. Among the 20 amino acid monomers, aspartic

acid (Asp) is iodomethanes (I-THMs), iodoacetic acids (I-HAAs), iodoacetonitriles (I-HANs) and iodoacetamides (I-HAcAms); asparagine (Asn) and tyrosine (Tyr) are also important precursors of I-HANs and I-HAcAms. In addition, the generation of I-DBPs can be controlled by increasing the alkalinity and hardness of the water body, using free chlorine, disinfectants such as peroxymonosulfate, and regular hydraulic flushing.

5.2 Outlook

In this paper, the formation and transformation rules of DBPs under the action of different PCPs were studied when EPS was used as the precursor, and the action pathway and mechanism were expounded. This will help the functional departments of water affairs to control the generation and transformation of DBPs, and provide a scientific basis for formulating relevant laws and regulations. The environment of the pipeline network transmission and distribution system is complex, and there are still many questions that need to be further studied and answered. Through the research of this paper and the understanding of cutting-edge theoretical technologies in this field, I think future research can focus on the following aspects:

(1) Study the possibility of DBPs generation and trace pollutant transformation when the pipeline material itself (organic macromolecular substance) or its extracts are used as precursors.

(2) In-depth study of the composite effect of different pipe network corrosion products (metal ions and metal oxides) on the formation and transformation of disinfection by-products.

(3) Establish a drinking water disinfection model, and screen out the most appropriate disinfection method and dosage through the analysis of water quality conditions, so as to ensure the safety of drinking water and minimize the generation of DBPs and trace pollutants.

(4) Study the mechanism of disinfection by-products generated when peptides (for

example, Asp-Asp-Asp) are used as precursors, and pay attention to their research pathways and intermediate products.

(5) Pay attention to the situation of industrial production of iodine-containing wastewater, and pay attention to the iodine content of treated wastewater and the impact on drinking water safety.